FACULDADE DE ENGENHARIA DA UNIVERSIDADE DO PORTO

Biped Locomotion Systems
Analysis, Modeling and Control

Diana Alves Lobo Guimarães

Master Degree in Electrical and Computer Engineering

Supervisor: Fernando Manuel Ferreira Lobo Pereira

July 23, 2013

Abstract

This dissertation concerns the analysis, modeling and control of the human locomotion with a view to the design of advanced systems supporting natural mobility, and, thus, promoting inclusivity and quality of life.

It starts with an overview of the state-of-the-art in modeling and control of the human locomotion, as well as a review of key background in nonlinear control and hybrid systems framework. Then, an analysis of human motion is performed in order to extract requirements to be satisfied by a motion control system. This leads to the specification of the overall control architecture and to some control design options that are discussed in detail. In order to properly formulate the associated control problems, a detailed and comprehensive kinematic and dynamic motion modeling is done by resorting to the so called DH method (Kinematics), Euler-Lagrangian method (dynamics), and techniques of impact mechanics. Finally, some simulation results of the implemented models are presented and some conclusions are taken.

A preliminary observation of locomotion quickly reveals its huge complexity. It is cyclic but composed of two major phases: double support and single support. Both of the phases encompass several stages, such as heel strike, midstance and push-off. The more significant changes occur in the sagittal plane. To avoid falling down when standing still, the body autonomously maintains its COG inside the support base formed by the feet. All the body segments have a role in system stability and accomplishments.

Humanoid robots can already walk at human speed and go up and down stairs or slopes.Multiple control methods were tested, often based on ZMP stability criterion.

The industry dedicated to the development of mobility solutions for disabled people is a growing sector of the economy, despite the current financial situation worldwide. For people that walk with abnormal gait due to muscle weakness, balance issues or similar issues, the state of the art solution is a hand-made carbon fiber frame with gyroscopes and a lock /unlock controller in the knee. Other solutions exist for paraplegics or amputees.Nowadays, most of the solutions involve electronics and, for this reason, they follow international standards for electromagnetic compatibility and low voltage levels, among others.

The idealized system presents a distributed architecture organized by layers as a way to guarantee adaptivity, robustness and (sub-)optimality. The low level controllers make use of a nonlinear technique to track the reference provided by the MPC, which is responsible for their optimization and for the feasibility verification in the upper layers. When the system safety is at risk or the a priori motion plan is impossible to archive the walking parameters or references can be adapted.

The walking machine model is composed by three sub-system (stance leg, swing leg and trunk) that cooperate to allow that the abstraction of balance, that constitutes a virtual system, to converge to a limit cycle.

The simulations done in the different domains proved sometimes the need of a different or additional approach/features. Once they were introduced, the requirements looked plausible.

Agradecimentos

Ao Prof. Fernando Lobo Pereira, por ter aceite orientar este projecto, por todas as contribuições dadas para melhorar esta dissertação e pela paciência para responder a todas as minhas questões.

E porque "é preciso uma aldeia para educar uma criança", agradeço a todos os que estiveram comigo neste percurso nos últimos 5 anos. Os seus nomes não seriam necessários, pois eles sabê-lo-ão, mas de qualquer forma: ao Jingle, Ricardo, Zé e Cristiano, que estiveram comigo nos primeiros anos. É sempre muito bom reencontrá-los!; ao ID, Kanguru, André e André, por todos estes anos de bons momentos e horas de estudo; ao Daniel e à Graça, por serem aquelas surpresas agradáveis que se encontra ao longo do caminho.

A muitos outros teria que agradecer, por me terem ajudado a ultrapassar os obstáculos ao longo dos anos ou por os terem colocado no caminho, pois isso fortaleceu-me.

Ao Enhamed, Teresa e Miguel. Pelo carinho e palavras nos momontos necessários.

Aos meus pais e ao Filipe! Por tudo.

Diana Lobo Guimarães

Contents

List of Figures

List of Tables

Abbreviations and Acronyms

CNS	Central Nervous System
COG	Center of Gravity
COM	Center of Mass
COP	Center of Pressure
DARPA	Defense Advanced Research Projects Agency
DBM	Dynamic Balance Margin
DOF	Degree(s) of Freedom
DH	Denavit-Hartenberg
ESPF	Energy Storing Prosthetic Foot
FRI	Foot Rotation Indicator
GRF	Ground Reaction Force
KAFO	Knee Ankle Foot Orthosis
MPC	Model Predictive Controller
PNS	Peripheral Nervous System
R&D	Research and Development
ROM	Range of Motion
SLK	Self-learning Knee
VMC	Virtual Model Control
ZMP	Zero Moment Point

Glossary

Balance	"a stable situation in which forces cancel one another" [10]
COG	Point where the resultant torque due to gravity forces is zero
COM	Point where the mass movements on one side of any plane are equal to the mass movements on the other side
COP	Point on the ground where the resulting GRF is applied
DBM	it gives the information of how far from unbalance the body is
Gait	Sequence of lift and release events for the individual legs (6 for humans)
GRF	force applied to a body by the ground as a response to the interaction body- ground (Newton′s Law of action-reaction)
Holonomic Constraint	integrable set of differential equations that describe the restrictions on the system′s motion. It can be written in the form $f(x_1,...,x_n) = 0$. Otherwise, it is called non-holonomic
KAFOs	Orthosis "designed to provide support, proper joint alignment to the knee, foot and ankle, assist or substitute for muscle weakness, and protect the foot and lower limb." [11]
Magneto-rheostatic fluid	Fluid whose viscosicity changes with the intensity of the applied magnetic field. Used as a shock absorber in prosthetics
Moment of inertia	Opposition to change of state of motion of a rotating body
Non-conservative Force	The work done on a moving object is dependent of the object′s path
Orthosis	Device to aid the healing process by relieving the joint, or, in the case of chronic situations, to relieve the joint by offering consistent support
Postural control	"the ability to/act of maintaining, achieving or restoring a state of balance during any posture or activity (...) strategies may be either predictive or reactive" [10]

Principle of Virtual Work	"The work done by external forces corresponding to any set of virtual displacements is zero" [12]
Prosthesis	Device designed to replace a missing part of the body
Rigid Body	body in which the distance between any two points remains constant in time, independently of the external forces acting
Wear and Tear	Damage that inevitably occurs, even if the product is used with proper care and maintenance
ZMP	"Point where the center of gravity is projected onto the ground in the static state and a point where the total inertial force composed of the gravitational force and inertial force of mass goes through the ground in the dynamic state." [13]

Chapter 1

Introduction

1.1 Why this Dissertation Project?

In daily life a person has to use his motor skills to overcome multiple situations and obstacles. The more common ones are flat ground, slopes and stairs, all of them with different degrees of roughness. The locomotion system will act differently in each one of these situations, adjusting the motion parameters (walking speed, step length or torso position). Thus, human locomotion fits clearly in the multi-phase systems category. People with locomotion disabilities are sometimes not able to do the required adjustments on their own.

In this dissertation, the human biped motion was investigated with a view to the design of control systems for robotic devices that will either enable or at least support this type of locomotion. Such a control system would enable people with balance issues to walk more safely in multiple environments, which are sometimes inaccessible to wheelchairs. This brings several advantages that include fewer motion constraints, which results in greater inclusivity by enabling locomotion on much less structured terrains (beaches, hills, etc.) and on a wider range of structures (stairs, unstructured trails, reasonably inclined grounds), and improving the health of the user. This last point is particularly important since, by walking in the up-right position and by stimulating an increased muscular activity blood circulation increases and, consequently bone loss caused by absence of stress is prevented. Moreover, the fact that the user is able to move up-right and do so with greater degrees of freedom and in a way much more similar (relatively to the wheelchair alternative) to that of other humans helps to eliminate psychological and mental barriers.

Finally, it should be pointed out that society would also benefit economicaly, because less resources would be spent in public accessibility improvement projects and, much more significantly, in health assistance.

1.2 Scope and Goals

This dissertation is written to obtain the Master Degree in Electrical and Computer Engineering.

It aims to help improve disable people's quality of life by studying biped locomotion systems and, based on the obtained models, design a control system capable of recognizising the present environmental conditions and adapting itself to ensure stability, according to the defined criteria (center of gravity position, joints' angles, among others). It should correct permanent locomotion anomalies and also be robust in dealing well with unpredicted environmental disturbances threatening the system integrity.

1.3 Methodology

Obviously, the design of a full fledged state-of-the-art global control system for a human biped locomotion system is a huge ambition that naturally is out of the scope of this dissertation, given the time and resources available. Thus, we will just provide a preliminary investigation that will contribute towards a solid foundation for the future design of a locomotion system. With this target in mind, this dissertation proceeds with a rigorous engineering and scientific effort anchored on a Systems Engineering Process based methodology, [14], that should prevail the methodological framework in the system's future development.

As a preliminary step in the process of the design of a new competitive solution, a market survey was done to identify existing solutions (with emphasis on their recent evolution) and outline their strengths and weaknesses.

Then, we proceed with a functional analysis providing a characterization of the identified challenges, followed by the specification of the functionalities and associated requirements to be considered in the system to be designed. This effort includes the detailed modeling of the system from the mechanical point of view as well as a thorough analysis of various instances of human biped locomotion. Subsequently, the key design options of the control architecture and associated subsystems will be made in such away as to ensure that the system provides the desired functionalities subject to the extracted requirements. This specification will involve not only a set of comprehensive simulation runs to chech the suitability of the obtained models - kinematic, dynamic, constraints, and performance functionals-. but also the use of formal results in Control and Optimization theories in the framework of hybrid systems in order to ensure that the specified properties are guaranteed. Once a suitable an overall system organization into multiple heterogeneous subsystems and of the associated control structure composed by an arrangement (with a hierarchic component) of intertwined control problems, is obtained, the ensuing stages will involve the synthesis of each one of the various controllers, with the corresponding performance analysis and testing under the set of specified environmental conditions.

1.4 Document Overview

The current chapter shows the motivation and the goals of this dissertation along with the methodology.

The next chapter displays the literature review on state-of-the-art humanoid robots and the used modeling and control methods.

In Chapter 3 is presented a market reasearch realized to rise the knoledge about orthopedic devices for people with disability and the exising gaps.

Chapter 4 analyzes the human locomotion.

Chapter 5 presents the problem and idealized system architecture.

In Chapter 6 the fundamental theoretical background concepts are described.

Chapter 7 explains the model developed.

Chapter 8 describes the obtained results.

Finally, brief conclusions are provided in the last chapter.

Chapter 2

Review on Control of Biped Systems

2.1 Introduction

Legged locomotion is harder to duplicate than wheeled locomotion, due to the greater mechanical complexity introduced by the extra DOF needed. Regardless, legs are more efficient on soft ground because they take advantage of discontinuous contact with the ground, which eliminates rolling friction. Besides, nature and man-made environments are unstructured and soft-surface based, respectively. With the presence of obstacles like steps or slopes, legs are much more suitable for these environments, [15].

This restates the need of finding a good legged solution for disabled people.

However, as it happens in any other R&D field, solutions are not tested in humans right away, so after computer modeling has been done, robots are used.

Humanoid robots have other purposes, such as entertaining or helping the elderly in daily tasks, but they allow better understanding of the influence in locomotion of some parameter variation – foot shape, weight distribution and posture.

Nowadays, detail level goes already in the toes: Waseda University (Japan) developed Wabian-2 that has passive toes and feet with an internal arch, just like humans, while in Tokyo a robot with active toe joints (see back foot in figure 2.1 on the left) was proven to walk faster and to overcome higher steps. In fact, PetMan can walk 7.08 Km/h and Honda's 2011 robot can run at 9 Km/h, [16].

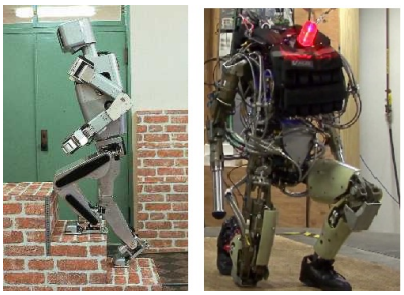

Figure 2.1: H7 (left) and PETMAN

2.2 Control Methods

To reach the walking speed that humanoid robots have today, researchers have abandoned the passive walking idea and have developed dynamic walking robots.

The main practical differences between the two walking strategies is that in passive walk the robot may stop at any time without the risk of falling, however the walking speed is 10 times slower and requires wider movements (synonymous for increased energetic waste) than in the dynamic approach.

Regarding the control method, passive walk balance control is performed based on the COG projection position. In dynamic walking, the need to control inertial forces resulting from body acceleration and matching external disturbances led to the consideration of the ZMP control method. The ZMP can also be used as a stability criterion.

The ZMP control strategy can be used differently depending on the complexity of the developed model. A model which considers a large number of links and its individual inertia generates a precise walking pattern by solving ZMP dynamics' equations. On the other hand, a not-so-complex model allows online pattern generation, despite performing a not-so-exact ZMP trajectory, due to model limitations and the system stability being dependent of the sensor reliability.

Both approaches have been used by researchers, leading to models going from the single inverted pendulum up to many links.

In the most complex models, different simplifications were done, such as not considering the feet [17] [18] [19] (working so with a 5 links model), considering a constant height for the hip [17], analyzing only the sagittal plan [17] [18] [19] or "imposing holonomic constraints on the robot's configuration parameterized by a monotonically increasing function of the robot's state" in order to reduce the stability analysis problem "from a 5-dimensional to a scalar Poincaré return map", [18].

Some authors have chosen to build a controller to guarantee that robot's feet have null velocity in the heel strike moment [13], whilst others develop an impact model based in the boundary conditions, [17].

According to [18], a pre-computed ZMP trajectory tracking using PID and a computed torque or sliding mode was compared by Tzafestas; Park and Kim did it combining computed torque with gravity compensation, while Fujimoto combined it with foot force control; Mitobe et al. tried using computed torque to regulate swing leg and COM' position.

The trajectory equations come often from a kinematic analysis based on the DH Method and for dynamics the Euler-Lagrange Method is used.

Other authors have distinct perspectives.

Standing balance is presented as an optimal control problem in [20], where a Linear- Quadratic Regulator (LQR) "selects trajectories that minimize an objective function which weighs the deviations of the controls and states from nominal", and the control scheme, being the controller of a nonlinear optimal feedback form. This author also studies the impact of delay (realistic neural delays are introduced in [21]) and proposes a Model Predictive Control Scheme.

A controller based on a 3D gait prediction is suggested in [22]. The authors of this paper combined the "state-of-the-art walking controllers from the robotics field and state-of-the-art musculoskeletal models in the biomechanics field" to predict the consequences of lower limb surgeries.

In [23], the trunk position in the walking direction is used to help maintain stability (if COG is too ahead of the support foot, the trunk will lean backward), and the influence of the arms movement is analyzed in [24].

Unlike [17] [18], there are authors that consider feet the main concern in robot motion. Authors of [25] propose the implementation of force sensors in the sole of the feet to calculate the real ZMP position and compare it with a database of gaits with different parameters that will be adjusted online by a neuro-Fuzzy controller. The paper [26] tests a foot positioning compensator (FPC) "to adaptively modify the robot's foot positioning based on the current and a short period of history robot states", and, to complete the control, the machine learning approach is employed " to find the relationship between the amount of foot positioning compensation and the actual dynamics" of the remaining body. In the same year, [27] tried to make their robot walk more like a human by adding a toe joint and focusing in its behavior during the support and swing phase and adding the possibility of stretching the support leg's knee.

By abandoning the walk on flat floor problem, an interesting comparative study between analytical method (DH based), Neural Networks and Fuzzy Logic performance in finding optimal gait for ditch crossing by a 7 links Humanoid was conducted by [1].

To walk on slopes, [28] used 3 tactile sensors placed in triangle on each foot, while [13] chosed a network of online controllers.

Also based on the network of online controllers, the same authors present a solution for stairs in [29].

Curiously, [30] refrained from the use of technics such as computed torque or adaptative control, because from their point of view, they were effective for the trajectory tracking but complex, time-consuming and needed a precise and accurate model. Therefore, they chose a Iterative learning control method.

Finally, just to mention that not many authors have chosen the Virtual Model Control (VMC) instead of the ZMP. The Spring Flamingo Bipedal Robot is an example of this. VMC is an ad-hoc method that adds components like springs, dampers or potential fields in an intuitive location to create forces and torques that generate stability, avoiding the need of a complete model.

2.3 Control Architectures

From what has been stated above, it becomes clear that the most used architecture has three main blocks: an (offline) trajectory generator, a (network of) controller(s) and a stabilizer.

The function of the stabilizer is to react in real-time to external disturbances, giving robustness to the system. The figure below, shows the architecture chosen in [31] for the SHERPA robot, where an impact controller was also included.

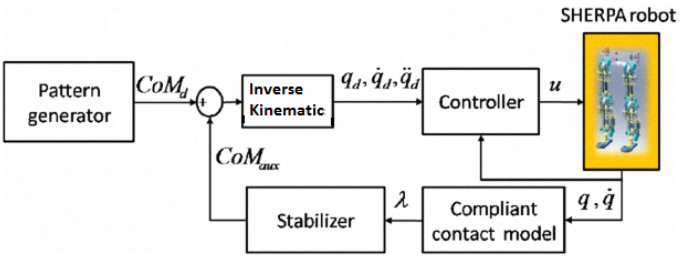

Figure 2.2: Control architecture of SHERPA robot

The ZMP based trajectory generator block is in detail below. The "Optimal" block is where COM trajectory is computed.

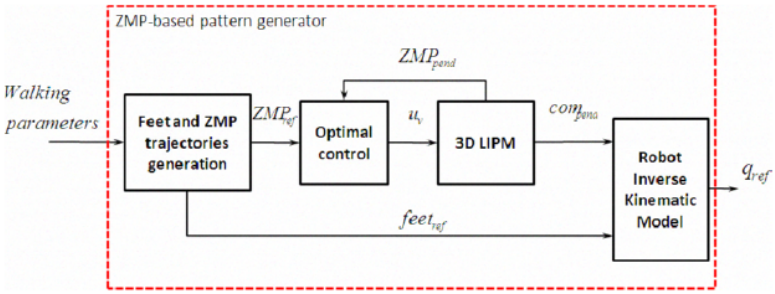

Figure 2.3: ZMP based trajectory generator block

The PD controller with gravity compensation in [32] works as displayed in figure 2.4, where q and $\dot{q}$ denote the current position and velocity while q_d and $\dot{q}_d$ are the desired ones.

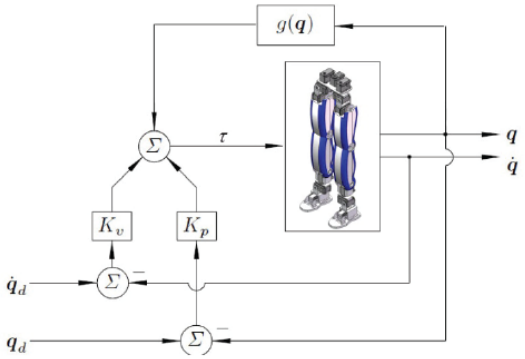

Figure 2.4: PD + gravity compensation controller

An example of Neural Network control is presented in the figure below, where b stands for bias and w for the weight assigned to each neuron. The number of neurons and layers have a significant impact in the overall performance. This particular author chose a two module architecture and applied a linear activation function in the input layers and Tan-sigmoid in the remaining ones.

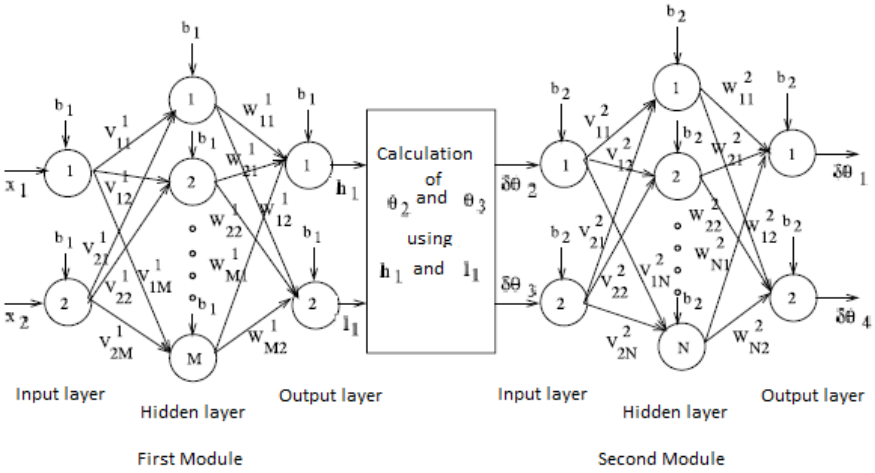

Figure 2.5: Neural Network Controller (taken from [1])

A very different architecture is proposed in [30], with the locomotion being viewed as a coordinated control effort. This interesting work simulates the use of a prosthetic leg and uses an hierarchical architecture in the context of a master-slave framework.

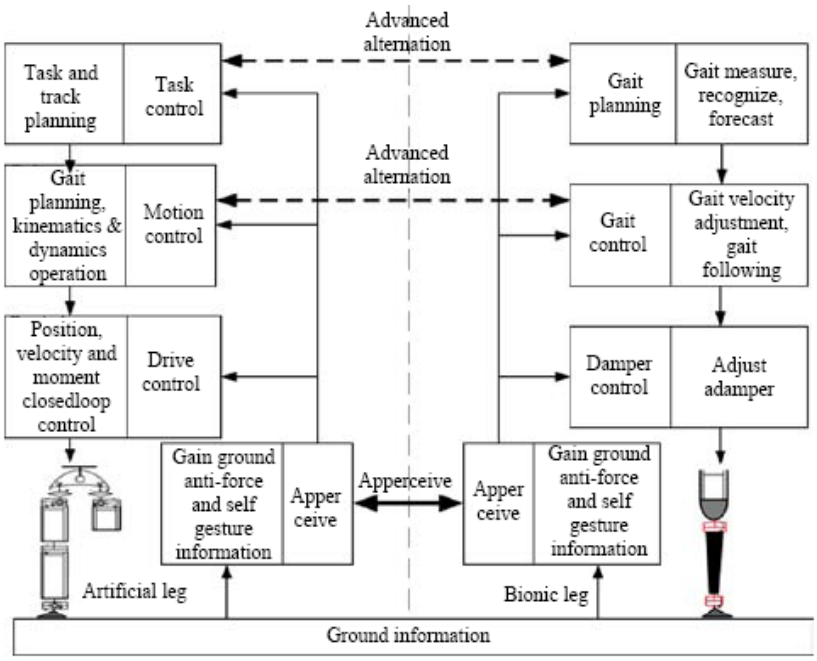

Figure 2.6: Hierarchical architecture in a master-slave coordenative control effort

The leg on the left simulates a healthy human leg and on the right is the prosthetic limb.

The paper explains that the task layer "decides what to do according to environment information or human command." As a master leg, it "decides the task of the whole biped robot system". In plan layer, the kinematics and dynamics equations are solved for gait control purpose, and the

planned gait is verified to see whether it is satisfying the constraint conditions of the coordination model. The drive layer is the actuation one. The slave leg has also three layers. The higher is for monitorization of the other leg′s motion. The middle layer, besides solving kinematic and dynamic equations, it also performs gait optimization.

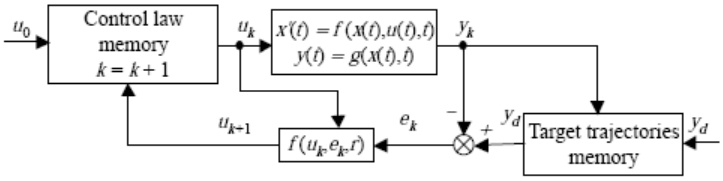

Figure 2.7: Iterative learning controller conceptual diagram

Paper [33] sees the biped robot as a hybrid system with real-time requirements and used ORCCAD to design the robot controller architecture. The authors made this choice because ORCCAD "allows the specification, the simulation and the implementation of robotic elementary actions (Robot-Tasks) integrating discrete events and continuous-time aspects. The overall robotic mission (Robot Procedure) is described by composing the Robot-Tasks through a synchronous language". A Robot-Task is showed below.

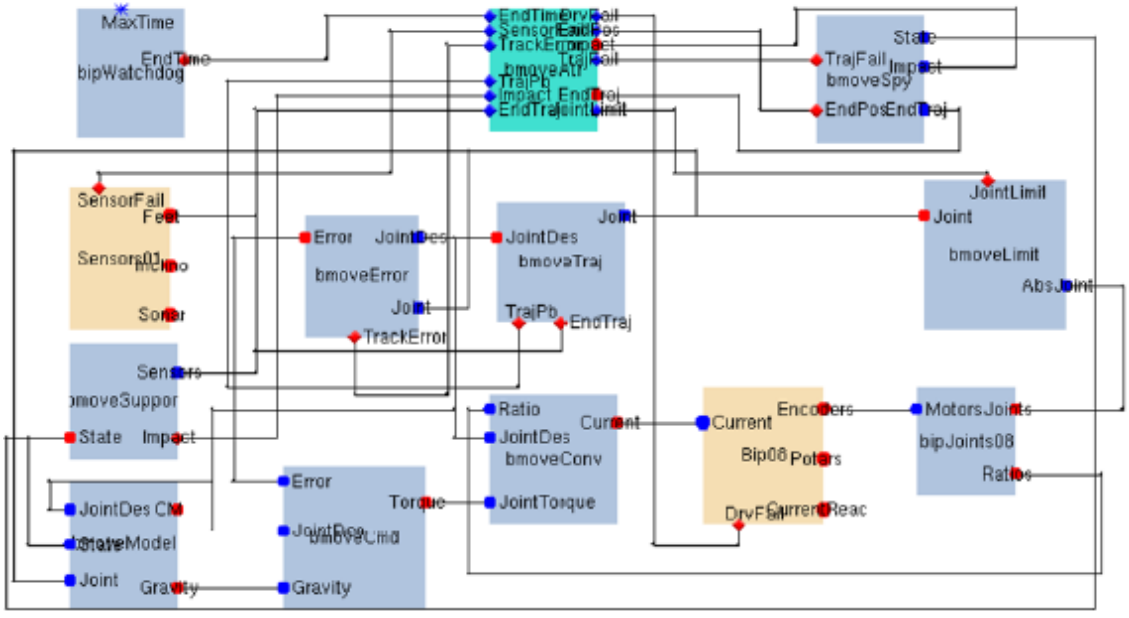

Figure 2.8: "Robot Task" in ORCCAD

But, before thinking in such a low level architecture, it is common to choose a intuitive path to get a global perspective of the different stages of the biped system, designing for example a state

machine, as displayed in figure 2.9

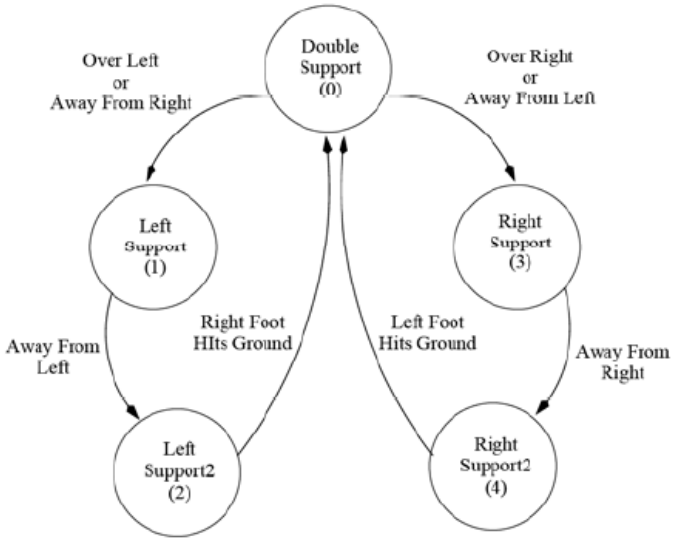

Figure 2.9: State machine for a biped robot (taken from [2])

This state machine maps only the motion in sagittal direction.

It becomes clear that, for walking, the sets of states 0,1,2 and 0,3,4 alternate. State 3 represents the period of time when the left foot has pushed the ground and is swinging still behind the support leg. State 4 lasts from when the swing foot gets ahead of the support leg until it touches the ground. The same happens in states 1 and 2 for the opposite side.

Chapter 3

Market Research on Applications for People

3.1 Context

The prostheses' industry was initially developed to find a better solution for those who lost their limbs in the World Wars.

These days, individuals with congenital malformations from birth or affected by diseases like diabetes, cancer or any other that demands surgical limb amputation to stop its propagation benefit from this development.

The 2011 World Report on Disability from the World Health Organization [34] indicates that 35% of the world population has, in some way, its mobility affected, 54% of those under 60 years of age.

Between 1998 and 2006, there was a 37% rise of obesity diagnosis. In 2010, the USA counted up to 1,7 million amputees and only 0.1% were caused by military incidents. Forecasts predict that 29 million Americans will have diabetes in 2050, many of them losing one or even both legs, which will be a large contributing factor to the existence of 28 times more amputees. [35]

The data presented above support the prosthetic industry's expectations of growth. The orthotics field appeared at the same time and also had the World Wars as big propeller. The market is controlled by five major players: Otto Bock HealthCare, Össur, Ohio Willow Wood , Fillauer e Hanger Orthopedic. [35]

As the last three companies are located respectively in Ohio, Tennessee and Maryland (USA), this leaves the European market more open for the Icelandic Össur and the German multinational company Otto Bock. There is also straight collaboration between some of the companies, for example Otto Bock and Hanger Orthopedic, because Hanger does not have a technology development department, so it sells German technology in a different geographical area.

There are, of course, a number of smaller corporations trying to win market share. They attempt it in two different ways: with very inviting prices or with state-of-the-art technology. Companies as the british Blatchford (whose commercial section is known as Endolite in the USA and

who earned major advertisement during the 2012 London Paralympic Games Opening Ceremony) and the American Freedom Innovations (founded in 2002) with the iWalk (launched in 2006 by Hugh Herr, MIT Media Lab's Biomechatronics Group director) bet on state-of-the-art technology. Lower prices are usually an attempt to capture the attention of developing countries, but present a limited functionality product.

The estimated annual profit of this industry is 2,15 thousand million euros. Otto Bock alone reached 487,5 million euros in 2011 - a 9.5% increase compared with the former year, [36].

Being highly technologically advanced together with a very specific target-audience makes it a low volume business. The profit comes from the considerably large unitary price asked for the development and maintenance of a highly complex and customized system. Delivering a high quality and safe product to the consumer is such a top priority that the state-of-the-art products usually exceed the demand of international standards, as electromagnetic compatibility (IEC 61000 family or ISO 13766:2006), low voltage levels (directive 2006/95/EC) and mechanical prostheses and orthotics testing and components standards (ISO 13405-1:1996, ISO 22523:2006, ISO 22675:2006 or ISO 13404:2007). [37]

3.2 Prostheses

3.2.1 Background

Prosthetics have experienced a radical change. Until 1980, prostheses had the function of establishing artificial, purely-mechanical connections to the ground. The well-being of the user was low. Prostheses caused swelling and a high level of fatigue.

In 1981, the first prosthetic foot able to store energy (ESPF) was designed and, in 1997, the first microprocessor-controlled prostheses with integrated sensors became available. (figure 3.1)

Figure 3.1: Leg prostheses evolution until today by date of creation

Modern solution generation is less than 15 years old and provides a close-to-natural gait in daily life situations: even ground walking, going up and down stairs and ramps. Its price ranges

from 4600 and 6200 euros for below-knee prostheses and 7700 to 11500 euros, but can reach 27000 euros, for above- knee prostheses, [38].

The cost would be even higher if there was not so much "wear and tear" that forces a replacement in 4 to 5 years time.

Low cost solutions like LCKnee and SATHI friction knee, [38], (developed in Canada and India respectively) can be bought for an average price of 40 euros (only the knee joint, not the mechanical stucture). These joints obviously have limited functionality, as hand-actuated mechanical blockage, low fault tolerance, inadaptability to locomotion conditions and/or less well-being.

In the next section, technological details for knee and ankle joints will be explored.

Hip solutions and others will be left out, because they present no significant further innovation interesting in this dissertation context.

3.2.2 State-of-the-Art Technology Details

The idea conceptualized in the ESPF is quite simple: the prosthetic foot heel is compressed during contact with the ground, storing energy, which is returned during the last phase of ground contact to help propel the body forward.

In this decade, the carbon fiber has also started being used.

The appearance of the C-Leg in the late 90s made the combination of ESPF with something novel for that time: a hydraulic knee-joint with sensors on the knee, measuring bending angle and angular velocity, and on the ankle, strategically placed to have a good leverage point, measuring the bending torque and the applied strain, with the data being sent to a microprocessor that refreshes the hydraulic actuator resistance in real-time and the controller recognizing and assisting two phases in the locomotion: stance and swing.

In the stance phase, the controller helps to stabilize the leg, so it can support the body weight, making sure the knee is fully extended (with a configurable tolerance) and at least 70% of the body weight is in the tip of the prosthetic foot before releasing the joint. In the swing phase, the controller provides dynamic control, decreasing the velocity to make the impact with the ground less violent and uncontrolled. The ankle sensor gives extra reliability and better dynamic tuning.

The microcontroller also has a customizable reaction to unpredicted events and a mode for sports and other physical activities, such as riding a bicycle.

Despite the two weeks long and easy to replace battery and smaller learning curve, the Blatchford / Endolite's Smart Adaptive Knee presents a lack of control in the swing phase, no adjustable hydraulic resistance (to help improve the user's posture) and easy to ruin hydraulics that make it less convincing for the users,[39].

The RHEO KNEE, released by Össur in 2005, deviates from the C-Leg, but without the sensor in the ankle. It uses software to detect the current state and which state should follow, based on the weight, the velocity detected by the sensor located in the knee and a statistical analysis of past events. This way of operating is called self-learning knee (SLK). Its main drawbacks are no support in the swing phase and magneto-rheostatic fluid hydraulics, which translates into high

battery consumption and a totally free joint in both phases once the battery is over. The attractive price mitigates these drawbacks and makes it a competitive choice.

Plié Knee, launched by Freedom Innovations in 2007, has the fastest reaction time to an environmental change, because it reads the sensors 1000 times per second, a refreshing rate 20 times higher than C-Leg and 50 times higher than the human body. The hydraulics resistance changes with pressure and position fluctuations rather than velocity. Being a SLK with unexpected knee joint actions provokes some uncertainty in the costumers' decision, [40].

The table below summarizes operating mode and main features of the three most known state-of-the-art leg protheses

Table 3.1: Prostheses features comparative analysis

Feature	**C-Leg**	**Rheo**	**Pile**
Sensors information (location)	bending velocity and angle (knee); bending torque and applied stain (ankle, with good leverage point)	bending velocity and angle (knee); current state detection software and statistical analysis of past events to decide future	equal to Rheo
Weight (Kg)	1,145	1,520	1,225
Height (mm)	196 or 214	236	235
Maximum bending angle (degrees)	125	120	125
Sensor reading (1/s)	50	(unspecified)	1000
Battery: composition; autonomy (h) ; complete charge time (h)	Lithium ion; 40 to 45; 5	Lithium ion; 24 to 48; (unspecified)	(unspecified); Aprox. 24; (unspecified)

In 2010, Össur released PowerKnee, the evolution from Rheo Knee, adding a climb stair functionality (triggering the muscles activity with an engine) and two sensors (gyroscope and accelerometer) in the knee joint to have the floor slope perception.

For 2012 OttoBock released Genium, C-Leg's update, including a gyroscope and accelerometer, accepting a 135 degree bending angle and bending automatically up to 17 degree to benefit the user's posture, improved autonomy battery (4 or 5 days) with an user-friendly interface and saving mode. It also provides extra safety to overcome obstacles, the ability to stand longer periods of time, walk backwards or go up and down stairs with the prosthetic leg leading. The higher IP

protection (IPx4) makes it possible for the prosthesis to be exposed to water jets.

Figure 3.2: Last generation knee joints: Genium (left) and PowerKnee

Both, Genium and PowerKnee, are featured with computer assisted alignment. This is, in fact, something that has expanded in the past few years. The biomechanical research - the knowledge of the points of interest positioning during the locomotion phases and in static balance - has led to the development of tools, typically platforms using laser, to show the current positioning and applied forces on each body segment, enabling a correction through joint regulation, using the computer or manually. Other sections in concurrent development are socket technology, [41], which tries to find the right cloth for different types of residual limb and to develop closure systems to extract the air between the mechanical structure and the cloth socket (improving comfort) and the residual limb software modelation to autonomously produce the mechanical piece to support the applied load (black part with white inside in figure 3.2), replacing the traditional handmade plaster alloy cast.

This last business sector is so successful that companies are created exclusively to sell customized add-ons (figure 3.3) with the purpose of giving the leg visual symmetry back to the amputee or making a double amputee have limbs that match his/her body type, [42].

Figure 3.3: Customized add-ons (shape symmetry)

Concerning prosthetic feet and ankle joints, there is a wide mechanical genesis variety, minimizing energy consumption or appropriated for outdoor activities (figures 3.4 and 3.5).

Figure 3.4: mechanical prosthetic feet (taken from [3])

Figure 3.5: Echelon (left) and Triton mechanical feet

These prostheses bring new abilities such as standing on an inclined ground, sitting with the prosthetic foot tip and heel touching the ground or rotating over the ankle's axis (figure 3.6).

Figure 3.6: Conventional mechanical foot (left) and state-of-the-art mechanical foot

The position change is induced by ground impact and is based on the constriction of the springs. Thus, the response time is approximately one second.

Therefore, the new generation is electronic and can refresh the ankle angle even in the swing phase, duplicating human foot angle changes.

Proprio Foot from Össur and BiOM PowerFoot from iWalk excel in this generation. BiOM has a stoning complexity: 12 inertia, force and position sensors; actuator capable of providing up to 20 Jooule of energy, as a healthy human calf muscle would do to enable an intended movement speed, and 3 microprocessors with a dynamic standard movements library. All this to refresh the angle, stiffness and damping factor 500 times per second, [43].

Össur's product weighs 1,468 Kg (having a 168mm minimum height) and the iWalk weighs 2,041 Kg.

Figure 3.7: Proprio Foot (left) and PowerFoot ankle joints

As you can see, there has been a great technological development in the last twenty years, mainly thanks to the development of material sciences and embedded systems, with the trend being more, smaller and lighter electronics embedded in a prosthesis, giving the amputee a perfectly natural gait and the same (or even better) abilities then a non-disabled person. According to Hugh Herr, another twenty years from now, it will be possible to make the brain respond effectively and efficiently to the information coming from the prostheses sensors. This closed loop will enable a leg amputee to feel the texture of the sand as he walks on the beach, [44].

3.3 Orthoses

Leg orthoses have two main goals: to keep limb alignment and impose or deny total extension or bending. Two types of users were identified: people with permanent or temporary impairment (healing from surgery or other). The last situation will not be studied. Until 2002, orthoses were completely mechanical with a hand activated lock to allow sitting.

Figure 3.8: classical KAFO (side and front view)

In that year the first stance control KAFO appeared, [45], and their operating principle is: “The automatic lock is initiated by knee extension, and is only released to swing freely when a knee extension moment and dorsiflexion occur simultaneously during terminal stance”, [46].

As not every user can do total knee extension or significant foot dorsiflexion, in the following half a dozen years manufactures have developed KAFOs with different operating principles using gyroscope like prostheses do, but the actuator was still an electromagnetic activated spring.

In May 2012, the adjustable resistance hydraulics actuator was embodied in an orthosis, enabling dynamic control in real-time (see figure 3.9).

Figure 3.9: Gyroscope sensor (left) and hydraulic actuator (right)

3.4 Applications with a Different Perspective

There are some interesting applications with a different aim and with other target users. For example, Rewalk (created in 2011), WalkAide, and the Israelite product Re-step (created in 2008) (see figure 3.10).

The first is designed for paraplegic people, and, for that reason, is a more complete and complex product, similar to an exoskeleton.

WalkAide performs electrical muscle stimulation to overcome the communication interruption that inhibits natural foot lifting (foot drop disease).

Re-step is a very smart walk-teaching pair of shoes that "changes the sole height and inclinations in a specific order. The shoes measure the parameters of your gait and in addition a PC displays progress and recommendations", which helps train the brain, [47]. It is directed towards people with cerebral palsy or with advanced age, but it can be used by anyone trying to improve balance because it has a training purpose, not a permanent use one.

Figure 3.10: Different target users products: Rewalk (left), WalkAide (middle) and Re-Step

Chapter 4

Human Locomotion Analysis

Locomotion is processed through the cerebral cortex and thalamus, situated in the forebrain.

A locomotion disorder can be triggered by cerebral cortex or thalamus malfunction. Another possibility is to be consequence of communication anomalies between peripheral nervous system (PNS) and central nervous system (CNS), composed by the brain and the spinal cord. It can also be a local problem, such as abnormal bone/joint alignment or muscle weakness.

Locomotion modifies human posture over time in three different planes (figure 4.1)

Trajectories in the sagittal plane suffer the most changes (as people walk forwards or backwards), but trajectories in the frontal plane can also be important because abnormal trajectories with significant amplitude can influence stability.

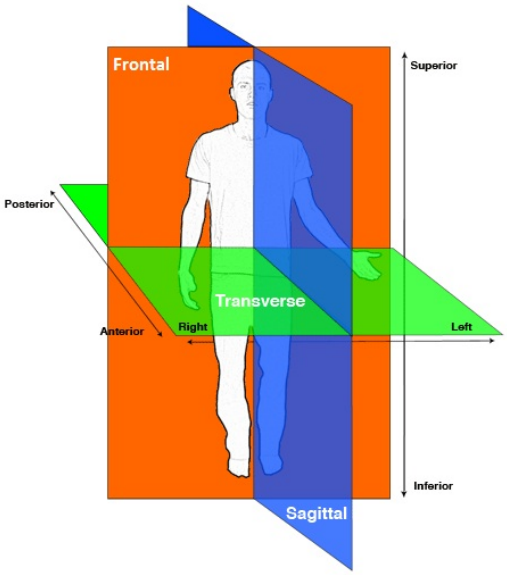

Figure 4.1: Locomotion plans

Locomotion can be performed in multiple situations, such as:

- On a flat surface,
- On an uneven surface,
- Walking up or down a slope,
- Climbing or descending steps

In any one of these, the friction coefficient might be considered.

According to expression 4.1, human gait adds up to six changes of state.

$$N = (2k-1)! \tag{4.1}$$

where N represents the different states and k the number of legs.

However, three of them are not so interesting, since they represent hopping.

Thus, by considering the following states:

1. Both legs on the ground;
2. Left leg on the ground and right leg in the air; and
3. Right leg on the ground and left leg in the air.

it is possible to stand still, rotate on both sides and walk.

Standard values for body segments weight in percentage of total body weight can be viewed in table 4.1. The segments length in percentage of body height is displayed in figure 4.2, and the location of each body segment COG is in table 4.2.

Table 4.1: Standard body segments weight in percentage of total body weight (taken from [8])

Segment	**Males**	**Females**	**Average**
Head and Neck	6.94	6.68	6.81
Trunk	43.46	42.58	43.02
Thigh	14.16	14.78	14.47
Shank	4.33	4.81	4.57
Foot	1.37	1.29	1.33

Table 4.2: Standard COG location in percentage of each segment height (taken from [8])

Segment	**Males**	**Females**	**Average**
Head and Neck	50.02	48.41	49.22
Trunk	43.10	37.82	40.46
Thigh	40.95	36.12	38.54
Shank	43.95	43.52	43.74
Foot	44.15	40.14	42.15

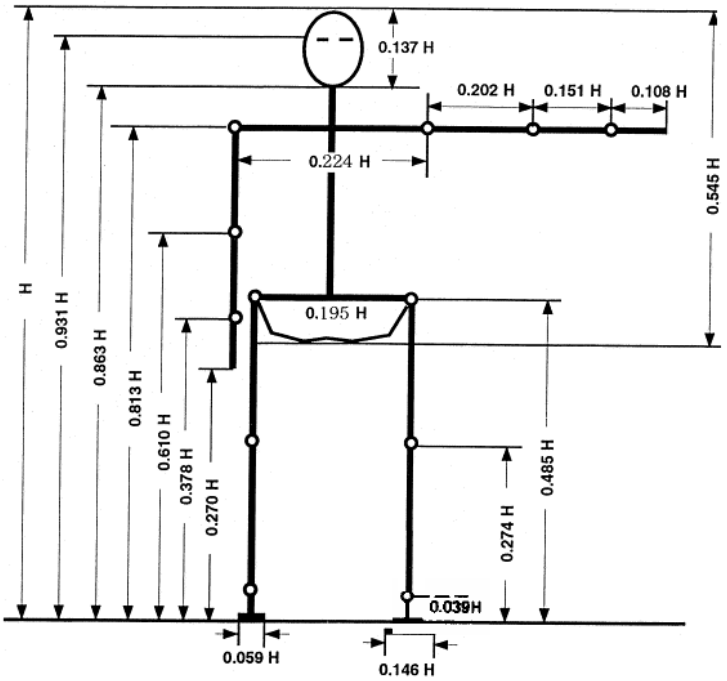

Figure 4.2: Body segments length (in percentage of body height)

In an adult, the horizontal distance between heel and toe is between 24 to 28 cm. The angles' representation is in the imaage below.

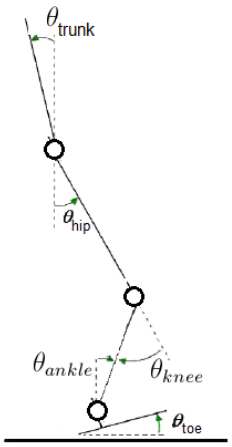

Figure 4.3: Leg angles

The ability to stand still and walk are going to be analyzed in detail in the next sections.

4.1 Standing Still

Motionless standing is possible if an equilibrium position is accomplished. It happens when the sum of all forces and torques applied to the body equals zero, simultaneously.

Equilibrium can be classified as stable if a lifting of COG is necessary to break it, or unstable if a small perturbation will change the COG position.

Static balance/stable equilibrium is accomplished if the COG vertical projection does not leave the support area, as shown in figure 4.4.

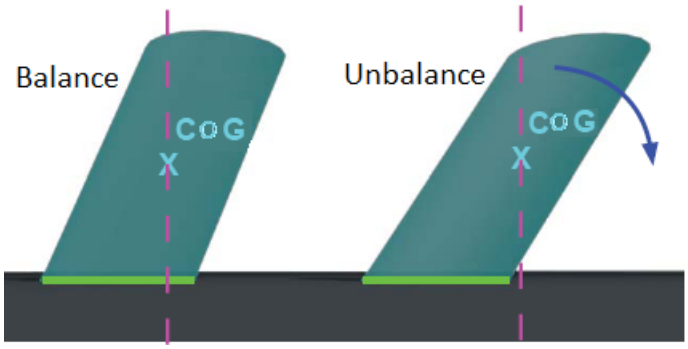

Figure 4.4: COG vertical projection determining balance existence

In a human, the base of support is the space between the feet. It can assume multiple configurations and each one of them benefits the stability in different directions.

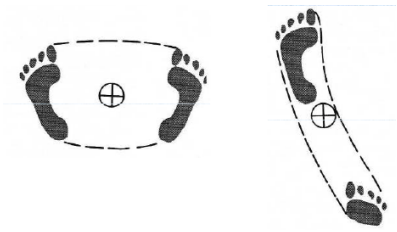

Figure 4.5: Human base of support configurations

The base of support can assume multiple configurations with the situation on the left increasing resistance to forces acting in the sagittal plane, while the other situation benefits stability to forces acting in the frontal plane.

In a human in the standing position as illustrated in figure 4.1, the COG is located around 55% of a female's height and around 57% of a male's height. Besides gender and body pose, age and body mass or built/shape also have an effect on COG position.

Humans are capable of controlling the body posture by performing very small predictive corrections, unwittingly. These corrections are commonly made by actuating one or both of the main control cores: ankle or hip. Moving the feet or grasping with a hand are alternatives for bigger

corrections. Hip strategies are typically used when support area is small, [48].

In a balanced posture, all the leg joints will be zero degrees and, according to a study available in the US National Library of Medicine National Institutes of Health Search, [49], "The joint contractures at ankle angles > 5 degrees of plantar flexion, knee angles > 19 degrees of flexion, and/or hip angles >19 degrees of flexion produce a potentially unstable posture".

In what concerns the weight distribution, a non-neutral COG position in the frontal plane will make limbs bear a disparate amount of weight, proportional to the distances ratio, damaging the individual's health, since a good posture is key to decrease stress in body structures (muscles, bones, ...) and energy waste.

4.2 Walking on Level Ground

Several authors propose different standard values for walking speed and step length and cadence for men and women. Table 4.3 summarizes the different studies.

Table 4.3: Standard values for walking speed, step length and cadence for men and women proposed by distinct authors (taken from [9])

Characteristic	Male: Mean (SD)	Female: Mean (SD)	Source
Walking speed (m/s)	1.37 (0.22)	1.23 (0.22)	Finley and Cody
	1.37 (0.17)	1.32 (0.16)	RLA
	1.22–1.32 (unspecified)	1.10–1.29 (unspecified)	Oberg et al.
	1.34 (0.22)	1.27 (0.16)	Kadaba et al
Stride Length (m)	1.48 (0.18)	1.27 (0.19)	Finley and Cody
	1.48 (0.15)	1.32 (0.13)	RLA
	1.23–1.30 (unspecified)	1.07–1.19 (unspecified)	Oberg et al.
	1.41 (0.14)	1.30 (0.10)	Kadaba et al
Step cadence (steps/min)	110 (10)	116 (12)	Finley and Cody
	111 (7.6)	121 (8.5)	RLA
	117–121 (unspecified)	122–130 (unspecified)	Oberg et al.
	112 (9)	115 (9)	Kadaba et al

The complete walking (or gait) cycle shown in figure 4.6 is divided into stance and swing phases.

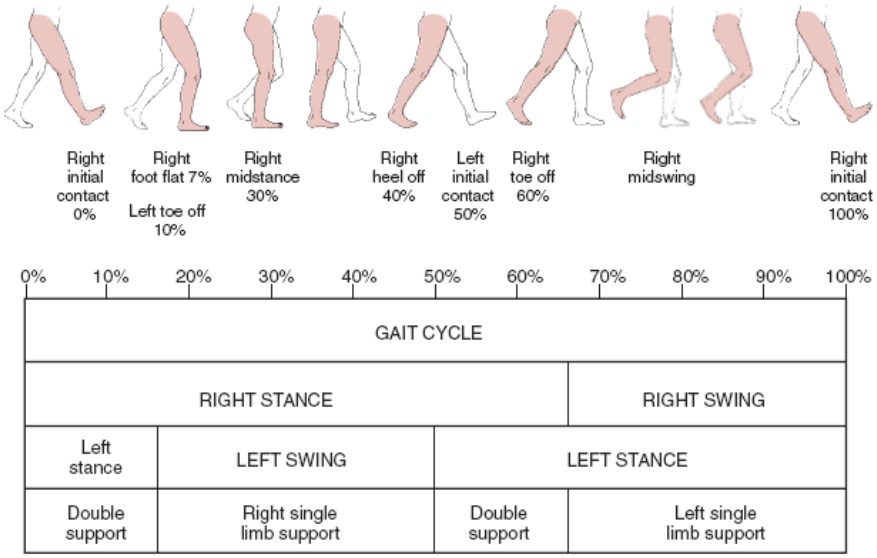

Figure 4.6: Complete gait cycle

As it can be seen, double support stage represents only 10% of the gait cycle.
Stance phase takes about 60% of the cycle and can be split into:

- Heel strike or initial contact
- Foot flat
- Midstance
- Heel off
- Toe push- off

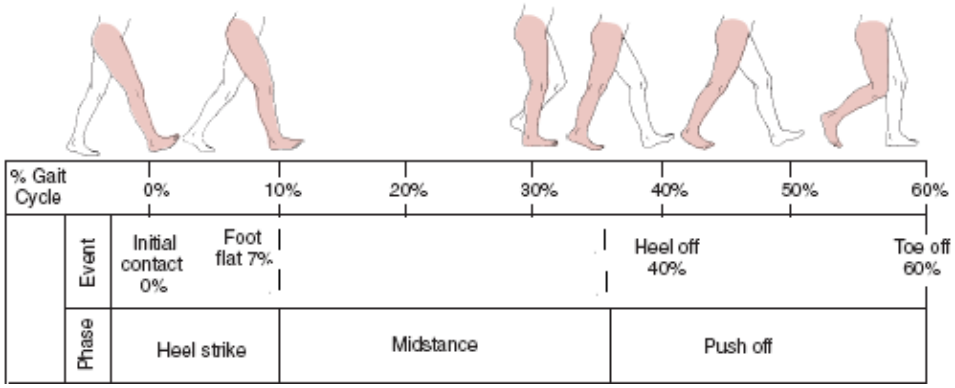

Figure 4.7: Stance phase in detail

The swing phase lasts the remaining 40% of the cycle and also has three separate moments:

- Initial acceleration
- Midswing

- Deceleration

Humans often develop their own style of locomotion, the one wich is most efficient according to the physiognomy of the individual. Nevertheless, everyone is able to adopt a different motion style if they are trying to walk at a different speed, overcome an obstacle, or even regain balance.

Although some things, like maximum foot height or knee-bending amplitude, can create a very different walking style, they can be seen just as a variation of parameters. A style is more related to the order of events in the proximity of the exchange of single support to double support.

Next, we characterize the four most common styles.

- Style of locomotion 1

  The support foot remains flat on the ground until the heel-strike of the opposite leg. It intends to maximize the ground contact surface to increase stability and is only possible with small steps

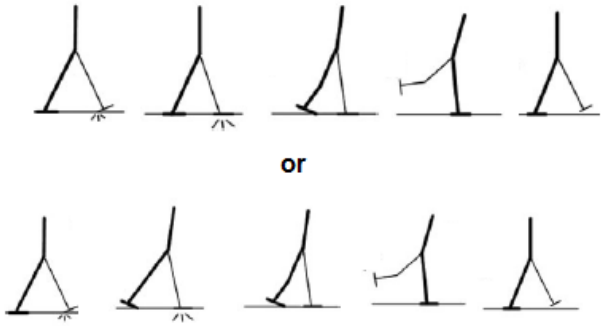

Figure 4.8: Style of locomotion 1

- Style of locomotion 2

  The order of events is heel-lift, heel-strike, toe-strike and toe-lift. This is considered the standard style

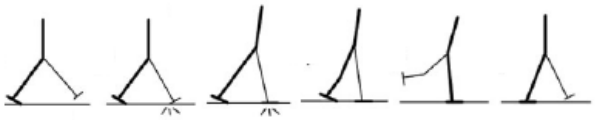

Figure 4.9: Style of locomotion 2

- Style of locomotion 3:

  The order of events is heel-lift, toe-lift, heel-strike and toe-strike. This foresees larger steps and a near to running motion

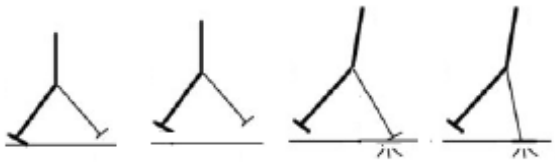

Figure 4.10: Style of locomotion 3

- Style of locomotion 4:

  The order of events is heel-lift, heel-strike, toe-lift and toe-strike. This style is common when stepping over obstacles

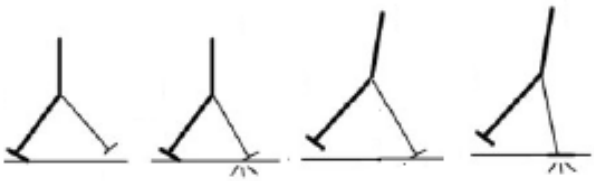

Figure 4.11: Style of locomotion 4

As a person walks, their COG will experience a vertical oscillation of 5,08 centimeters. Figure 4.12 displays when the maximum and minimum occur.

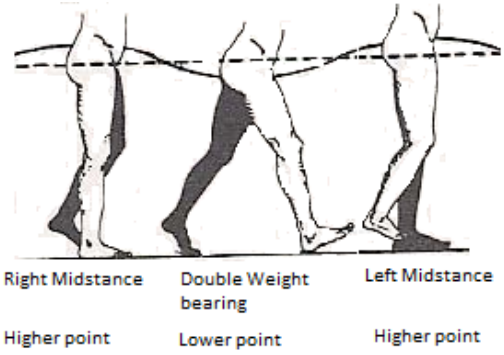

Figure 4.12: COG oscillation

Other features that cannot be left without analysis are the range of motion (ROM) of each joint (hip, knee and ankle), applied torques, GRF vector and COP location.

Table 4.4 shows the ROM for a person without any physical limitations, during motion on level ground (sagittal plane).

Table 4.4: Leg joints' ROM when walking on level ground (sagittal plane)

Joint	**ROM (in degrees)**
Hip	[-20; 30]
Knee	[0; 60]
Ankle	[-25; 7]

With negative values representing hip extension and ankle plantar flexion.

This numbers are confirmed, with minimal changes, by a different author, [50], who found that "during normal ambulation, the normal range of motion at the ankle is from 20^o plantar flexion to 15^o dorsiflexion. The knee moves 65^o from flexion to extension. At the hip, about 6^o of adduction occurs and a 45^o range is necessary from flexion to extension."

For a person with a proper gait pattern and using no gait changing footwear, COP describes the trajectory shown in figure 4.13

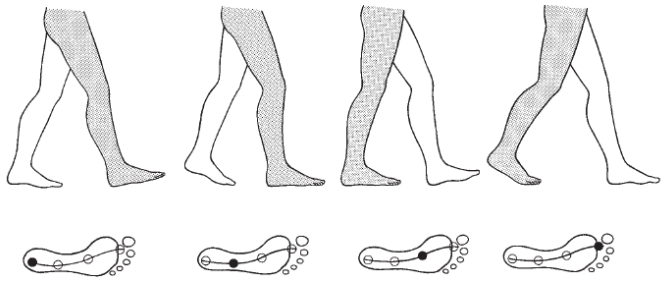

Figure 4.13: COP trajectory

Angle values, applied torques and GRF vector for the previously identified stance and swing phases' milestones are displayed in figure 4.14 and 4.15. Notice that only joint angles are not null in the swing phase.

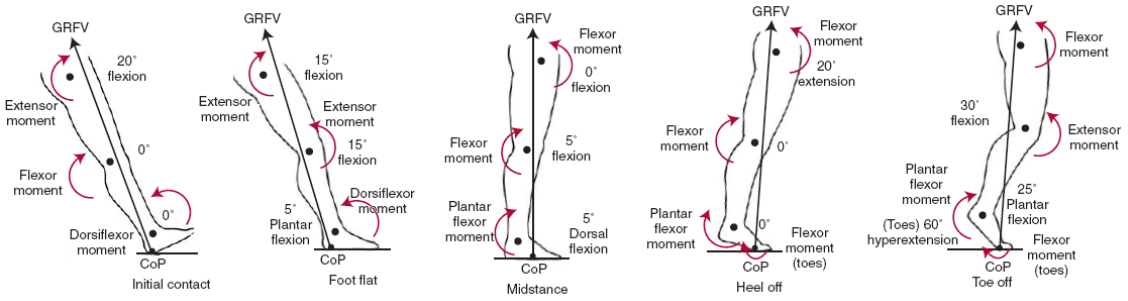

Figure 4.14: Joints' angle, applied torques and GRF vector in stance milestones

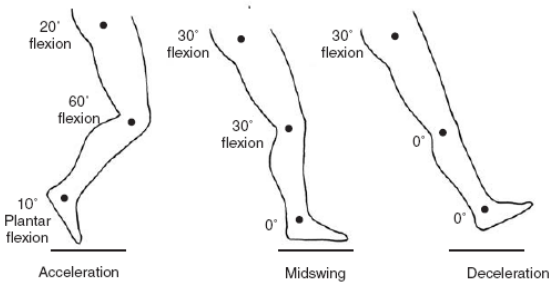

Figure 4.15: Joints' angle in swing milestones

The GRF vector has a component in every motion plane, however the magnitudes in the direction of motion and in the lateral direction are 10 and 100 times lower than the vertical one, respectively, [51]. Usually only the sagittal component is considered. The maximum values occur just after the heel touches the ground and in toe push-off (COG lower points). The local minimum occurs in the midstance (COG higher point).

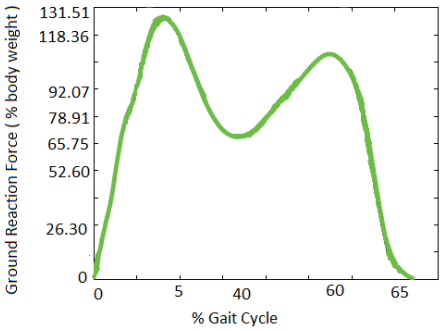

Figure 4.16: GRF over the stance phase

ZMP and FRI are the most common stability criteria for motion.

ZMP can be used as a stability criterion, since if the ZMP "strictly exists within the supporting polygon made by the feet, the robot never falls down",[13]. FRI is based in the position of instantaneous center of rotation towards the knee line. Figure 4.17 illustrates both.

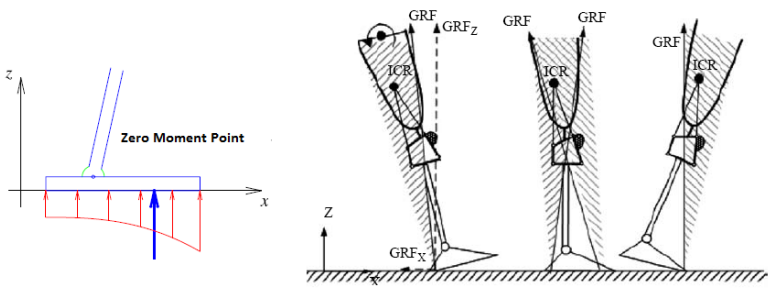

Figure 4.17: ZMP and FRI stability criterions

Next, we illustrate with a number of diagrams the evolution of the key motion variables of hip, knee, ankle and foot over the gait cycle, considering angles and torques' normative values. This figures were redrawn from [9], and the mean value is drawn in a solid black line and the mean value plus standard deviation is represented by the red dotted line. Since the joint displacement depends on multiple factors, figures of the displacement variation with gender, weight and type of shoes are also included (taken from [52]). A generic pathologic gait is also shown.

- **Hip**

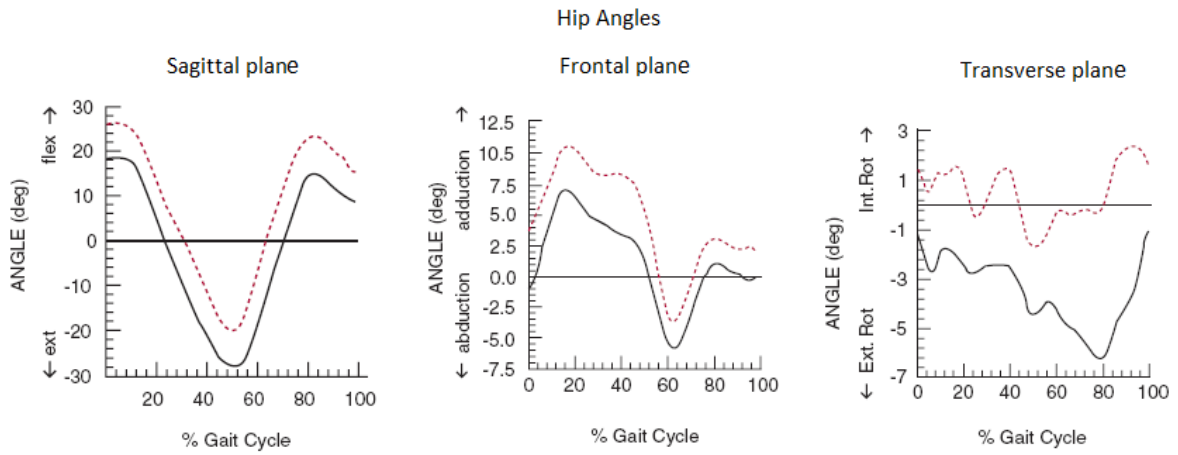

Figure 4.18: Hip joint angle's evolution over the gait cycle

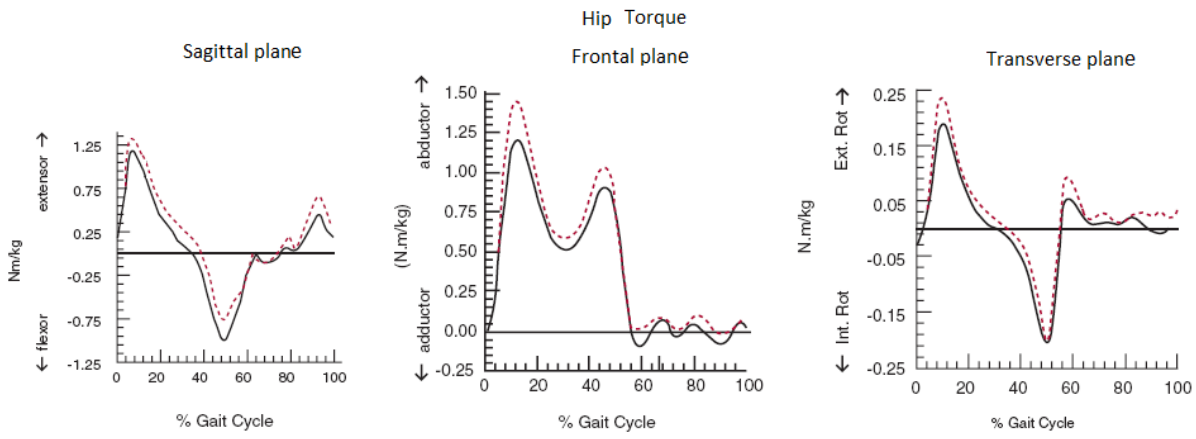

Figure 4.19: Hip joint normalized torques' evolution over the gait cycle

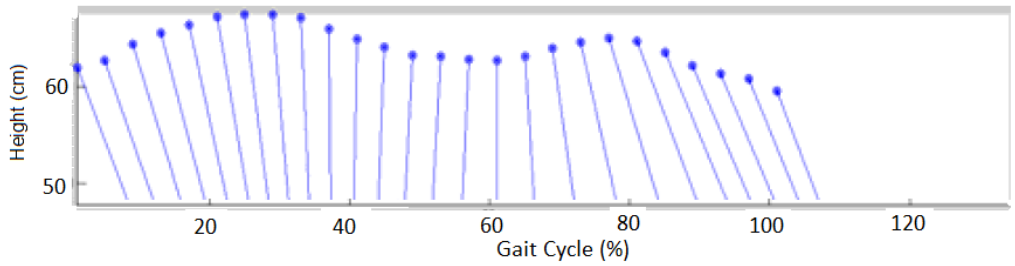

Figure 4.20: Ilustrative hip displacement (in cm) over the gait cycle in the sagittal plane (taken from [4])

- **Knee**

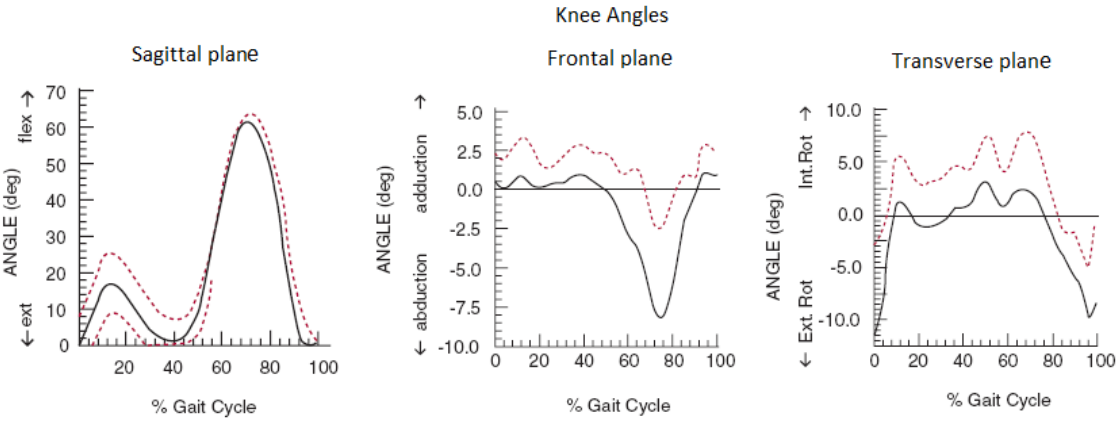

Figure 4.21: Knee joint angle's evolution over the gait cycle

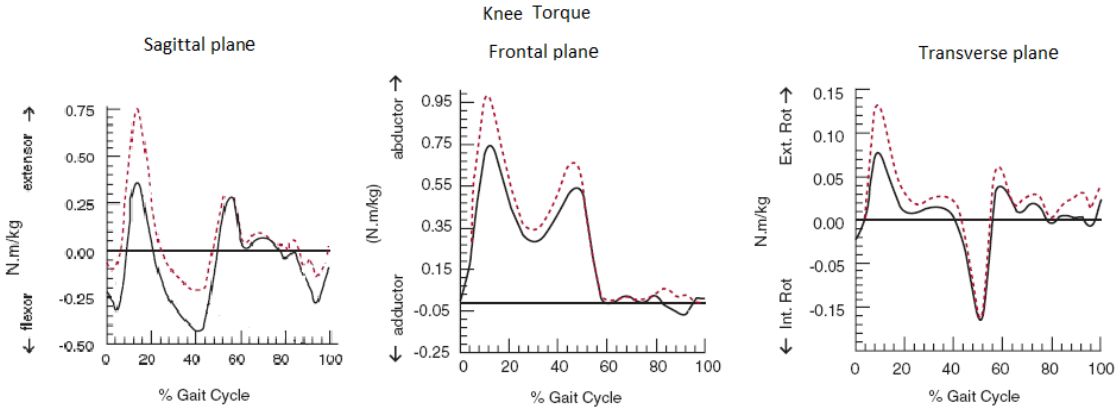

Figure 4.22: Knee joint normalized torques' evolution over the gait cycle

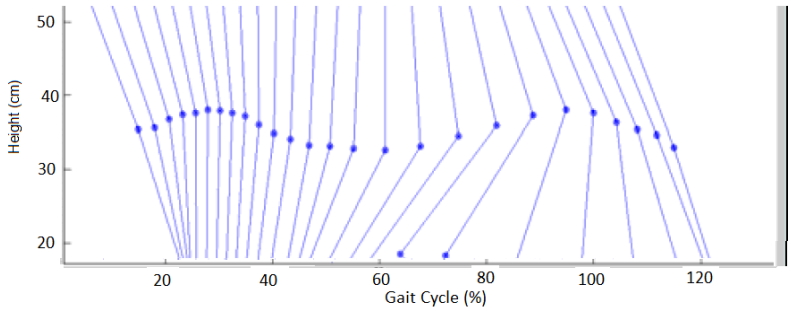

Figure 4.23: Ilustrative knee displacement (in cm) over the gait cycle in the sagittal plane (taken from [4])

- Variable size heel shoes

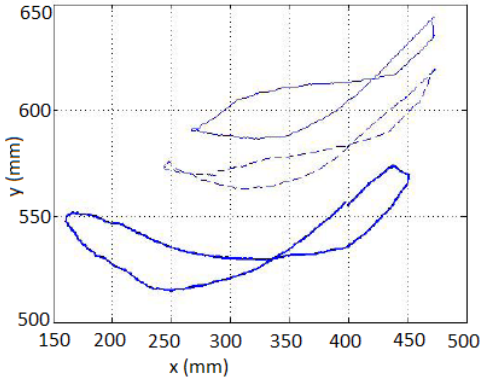

Figure 4.24: Knee displacement (in mm) for 10 mm heel (bold line), 80 mm heel (dotted line) and 110 mm heel

- carrying a 6 Kg backpack

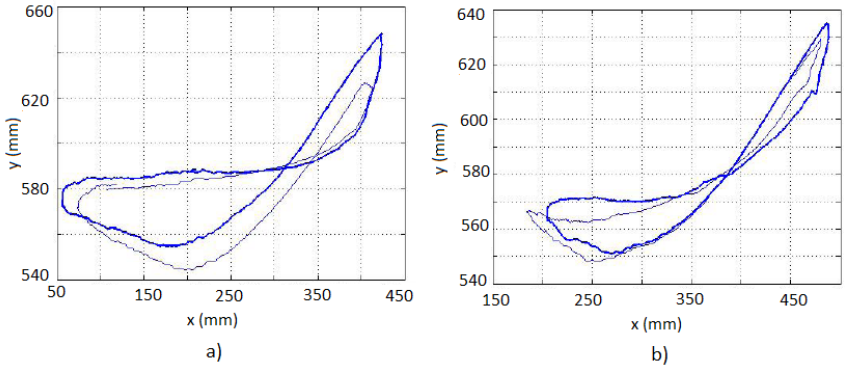

Figure 4.25: Knee displacement (in mm) when individuals a) and b) carry a load - without load (bold line) and with load

- Disabled gait pattern

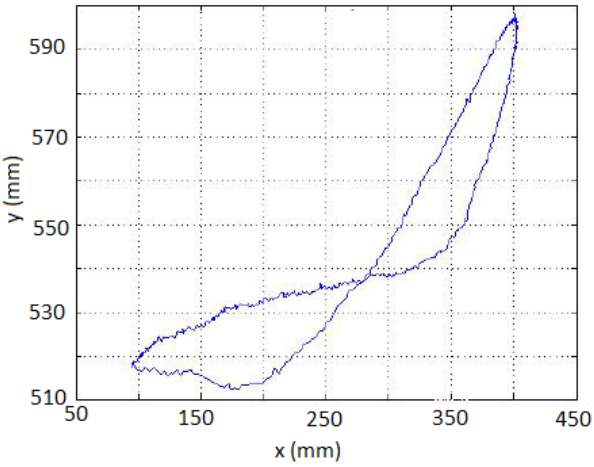

Figure 4.26: knee displacement (in mm) on a unknown disability

- Ankle and Foot

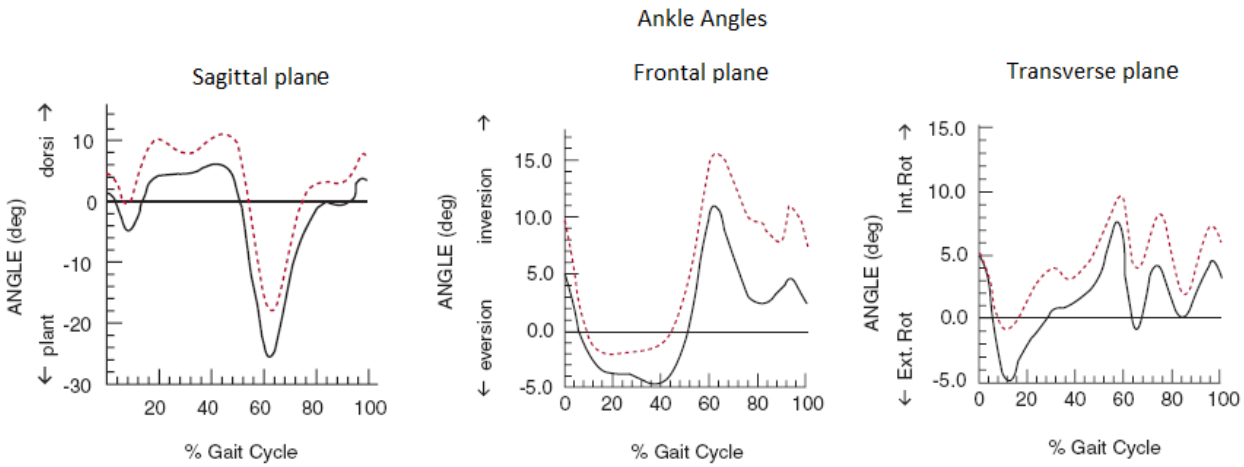

Figure 4.27: Ankle joint angle's evolution over the gait cycle

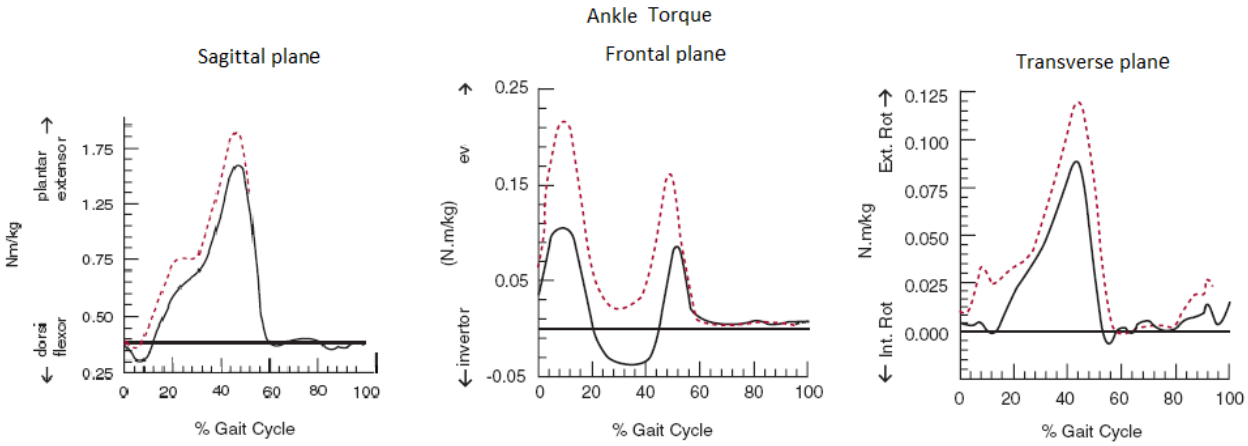

Figure 4.28: Ankle joint normalized torques' evolution over the gait cycle

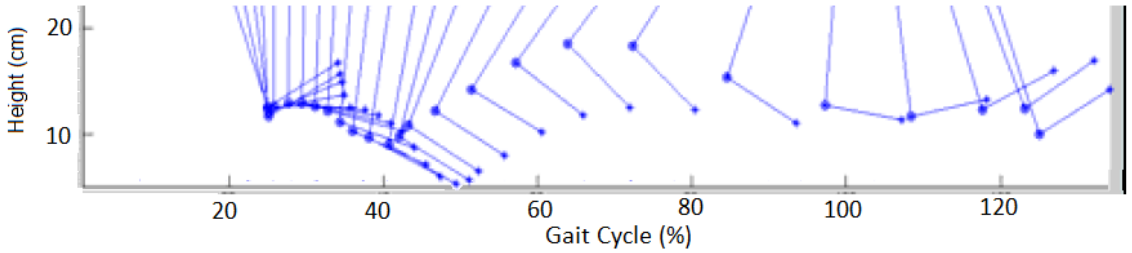

Figure 4.29: Ilustrative ankle and foot displacement (in cm) over the gait cycle in sagittal plane (taken from [4])

The above figure is not fully correct, since the heel should be the first thing to touch the ground (height= 0 cm), not only the toe.

- Man/ Woman

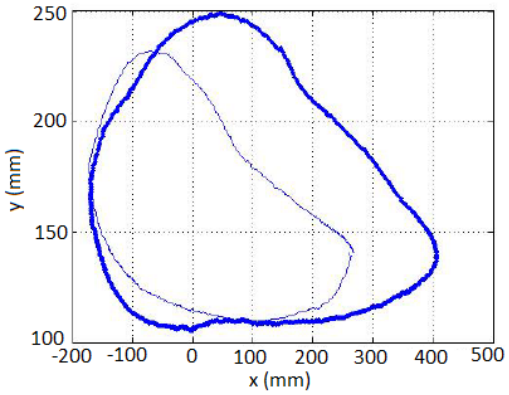

Figure 4.30: Ankle displacement (in mm) for man (bold line) and women

- Short/ Tall

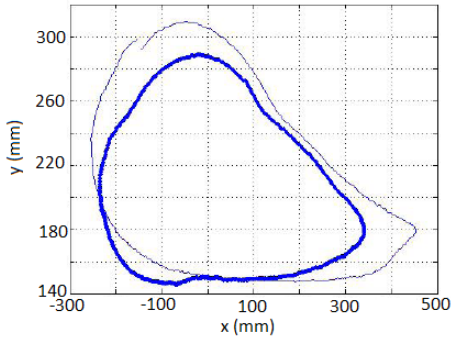

Figure 4.31: Ankle displacement (in mm) for a short (bold line) and a tall person

- Slim/ Overweight

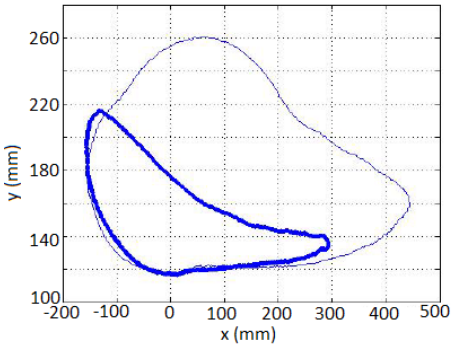

Figure 4.32: Ankle displacement (in mm) for a slim (bold line) and a fat person

- Variable size heel shoes

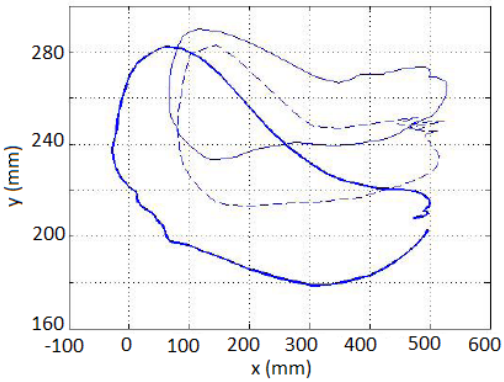

Figure 4.33: Ankle displacement (in mm) for 10 mm heel (bold line), 80 mm heel (dotted line) and 110 mm heel

- carrying a 6 Kg backpack

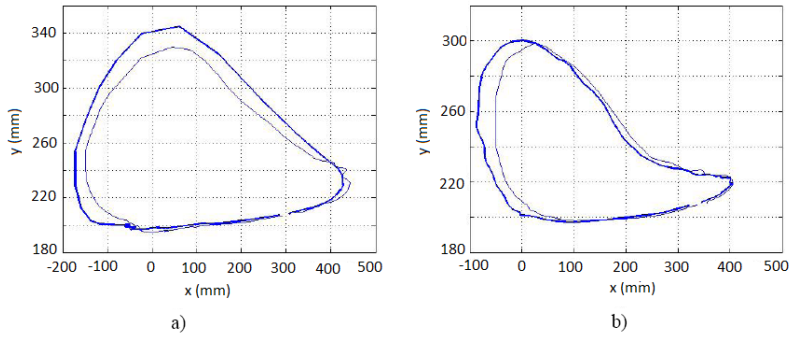

Figure 4.34: Ankle displacement (in mm) when individuals a) and b) carry a load - without load (bold line) and with load

- Disabled gait pattern

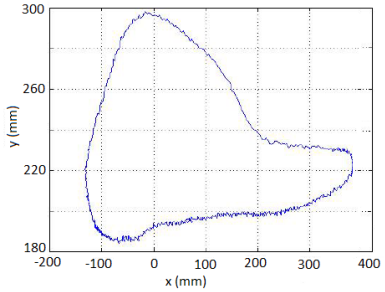

Figure 4.35: Ankle displacement (in mm) on a unknown disability

Focusing now on the feet and toes (tip of feet), by looking at figure 4.36 we can learn how both feet change position alternately over time when walking, is visible the change from standing still to the beginning of walking.

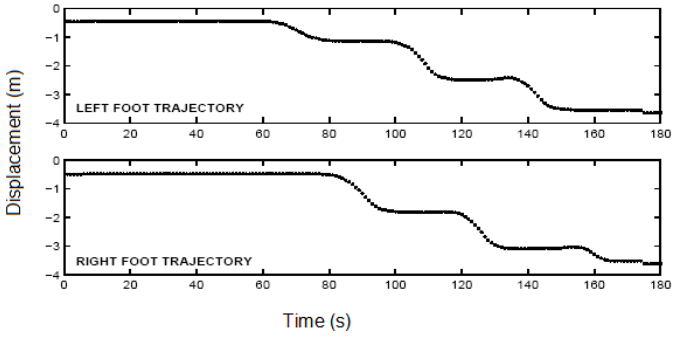

Figure 4.36: Feet coordinate displacement in the direction of motion

The above figure gives a good general idea of the coordinative effort needed.

Figure 4.37 shows the evolution of the toes' velocity and vertical displacement over the gait cycle.

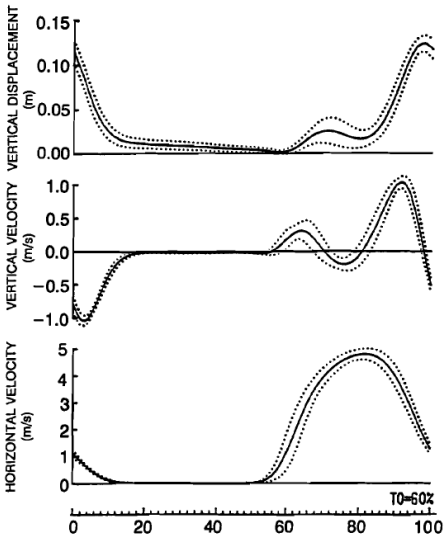

Figure 4.37: Toe vertical displacement (in m) and velocity (in m/s) (taken from [5])

- Upper Body

The upper body can harm or help stability, thus a complete model should also consider its motion.

This is illustrated in figure 4.38.

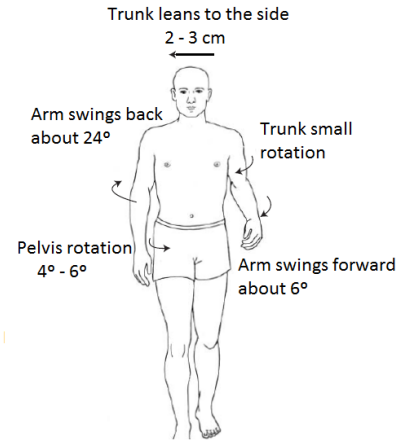

Figure 4.38: Trunk motion when walking

4.3 Climbing Stairs

The gait cycle of stairs climbing is quite different from the walking one.

Modeling it is important when trying to obtain a robust and complete system.

The figure below shows an able-body person's standard gait cycle for stair climbing.

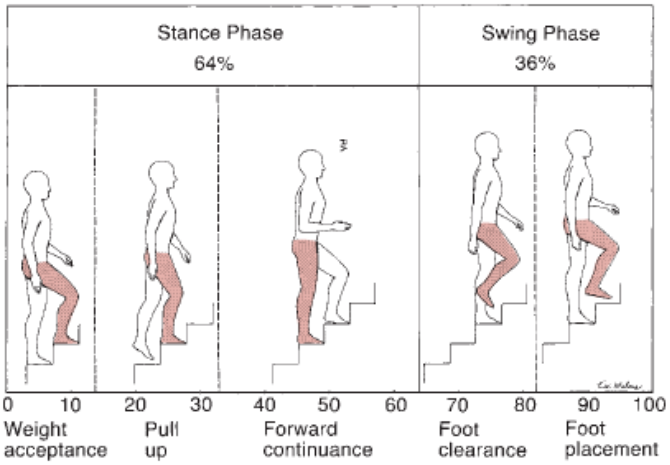

Figure 4.39: Stairs climbing gait cycle

Throughout this chapter we had the chance to gather all the information necessary to make the developed model closer to human reality.

Chapter 5

Problem Statement and Approach

5.1 Problem Statement

From the literature review and market research (see chapters 2 and 3), multiple challenges were identified and became clear the necessity to develop a system to provide stability during walking. It is directed to people with deformation of the walking pattern, absence of limb motion or with balance issues.

The way to do it is develop a set of preliminary studies, which are essencial to develop an architecture that could later be articullated with/ help improve the existing products.

Human locomotion has been studied to allow the existence of human-like/bio-inspired robots and developments have been done to apply in robots, but the truth is only a very small part the control methods developed are used in benefit of people.

Please note that the complexity of such system does not allow it to be completed in the 5 months' time that correspond to this dissertation work. Nevertheless, the goals are mentioned to give a full perspective of the project.

The control system must fulfill the requirements in the table shown below.

In the Degree of Subsidiarity column, "1" represents the highest level of priority and N/A stands for non-applicable.

Table 5.1: Locomotion control system requirements

Number	**Requirement**	**Degree of Subsidiarity**
1	respect the boundary conditions of position, velocity and acceleration imposed by leg coordenation and human body limits	1
2	guarantee stability during every stage of locomotion in standard conditions	2
3	guarantee stability despite changes due to object transportation and shoes	2
4	be robust to external perturbations	3
5	track and correct limb trajectory	4
6	allow motion at the usual human velocity	5
7	minimize energy cost	6
8	act in real-time	N/A
9	minimize equipment volume	N/A
10	minimize equipment cost	N/A

In spite of the limited scope of the analysis of the required motion performance presented in this dissertation which was based in a few key literature references, [48][49][9], it is clear that the following requirements have to be considered:

1 Articulation of long time (say, as defined by the scope of the available a priori or sensed data, which might well be infinite) and short time horizon 'optimal' control strategies in spite of the, possibly conflicting, goals to be considered in the different time horizons.

2 System's integrity. The control system should be designed in such a way that all the constraints to be satisfied by the various subsystems are satisfied. These constraints arise from the external environment due to a priori known features but also due to perturbations and to the, usually unexpected, associated variability. This may lead to control references that need to be adjusted "on-the-fly".

3 Scalability in time and space. Scalability is required not only to deal with complexity and the heterogeneity of subsystems with very diverse process dynamics to be considered, and multiple goals to be targeted and performance criteria to be optimized, but also with the fact that these might be relevant over different time scales. Modularity is an important feature enabling this requirement to be fulfilled. As it has been recognized in the some of the surveyed literature, for example [30], a multi-stage structure is required to coordinate the various modules in order to ensure local strategies contributing to common goals.

4 Coordinated decentralization of the decision and control system. This requirement emerges from the need to take into account local specific issues to be addressed by exploiting local degrees of freedom, at a given time scale with shared constraints that arise from the other subsystems and the environment. It should enable the organization of the system in a discrete set of 'independent' nodes, each one acting with partial information but also coordinating indicators to enable automatic adaptation of control references.

5 Adaptivity to take into account trends associated with environment changes, such as ground morphology and physical properties, and weather conditions. By incorporating the most update perception provided by the user or the overall system sensors, the optimization underlying the control synthesis will yield results better adjusted to the user expectations.

6 Robustness of the solution with respect to modeling uncertainties and perturbations. Data gathering, sensing and computational limitations as well as human factors entail the omnipresence of modeling uncertainties and perturbations. This requirement is fulfilled by appropriate feedback control systems designed at subsystem level as well as appropriate choices of targets and performance criteria.

5.2 Approach

To succeed, and after analyzing the functionalities needed, the following concept of the system was developed: a high level controller would collect information from the high level sensors like vision and low level sensors like gyroscopes, accelerometers and force sensors, identify the current environment and perform the corresponding control action. The supervisor controller is also responsible for deciding to change the reference or the boundary conditions when needed.

Such a control architecture involves the following layers:

- **Planning layer**: It considers more global issues and takes information from the overall 'system' via the coordination layer and from pertinent external sources in order to generate "long-term" planning targets that are sent in to the coordination layer. The planning horizon is not necessarily predetermined and the planning layer will be run whenever significant inconsistencies are detected in the current plan as a result of the scrutiny of the execution provided by the coordination layer as well as significant evolution of pertinent externally generated knowledge. The data at the disposal in the planning layer also enables the update of global models that might be required to preserve meaningful planning targets in the light of prevailing pertinent data and the execution performance of the various subsystems.

- **Coordination layer**: It receives the planning targets from the planning layer and generates shorter term targets for each one of the subsystems being coordinated. It also receives status data from each one of these subsystems, integrates and provides feedback data to the planning layer. Moreover, the coordination layer may play a role in a decentralized

generation of "consensus" among the various subsystems inasmuch as the planning targets are not at stake. Notice that these operations may involve optimization procedures.

- **Subsystem layer or execution layer**: In each one of these subsystems, a resources optimization (possibly optimal control) sectorial problem is solved by taking into account the local performance functional, dynamics and constraints as well as the indicators provided by the coordination layer in the form of shared constraints with other subsystems, and, possibly with interaction with some neighboring subsystems. The shifting of coordinating targets might require either operational or structural changes at the subsystem which will have to be taken into account by the corresponding model update.

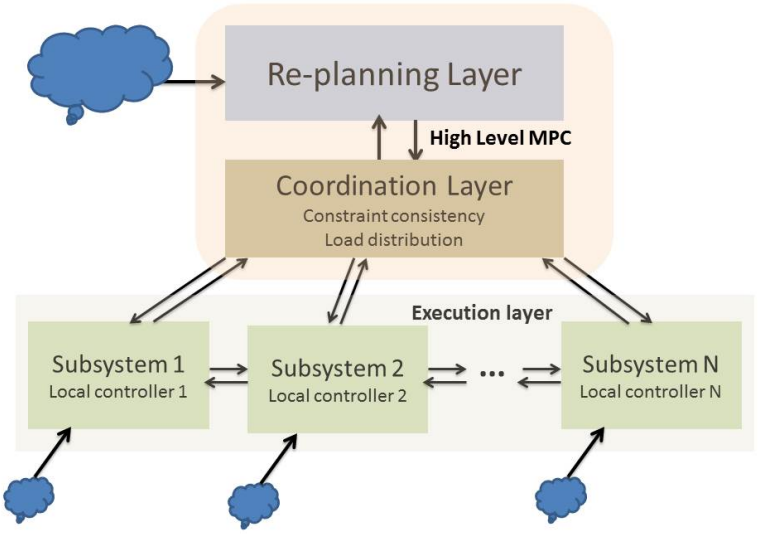

Figure 5.1: Layered Control Architecture

The clouds represent external information about the environment or the system status coming from the sensors.

This modular organization into subsystems allows to accommodate the spatial heterogeneity as well as the evolution over time that follows from the evolution of the environment as well as the evolution of the overall "health" of the system, notably, available power, uneven actuators load distribution. This ensures that adaptivity is built in the process of decision-making and control strategies generation at the various levels, as well as the scalability requirement. With respect to this point, we note that the operation of composition can be defined in the sense that this layered structure can be regarded a single block embodying a certain subsystem in a wider structure with the same architecture. The coordination layer ensures the articulation of short term goals at subsystem level with long term goals addressed by the planning level. Remark that the optimization problem solved at this level takes into account the physical feasibility constraints at the subsystem level via the coordination layer. Since each subsystem generates control strategies by solving an

optimization problem with “local” data, besides the indicator targets provided by the coordination layer reveals that, in general, decision-making is decentralized. Finally, the built in consensus generation capability and the adopted optimization procedures at the various levels of the proposed decision-making architecture entails the robustness requirements.

The particularization of the architecture should express the two different concepts behind the system: on one side is a machine capable of moving completely autonomously with a particular gait described by input parameters; another option is having a human able to generate motion (not necessarily always a desirable one) and the system would only bring the input missing to archive motion harmony. This last option would convert the dashed connection in a thick connect. The human would be seen by the system as an input perturbation, once there is no guarantee that the human motion would perform a positive action in the expected moment.

Such control architecture is illustrated below

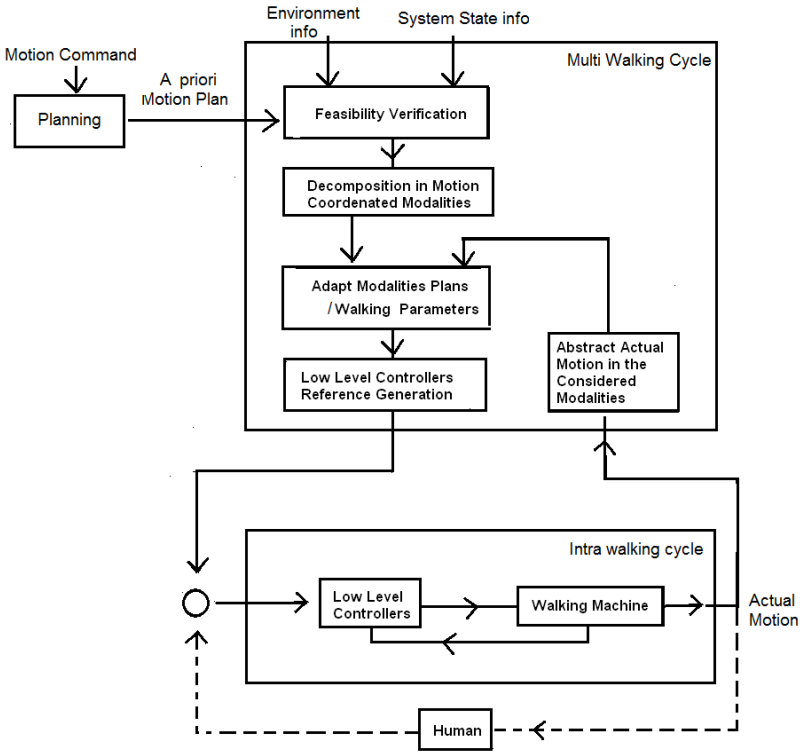

Figure 5.2: System Architecture

The purpose of the blocks in the figure:

block "Planning"

A human motion plan is quite abstract when it comes to consciousness. The goal is often related with reaching a final location and arrive there after a period of time, which

is established qualitatively. It can also concern the choice of the geographic path based on observation of the environment.

The abstraction has to be brought to a more concrete level (task done by the brain), translating it into a set of quantitative parameters as:

- Average speed of motion;
- Cadence;
- Walking distance;
- Walking time;
- Number of steps;
- Length and width of step;
- Swing foot maximum height; amd
- Waist oscillation.

Obviously, not all of them need to be specified, since there is a minimum set that allows the inference of the other. Although all combinations form a valid set. For example, {step width, number of steps and total time of motion} or {velocity of motion, cadence of motion and walk distance} are valid input sets, while {step width, number of steps and walk distance} is not.

The style of locomotion that most properly fits the motion specifications is chosen by the user, and the generated output is the a priori motion plan.

block "Feasibility Verification"

The consistency of the information provided will be checked. Its admissibility regarding the actuators limits and satisfaction of the constraints existing between sub-systems and with the environment is verified. The system state will also be sampled.

block "Decomposition in Motion Coordinated Modalities"

Each joint is viewed as an independent modality that can be classified as fundamental or secondary. A fundamental modality has its reference imposed by the stronger constraints that have been verified by the previous block. A secondary modality will be determined by taking into account the value of the fundamental modalities and the constraints that have not been met yet.

Given the difference of influence a modality has according to the role its sub-system is playing (stance leg or swing leg), the fundamental modalities have been selected differently for the stance and swing legs. So, for the stance leg, we have

- *fundamental modalities:* toe, ankle and knee; and
- *secondary modalities:* hip.

and for the swing leg,

- *fundamental modalities:* hip and knee; and
- *secondary modalities:* ankle and toe.

block "Adapt Modalities Plans / walking parameters"

If the information collected from the sensors indicates that the system safety is in danger or the energy consumption is too large, the supervisor can change the plan previously made for a modality or group of modalities, either fundamental or secondary. The priority will be to do the change that presents less energy consumption.

There is also the possibility of changing the walking parameters in case of impossibility to obey them due to the constraints.

The low level layer would have a structure similar to the one in figure 5.3

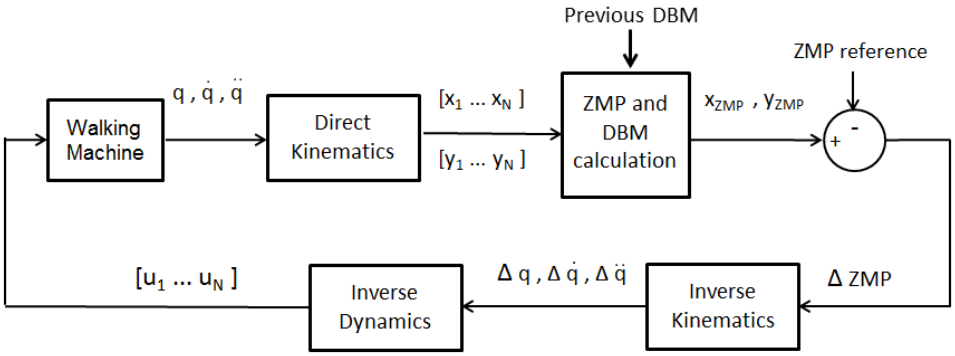

Figure 5.3: Low level layer

The low level controllers would receive the proper reference parameters, compute the error and send a signal to the actuators, which would be placed mostly in the ankle and knee. Its goal is to reject local perturbations. They could make use of different control techniques: sliding mode, backstepping or the simple PID.

Optimal Control Theory has a rich arsenal of tools to address the multiple challenges outlined above. Besides the wide range of paradigms, which include continuum time, discrete event and hybrid systems, the formulation of the optimal control problem is very general and flexible. It encompasses a wide classes of performance functionals, controlled dynamics (ordinary and partial differential equations, among others), state constraints (to be satisfied at given points in time and over time subsets), control spaces (from measurable functions to measures) and constraints, mixed state and control constraints, and isoperimetric constraints, among others. On the other hand for the most significant formulations there is a sophisticated body of results that have been proved under very weak assumptions on the data of the problem, thus ensuring, their applicability to a

wide range of applications. Focussing on the characterization and synthesis of control strategies, we single out:

- Maximum Principle of Pontryagin, [53, 54, 55, 56, 57], which yields an open loop control strategy by maximizing the so-called Pontryagin function. This involves, an adjoint function which have the useful interpretation of propagating back in time the gradient of the cost functional at the optimum, and can be regarded as the gradient of the Value Function (the optimum cost to go) along the optimal trajectory almost everywhere with respect to time.

- Dynamic programming, [54], which provides both a technique for verification of optimality, as well as, a means for the synthesis of the optimal control strategy in a state feedback form.

Any one of these classes of optimal control results can be used to provide the control synthesis required in blocks of the above described structure

This led to the selection of a Model Predictive Control scheme to the, whose optimal control foundations are outlined next.

An MPC requires the specification of two slider horizons - one input (or control) horizon and one output (or prediction) horizon - and tries to predict the future evolution of the system (over the output horizon) to optimize the control signal. This means it solves an optimal problem for N future iterations at time t and repeats the optimization at time t + 1 (the next iteration) based on the new sensors' measurements.

In figures 5.4 and 5.5 show the concept of operation and the block diagram.

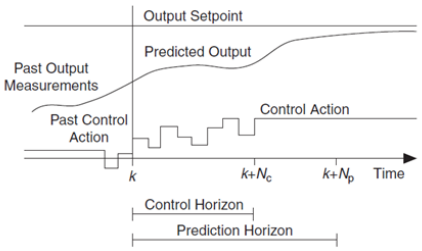

Figure 5.4: MPC

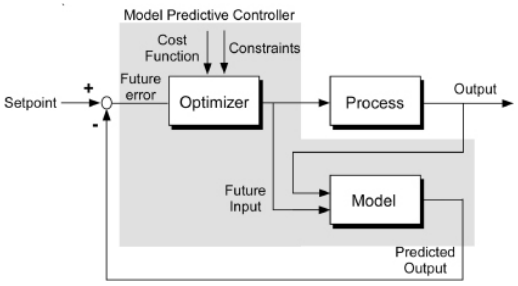

Figure 5.5: MPC block Diagram

The control horizon N_u is typically 10 times smaller than the output horizon N,[58], which, despite causing loss of performance, decreases computation time and allows the feasibility to be kept.

The high level MPC will generate a number of indicators that will translate into targets or constraints to be satisfied or approximated by the control problems of the Local Subsystems at the low level for a given finite time horizon. Remark that the specification of changes in models, functionals and targets - for example the desired long term equilibrium for the high level - can be incorporated in optimization processes at both levels of the structure as a result of the evolution of knowledge and of the effectiveness of the deployed control strategies. These changes in the formulation of the optimization problems can be either event-driven in the case of disruptive developments, or the result of a periodic review, being the rate at which these changes take place such that the overall stability of the scheme is maintained, and promote the adaptivity requirement of the overall system. On the other hand, the feedback nature of the MPC scheme will endow the overall system with robustness to perturbations.

Essentially, the very basic MPC scheme consists in a recursive procedure in which, once sampled the state of the system at the initial time, say $t = t_i$ and optimal control problem (P_T) is solved in a given optimization horizon $[t_i, T]$, and then applied during a time subinterval $[t_i, t_i + \bar{T}]$ with $\bar{T} \ll T$. At this point, the state of the system is sampled, the whole optimization horizon slides of $\bar{T}$ time units, and the whole process is repeated. Thus, this MPC scheme is as follows:

(1) Initialization. Let $t = t_i$, and consider the state of the system $x(t_i)$.

(2) Solve the optimal control problem (P_T) over $[t_i, t_i + T]$ to obtain an optimal reference trajectory x^* in this time interval.

(3) Compute and apply an optimal feedback control u^* during $[t_i, t_i + \bar{T}]$ to track x^* restricted to this time interval.

(4) Sample the state variable x at $t_i + \bar{T}$ to obtain $\bar{x} = x(t_i + \bar{T})$.

(5) Slide the time origin by $\bar{T}$ time units, let $x(t_i) = \bar{x}$, and go to step (2).

Remark, that even if the solution to the optimal control problem is open loop, the periodic sampling of the state variable together with the computation of the associated solution to (P_T), ensures the closure of the control loop to the required extent. If sampling at step (4) reveals no significant deviations of the sampled state $\bar{x}$ from the expected optimal value $x^*(t_0 + \Delta)$, then step (2) can be skipped. Other variations of the scheme may include the possibility of using the sampled data to upgrade the estimate of the model dynamics, changing time horizons as a function of the scope of the data provided by the system sensors. this information can be used to change "on the fly" constraint functionals and sets, and performance functionals. All these elements might be required to specify the optimal control problem (P_T), whose simplest formulation can be stated as follows:

$$
\begin{aligned}
(P_T)\ \text{Minimize} \quad & g(x(T)) + \int_{t_0}^{t_0+T} l(s,x(s),u(s))ds \\
\text{subject to} \quad & \dot{x} = f(t,x,u),\ \text{a.e.} \\
& x(t) \in X_t, \\
& u \in \mathcal{U} \text{ and } x(t_0) \text{ is given},
\end{aligned}
$$

where $f : [t_0, t_0+T] \times R^n \times R^m \to R^n$ defines the controlled dynamics of the system, $g : R^n \times R^n \to R$ is the endpoint cost functional, $l : [t_0, t_0+T] \times R^n \times R^m \to R$ is the running cost function, and $X_t \subset R^n$, and $U_t \subset R^m$ are, respectively, the pointwise state and control constraints. Optimality conditions are currently available for this problem under substantially weak assumptions on its data.

For further details on the MPC scheme, we point out [59, 60, 61, 62] and the references therein.

Since one key objective of the proposed resources optimization framework is to reconcile long term goals with short term goals, the MPC scheme proposed to the high level of the control structure should generate strategies that asymptotically approximate the solution to an "T_∞-horizon" optimal control problem that drives the system to the desirable equilibrium, that is, that solves a problem of the type

$$
\begin{aligned}
\text{Minimize} \quad & g_\infty(\xi) + \int_{t_i}^{T_\infty} l(t,x(t),u(t))dt \\
\text{subject to} \quad & \dot{x} = f(t,x,u)\ \text{ a.e.} \\
& \xi \in C_\infty,\ \lim_{t \to T_\infty} x(t) = \xi \\
& u \in \mathcal{U}.
\end{aligned}
$$

The function $g_\infty(\cdot)$ is the term in the performance functional that forces the system to be driven to the desired long term equilibrium. In order for the MPC scheme to yield solutions approximating the ones of the infinite horizon optimal control problem, the associated optimization problem (P_T) is defined as follows:

$$
\begin{aligned}
(P_T)\ \text{Minimize} \quad & V(t_0+T, x(t_0+T)) + \int_{t_0}^{t_0+T} l(s,x(s),u(s))ds \\
\text{subject to} \quad & \dot{x} = f(t,x,u),\ u \in \mathcal{U},\ x(t_0) \text{ given},
\end{aligned}
$$

where the function $V(\cdot,\cdot)$ is a value function defined by

$$
V(\tau,z) := \min_{u \in \mathcal{U}, \xi \in C_\infty} \left\{ g(\xi) + \int_\tau^{T_\infty} l(t,x(t),u(t))dt : \dot{x} = f(t,x,u),\ x(\tau) = z,\ x(t) \to \xi \right\}.
$$

Under appropriate assumptions, the value function can be obtained by solving an Hamilton-Jacobi partial differential equation

$$\begin{cases} \dfrac{\partial}{\partial t}V(t,x)+\min\limits_{u\in\Omega}\langle\dfrac{\partial}{\partial x}V(t,x),f(t,x,u)\rangle=0 \\ V(T,x(T))=g(x(T)). \end{cases}$$

For a good reference see [54]. In general, a solution to this partial differential equations in the conventional sense fails to exist, and the type of solution and the notion of derivative that have to be considered may depend on the ingredients of the problem. Moreover, the huge difficulties arising in the computational tractability in solving this equation are well known (for computational approaches and tools, see [63] and references therein). This constitutes a huge challenge in the current state-of-the-art in Optimal Control Theory.

In order to investigate an alternative approach to this problem, necessary conditions of optimality for a class of infinite horizon optimal control problems appears to be particularly well suited for the applications considered here, [64]. Consider the problem

$$\begin{array}{lll} (P_c)\ \text{Minimize} & h(x(0),\xi) & \\ \text{such that} & \dot{x}(t)=f(t,x(t),u(t)) & \mathcal{L}-a.e.\ [0,\infty) \\ & x(0)\in C_0,\ x(t)\to\xi\in C_\infty \text{ as } t\to\infty & \\ & u(t)\in\Omega\subset R^m,\ \forall t\in[0,\infty), & \end{array}$$

where C_0 and C_∞ are compact sets and the remaining ingredients are as above. In spite of the significant body of literature on this class of problems (see [65, 64] and references therein), the degenerative effect of very long time horizons still constitutes a huge challenge. The goal consists in deriving a maximum principle exhibiting boundary conditions at the final endpoint with maximal information. This should enable the appropriate propagation of a suitable Value Function from the final time to the current time. For this purpose, we consider $\xi\in R^n$ to be an equilibrium point as $t\to\infty$, i.e., there exists a feasible control process $(x(\cdot),u(\cdot))$ such that $\lim\limits_{t\to\infty}x(t)=\xi$, and $0\in\lim\limits_{t\to\infty}intf(t,x(t),\Omega(t))$, and, introduced the notion of directional inclusion at infinity.

Let $y(t)\in R^n$, $y(t)\neq 0$ a.e. in $[0,\infty)$ and $K\subset R^n$ be a pointed cone.We say that $y\in K$ directionally at infinity, i.e., $y\in_\infty^d K$, if $\hat{Y}\subset K_1$ where $K_1=\text{conehull}(K)\cap B_1(0)$ and

$$\hat{Y}=\left\{\hat{y}\in R^n:\exists t_i\to\infty,\ \lim_{i\to\infty}\frac{y(t_i)}{\|y(t_i)\|}=\hat{y}\right\}.$$

Below, we will denote by $y\in_\infty K$ either $y\in K$ or $y\in_\infty^d K$.

Then, the necessary conditions of optimality in the form of a maximum principle derived in [64] can be stated as follows:

Let the control process (x^*,u^*) be a solution to (P_c). Then, there exists a multiplier $(\lambda,p)\in$

$[0,\infty) \times AC([0,\infty), R^n)$ satisfying, $\lambda + \|p(\cdot)\| > 0$ (non-triviality)

$$\begin{aligned} -\dot{p}^T(t) &\in p^T(t)\partial_x f(t, x^*(t), u^*(t)), \quad \mathcal{L}-a.e. \\ p(0) &\in \lambda \partial_1 g(x^*(0), \xi^*) + N_{C_0}(x^*(0)) \\ -p &\in_\infty \lambda \partial_2 g(x^*(0), \xi^*) + N_{C_\infty}(\xi^*). \\ u^*(t) &\text{ maximizes } v \to p^T(t) f(t, x^*(t), v) \ \mathcal{L}-a.e. \text{ in } \Omega. \end{aligned}$$

Between the locomotion analysis done in the previous chapter and the implementation for the control system, a model needs the be developed and the resulting mathematical system properties have to be studied.

Chapter 6

Fundamental Theoretical Concepts

Although humanoid robot modeling uses concepts from the robotic manipulators, such as the DH convention (detailed in section 7.2.1 in chapter 7), some intrinsic characteristics of the legged locomotion systems make them require a different modeling approach and different analysis tools.

Apart from the need of carrying their own power and actuation subsystems, the two most relevant characteristics are the existence of impacts and periodic motion. This places us in the context of hybrid systems and limit cycle convergence/stability analysis.

6.1 Hybrid Systems

A hybrid system displays the evolution in time of both continuous and discrete variables. According to Lygeros ([66]), it is composed of

- a set of discrete states Q,
- a set of continuous states $X = R^n$,
- a vector field f : Q x X $\rightarrow R^n$,
- a set of initial states Init $\subseteq$ Q x X ,
- a domain D : Q $\rightarrow PS(X)$,
- a set of edges E $\subseteq$ Q x Q,
- a guard condition G :$E \rightarrow PS(X)$,
- a reset map R : E x X $\rightarrow PS(X)$

forming the tuple $H = (Q, X, f, Init, D, E, G, R)$. Notice that PS(X) stands for the power set of X (set of all subsets) and a set of control inputs U might be included.

Similarly to a finite state machine (or a generic directed graph) when the continuous variable x reaches the guard of some edge, the discrete variable may change (not mandatory), in which case, x is reset to the new value foreseen in the reset map and the system evolves to the next discrete state. Figure 6.1 illustrates a deterministic automaton.

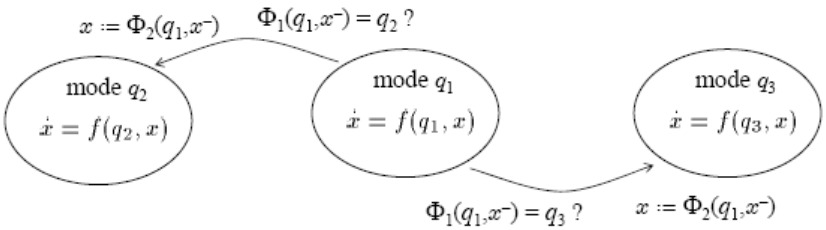

Figure 6.1: Hybrid deterministic automaton - taken from [6]

In the notation visible in the figure, Φ_1 corresponds to G presented above and Φ_2 to R and together form the transition map.

Modeling hybrid systems is "especially challenging", [66], due to problems in simulation when the existence and uniqueness of solution are not guaranteed. Dead-locks (permanent absence of conditions that would allow the system to change state) are a common and undesired situation and at the opposite end is the Zeno phenomenon - an infinite number of discrete transitions occuring in finite time. There is an identical phenomenon called chattering, which differs by not converging.

The case of non-uniqueness of solution, although allows uncertainty modeling, "requires additional care when designing controllers for such systems, or when developing arguments about their performance", [66], since the arguments have to be true for all solutions.

Some concepts already presented, or presented hereafter, are not exclusive of hybrid systems. For example, the existence and uniqueness of solution is also a concern in continuous dynamical systems but it is known that if f is **Lipschitz continuous** then $\dot{x} = f(x)$, $x(0) = x_0$ has a solution and it is unique.

Fundamental to finding the conditions of existence and uniqueness of solution is the concept of **Reachability**. A state is reachable if it is possible to get to in finite time from the current state. All the states reachable from a particular state form the reach sets, which are very important in control because they indicate the motion capability of the dynamical system.

There is also the notion of **backward reachability**, which defines the set of all states the system can be in at a time $t < t_0$ that allow the system to get at $t = t_0$ to a state belonging to a target set.

The concept of **attainability** is slightly different because it does not include all the states visited in the past.

Other two important properties are **safety** and **liveness**: while safety describes the ability to maintain in the set a solution that already belongs to it, liveness refers to the aptitude to bring into the set a solution that did not belong to it. Stability is naturally a safety property.

6.2 Limit Cycle

Focusing now on the periodic motion that characterizes legged locomotion, limit cycle and related concepts will be clarified.

A limit cycle is an asymptotically stable or unstable periodic orbit with no other periodic orbits nearby.

An orbit x is considered of period T if $\exists\, T > 0 : x(t+T) = x(t)\ \forall\, t$ and $x(t+n) \neq x(t)$ for any $n \neq kT$, k being a positive integer.

Poincaré-Bendixson Theorem, claims that if a closed region of phase space which does not contain any fixed points can be defined, then it must contain a closed-orbit" and since gradient potential fields - a category in which Lyapunov functions are included - can not have a closed-orbit, it is impossible to use unmodified Lyapunov analysis to examine limit cycle stability.

A way to study limit cycle stability is using **Poincaré map** (or return map). This method transforms the study of continuous-time stability of a limit cycle into the study of discrete-time fixed-point stability by defining a surface of section S of dimension n-1. This section can not be defined parallel to the trajectories. To obtain the discrete-time system, the continuous-time dynamics is sampled whenever S is crossed with the instant of the n^{th} crossing being $t_c[n]$, so $\dot{x} = f(x)$ becomes $x_p[n] = x(t_c[n])$. The Poincaré map is a mapping from S to itself defined by $x_p[n+1] = P(x_p[n])$.

P is hard to obtain analytically ([7]), but can be analyzed numerically. Once the map is obtained, eigenvalues can be inspected to infer stability. A limit cycle will always have an eigenvalue of magnitude 1, corresponding to the direction of perturbation which allows the system to flow along the orbit and all the others should have a magnitude smaller than the unity.

6.3 Nonlinear Control

A second order system, as the ones we will be dealing with can be written in the generic form

$$\ddot{q} = f(\dot{q}, q, u) \tag{6.1}$$

Note that time can be included as a parameter when dealing with a non-autonomous system.

A second order system, in its turn, can be viewed as a first order system of dimension two

$$\begin{aligned} \dot{x}_1 &= x_2 \\ \dot{x}_2 &= f(x_1, x_2, u) \end{aligned} \tag{6.2}$$

One useful tool to analyze a nonlinear system is the **phase portrait**. A phase portrait is a vector field plot of x_1 over x_2. It allows us to infer the behavior in the entire state-space for different initial conditions based on the behavior in the neighborhood of the equilibrium points. Therefore, it can also be used to analyze the effect of the designed controller. One of its properties is that the field lines cannot cross outside the equilibrium points and two adjacent field lines cannot flow in opposite directions.

6.3.1 Lyapunov Stability

Lyapunov theory regards the stability of equilibrium point instead of the stability of periodic orbits (Limit Cycle analysis). It is possible for a system trajectory to correspond only to a single point. Such a point is called an equilibrium point.

Definition of Equilibrium point: A state x_0 is an equilibrium state (or equilibrium point) of the system if once x(t) = x_0 and in the absence of disturbances, it remains equal to x_0 for all future time. It is called isolated if it is possible to define a region in its neighborhood that does not contain other equilibrium points.

Keep in mind, that if the equilibrium under study is not the origin, one can always introduce a coordinate transformation on R^n in such a way that the equilibrium of interest becomes the new origin.

The *Indirect Method of Lyapunov* uses the linearization to determine the local stability of the original system. The notion of *basis of attraction* enlightens how far from the equilibrium point can we be that the system will still move towards it.

Definition of stability of an equilibrium point: The equilibrium point $x_0 = 0$ is classified in the sense of Lyapunov as:

- stable if for each $\varepsilon > 0$ and each $t_0 \in R$ there exists a $\delta = \delta(\varepsilon, t_0)$ such that

$$\|x_0\| < \delta \Rightarrow \|x(t)\| < \varepsilon \quad \forall t > t_0 \tag{6.3}$$

Figure 6.2 illustrates the statement graphically

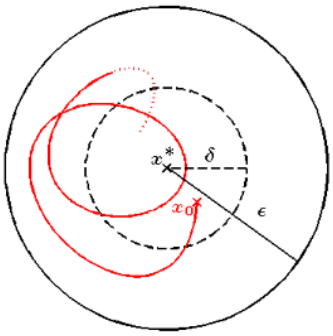

Figure 6.2: Graphical interpretation of Lyapunov stability definition

- unstable otherwise
- uniformly stable if the system is stable for time-varying systems, that is, a trajectory will converge to the equilibrium point at constant rate independentely of the initial time condition t_0

- asymptotically stable if stable and δ can be chosen such that

$$\|x_0\| < \delta \Rightarrow \lim_{t\to\infty} x(t) = 0 \tag{6.4}$$

That means a trajectory that starts near an equilibrium point converges to it. When this happens to a particular trajectory the system is *locally asymptotically stable* and when it holds for all trajectories it is called *globally asymptotically stable*. A non asymptotically stable equilibrium point is denominated marginally stable.

- exponential stable if $\exists\ \alpha, \beta$ in class K such that

$$\|x(t)\| \leq \beta\, e^{-\alpha t}\ \|x_0\| \quad \forall t > 0 \tag{6.5}$$

α is the rate of convergence.

The exponential stability is the strongest notion of stability. Yet, different systems demand the verification of different types of stability.

As you might anticipate, determining the equilibrium point of a system analytically can be hard or sometimes impossible. The *Direct Method of Lyapunov* allows the study of stability without doing it, though an "energy-inspired" function, based on a simple physical knowledge: any system that is dissipating energy will tend to an equilibrium point once its energy is getting closer to zero.

So, any function V(x) that respects the conditions

$$\begin{aligned} &V(0) = 0 \text{ and } V(x) > 0 \forall x \neq 0 \\ &\dot{V}(x) \leq 0 \end{aligned} \tag{6.6}$$

is designated *Lyapunov function*. Notice that $\dot{V}(x) = \frac{dV}{dx} f(x)$ is the derivate of V along the trajectory.

The Lyapunov's Theorem relates the the behaviour of V(x) and $\dot{V}(x)$ with the previous definitions of stability. It is described in table

Table 6.1: Lyapunov Theorem - stability of an equilibrium point

V(x)	$-\dot{V}(x)$	**stability**
locally positive definite	locally ≥ 0	stable
locally positive definite and decrescent	locally ≥ 0	Uniformly stable
locally positive definite and decrescent	locally positive definite	Uniformly asymptotically stable
positive definite and decrescent	positive definite	Globally uniformly asymptotically stable

The conditions of Lyapunov's Theorem are only sufficient, that is, if a particular Lyapunov function candidate to could not satisfy the conditions for stability does not mean that the equilibrium point is not stable. More than that, if we know (by physical intuition or other method) that a equilibrium point is stable then the *Converse Theorem* assures the existence of a Lyapunov function.

It is also possible to prove asymptotically stability when $-\dot{V}(x)$ is not locally positive definite, using *Lasalle's Invariance Principle*. However, it only applies to autonomous or periodic systems.[67]

6.3.2 Key Nonlinear Control Design Techniques

These are Lyapunov-based design techniques.

- Sliding Mode

Sliding Mode Control is a robust control scheme based on the concept of changing the structure of the controller in response to the changing state of the system. Thus, the control action is a discontinuous function of the system state.

The major advantage of sliding mode is low sensitivity to plant parameter variations and disturbances.

So, having a n^{th} order nonlinear system

$$\dot{x}^{(n)} = f(x) + g(x)\,u \tag{6.7}$$

with x being $[x\ \dot{x}\ ...\ x^{(n-1)}]^T$, the control action has two phases:

1. **reaching phase:** a trajectory x is driven to a desired trajectory or set point x_d, assuming that it is achievable in finite time with a finite control input
2. **sliding phase:** once x_d is reached x is maintained there $\forall\, t$

where x_d is a vector similar to x.

If we define a time-varying surface S(t) and map it in the state space by the scalar equation s(x,t) = 0, that is $S(t) = \{x \in R^n : s(x;t) = 0\}$, with

$$s(x,t) = \left(\frac{\mathrm{d}}{\mathrm{d}t} + \lambda\right)^{n-1} e \tag{6.8}$$

where $e = x - x_d$ is the tracking error and λ is a positive constant, then the problem of tracking the n-dimensional vector x_d is reduced to a problem of keeping the scalar quantity $s(x,t) = 0$.

For a second order system, s(x,t) is

$$s(x,t) = \dot{e} + \lambda e \tag{6.9}$$

It can be seen that s(x,t) is a weighted sum of the position error and the velocity error.

The dynamics

$$\dot{s}(x,t) = \ddot{e} + \lambda \dot{e} \tag{6.10}$$

which relates with the input by

$$\dot{s}(x,t) = f(x) + g(x)\,u - \dot{x}_d + \lambda \dot{e} \tag{6.11}$$

In the reaching phase, the control law must fulfill the sliding condition

$$\frac{1}{2}\frac{d}{dt}s^2 \leq -\alpha\,|s| \tag{6.12}$$

so that s becomes an invariant set, since the condition guarantees that s^2 (an index of proximity to the manifold) decreases along all system trajectories, converging to the desired state and being impossible to exit it afterwards. Furthermore, the surface will be reached in a finite time shorter than $\frac{|s(t=0)|}{\alpha}$, $\alpha > 0$.

Once it happens, the system enters in the sliding phase, where s = 0 and therefore the solution of equation 6.9 is an exponential function with time constant $\frac{1}{\lambda}$ (or generically $\frac{n-1}{\lambda}$).

The delay of actuation that is unavoidable in physical systems will prevents the swiching of control law to happen in the exact moment s reaches zero and forces to set aside a step switching control law, such as

$$u = -\beta(x)\ sign(s) \tag{6.13}$$

and brings the need to introduce a boundary layer around s to eliminate the unwanted high frequency switching known as chatering, which may force too much control effort or even excite unmodeled dynamics that contain unknown resonant frequencies causing instability in the system.

So, defining a boundary layer, whose thickness ε should be as small as posible to minimize the error but big enough to avoid chattering, we can replace the sign function for a smother sigmoid function such as *sat* or *tanh*, making

$$u = -\beta(x)\ sat\left(\frac{s}{\varepsilon}\right) \tag{6.14}$$

Be aware of the differences between the sign(s), $sat\left(\frac{s}{\varepsilon}\right)$ and $tanh\left(\frac{s}{\varepsilon}\right)$

$$sign(s) = \begin{cases} 1 & \text{if } s > 0 \\ -1 & \text{if } s < 0 \end{cases} \quad sat\left(\frac{s}{\varepsilon}\right) = \begin{cases} -1 & \text{if } s \leq -\varepsilon \\ s/\varepsilon & \text{if } |s| < \varepsilon \\ 1 & \text{if } \varepsilon \leq s \end{cases} \quad tanh\left(\frac{s}{\varepsilon}\right) = \begin{cases} -1 & \text{if } s \leq -\varepsilon \\ \frac{1-e^{-2\,s/\varepsilon}}{1+e^{-2\,s/\varepsilon}} & \text{if } |s| < \varepsilon \\ 1 & \text{if } \varepsilon \leq s \end{cases}$$

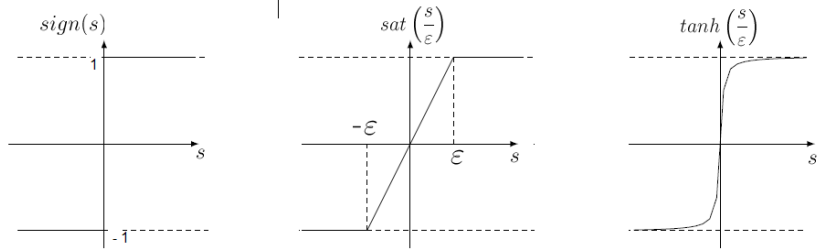

Figure 6.3: Usual sigmoid functions in Sliding Mode

When a stabilizable system is affected by uncertainty $\Delta(x,t)$, which only a bound $\rho(x) \geq |\Delta(x,t)|$ is known, as in

$$\dot{x} = f(x) + g(x)\,u + \Delta(x,t) \tag{6.15}$$

the success of Sliding Mode Control method depends on having a uncertainty that satisfies the **matching condition**

$$\Delta(x,t) = g(x)\,\tilde{\Delta}(x,t) \tag{6.16}$$

where $\tilde{\Delta}$ is an uncertain function that does not depend of f, since it is the only way (6.15) can be written as

$$\dot{x} = f(x) + g(x)\,\left(u + \tilde{\Delta}(x,t)\right) \tag{6.17}$$

and thus the input u can directly oppose (ideally cancel) the uncertainty.

- Backstepping

Backstepping is a systematic design procedure for dealing with uncertain nonlinear systems allowing the relaxation of the matching condition assumption.

It works by applying successive transformations to each variable and differentiating each fictitious control, until the actual control input u is reached.

This systematic procedure can be more easily understood with an example (taken from [67]) without loss of generality. Therefore consider the system

$$\dot{x}_1 = x_1 + x_2 \tag{6.18}$$

$$x_2 = u \tag{6.19}$$

The first step is to see the dynamical system as a set of separate sub-systems and treat them separately including the stabilization of its own variable. So, focusing in (6.18) and thinking of x_1 as the state variable that will be stabilized and x_2 as a virtual control input v we get

$$\dot{x}_1 = x_1 + v \tag{6.20}$$

Now we need to select candidate Lyapunov function such that x is stable. Trying

$$V_1(x) = \frac{1}{2}x_1^2 \tag{6.21}$$

which has derivative

$$\dot{V}_1(x) = x_1\dot{x}_1 = x_1^2 + x_1 v \tag{6.22}$$

So, if choose v properly, for example

$$v = -2x_1 \tag{6.23}$$

Turns (6.22) into

$$\dot{V}_1(x) = -x_1 \tag{6.24}$$

we can easily conclude that the conditions in (6.6) are respected and once $\dot{V}_1 < 0 \,\forall x \neq 0$ then x_1 goes asymptotically to the origin with the virtual input picked.

The second step is to garantee that x_2 tracks v, because we assumed in the beginning that $x_2 = v$ but their inital conditions may be different. We can define and regulate the following output

$$z = x_2 - v \Leftrightarrow z = x_2 + 2x_1 \tag{6.25}$$

Using the previous equation to replace x_2 in (6.18) we get

$$\dot{x}_1 = -x_1 + z \tag{6.26}$$

Differentiating z and replacing $\dot{x}_1$ and x_2(remember that $x_2 = v = -2x_1$) comes

$$\dot{z} = u + 2(x_1 + x_2) \Leftrightarrow \dot{z} = u - 2z + 2x_1 \tag{6.27}$$

For this sub-system we could choose a candidate Lyapunov Function V_2 identical to V_1 and as the resulting Lyapunov function is the sum of all the "sub-Lyapunov" functions [**?**, **?**] we are

capable of writing the total Lyapunov Function

$$V(x,z) = V_1(x) + V_2(z) \Leftrightarrow V(x,z) = \frac{1}{2}x_1^2 + \frac{1}{2}z^2 \tag{6.28}$$

and

$$\begin{aligned} \dot{V} &= x_1\dot{x}_1 + z\dot{z} \\ &= x_1(-x_1 + z) + z(u + 2z - 2x_1) \\ &= -x_1^2 + z(u + 2z - x_1) \end{aligned} \tag{6.29}$$

Selecting

$$u = -3z + x_1 \tag{6.30}$$

Results

$$\dot{V} = -x_1^2 - z^2 \tag{6.31}$$

As $\dot{V}$ is negative definite, we have asymptotical stability.
The final control law is

$$u = -3(x_2 + 2x_1) + x_1 \Leftrightarrow u = -5x_1 - 3x_2 \tag{6.32}$$

The repeated differentiation of nonlinear functions required and the need to bound the uncertainties in the higher derivatives led to the development of two related methods: Multiple Sliding Surfaces and Dynamic Surface Control.

6.3.3 Zero Dynamics

A nonlinear system

$$\begin{aligned} \dot{x} &= f(x) + g(x)\,u \\ y &= h(x) \end{aligned} \tag{6.33}$$

can, under certain conditions, be expressed as a chain of integrators and an other part which is not observable from the output y called the internal dynamics, [68]. The resulting system is said to be in the normal form

$$\begin{aligned} \dot{\eta} &= f_0(\eta, \xi) \\ \dot{\xi} &= A_c\,\xi + B_C\,\gamma(x)\,[u - \alpha(x)] \\ y &= C_c\,\xi \end{aligned} \tag{6.34}$$

where $[A_c, B_c, C_c]$ are in the canonical form and $\gamma(x) = L_g L_f^{\rho-1} h(x), \alpha(x) = -\frac{L_f^{\rho} h(x)}{\gamma(x)}$

Underlying this representation are the definitions of diffeomorphic transformation, relative degree (ρ) and Lie derivative (L_f and L_g).

The relative degree is determined by the order of the first output derivative that depends on u. The internal dynamics is formed by the $n - \rho$ undetermined DOFs (n being the system's dimension). Its stability is important since it can trigger unexpected and unwanted system behavior. A way to analyze it is to force the output and its derivatives to zero, obtaining

$$\dot{\eta} = f_0(\eta, 0) \tag{6.35}$$

This particular case of internal dynamics is called **Zero Dynamics**.

If the zero dynamics has an asymptotically stable equilibrium point in the domain, the system is a **minimum phase system**, which is very desirable. Otherwise, no matter what control input is applied, the internal dynamics remains unstable.

Controlling a system where $\rho < n$ requires an observer and that the ouput is controlled as a virtual input to stabilize the internal dynamics before driving the output to the desired value.

In linear systems, ρ is simply the difference between the number of poles and zeros and the stability of the internal dynamics is guaranteed if all the zeros are in the left semi-plane.

Chapter 7

Locomotion Modeling and System Properties

An human being develops walking skills in less than two years, even before being able to count to 10. Nevertheless, locomotion is a highly complex nonlinear task, involving a multivariable dynamic, with numerous configurations and unpredicted events.

When an individual has his daily life seriously affected because he is not able to maintain balance on his own, external devices can be employed. But, to do so, biomechanical studies and gait modeling are required.

The central problem in human locomotion modeling is to find a simple, but still complete and realistic model, because overly strong assumptions can rule out important dynamic issues, but doing none leads to a very heavy model, which is bad for real time processing.

7.1 Single Inverted Pendulum Model

The most basic model of locomotion is the planar single inverted pendulum approach and has been used by several authors.

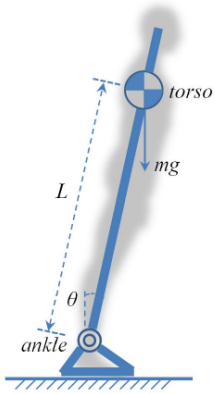

Figure 7.1: Single inverted Pendulum approach

The system respects Newton's Second Law, yielding the general equations below

$$ma = \sum \overrightarrow{F} \tag{7.1}$$

$$I\ddot{\theta} = \sum \overrightarrow{T} \tag{7.2}$$

More specifically, gravitational force is the only external force acting on the pendulum in figure 7.1, and its effect is canceled by the ground reaction force, causing no linear acceleration in both horizontal and vertical directions.

Regarding rotation, equation (7.3) can be written

$$I\ddot{\theta} = mgLsin(\theta) + u \tag{7.3}$$

where u, I and m are the ankle torque, the inertia and mass of the body, respectively. L and θ are as depicted in figure 7.1.

Be aware that

$$I = mL^2 \tag{7.4}$$

In a real situation (close loop), people regulate u to get the desired θ.

7.1.1 Equations for Standing Still

To remain still, right side of conditions (7.1) and (7.2) have to go simultaneously to zero, so u needs to be in the opposite direction of gravitational torque and any existing disturbance and have the same extent.

On level ground, the normative value for θ is zero degrees. Any deviation is expected to be corrected quickly, so the approximation $sin\theta = \theta$ is valid and equation (7.3) can be linearized around its (unstable) equilibrium point and written in the state-space form:

$$\dot{X} = \begin{bmatrix} 0 & 1 \\ \frac{g}{L} & 0 \end{bmatrix} X + \begin{bmatrix} 0 \\ \frac{1}{mL^2} \end{bmatrix} u \tag{7.5}$$

with

$$X = \begin{bmatrix} \theta \\ \dot{\theta} \end{bmatrix} \tag{7.6}$$

7.1.2 Equations for Walking

Each individual imposes a particular rhythm when walking. Considering the single pendulum approach, the walking frequency varies only with the distance L between the ankle and the COM, according to expression (7.7)

$$\omega = \sqrt{\frac{g}{L}} \tag{7.7}$$

- **Restricting to small steps**

The linearization performed above is still valid if the steps are very small (implying θ is not much larger than 5 degrees). Displacement can be found, even when a disturbance force or torque e with random direction is introduced. Considering $\tau = u + e$, rearranging equation (7.2)

$$\tau = mgL\theta - mL^2\ddot{\theta} \tag{7.8}$$

Divide by mg, which symbolizes the z component of the ground reaction force

$$\frac{\tau}{F_z} = L\theta - \frac{L^2}{g}\ddot{\theta} \tag{7.9}$$

Finally, replacing Lθ by the horizontal displacement, it is possible to obtain the ZMP dynamics equation for the sagittal plane

$$x_{zmp} = x_{com} - \frac{L}{g}\ddot{x}_{com} \tag{7.10}$$

A similar equation is valid for frontal plane, just replacing x_{com} by y_{com}

Since, human COM describes in every motion plane approximately a sinusoidal trajectory in a complete gait cycle, departing from the mean value in the double support phase, we can make $x_{com} = Acos\omega t$ and, combining it with equation (7.7), obtain

$$x_{zmp} = 2Acos(\omega t) \tag{7.11}$$

with A being the amplitude of the swing.

- **Removing the constraint**

Analyzing walking motion based on the single pendulum model without the small-steps constraint enters the nonlinear domain. Equation (7.3) can be rewritten in the generic form of a second order system.

The physical intuition about the inverted pendulum allows us to know that it has an unstable equilibrium point in the interval of $[-pi/2, pi/2]$ and a stable equilibrium point in the interval of $[pi/2, 3 * pi/2]$ (remember that the upright position was considered to be in $\theta = 0$). A way to confirm it is through a phase portrait of the system.

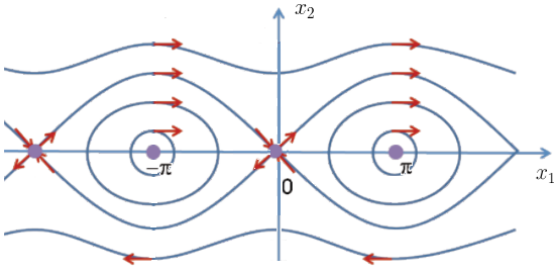

Figure 7.2: Phase portrait for the single pendulum in the entire state space - taken from [7]

Image 7.2, where $x_1 = \theta$ and $x_2 = \dot{\theta}$, shows an unstable node at $x_1 = 0$, which implies that the linear system state matrix has one positive eigenvalue and one negative eigenvalue, both real (the trajectory is called a saddle point)

The trajectory that is the border of two different behaviors is designed separatix.

Observe that the ellipses around $-\pi$ and π has a purely imaginary pair of eigenvalues (called oscillation or center) and results of presupposing the nonexistence of dissipative forces or input. In a more realistic situation the trajectories there would be as in the Figure below. In such situation the eigenvalues are imaginary with the real part being negative, which is called a stable focus.

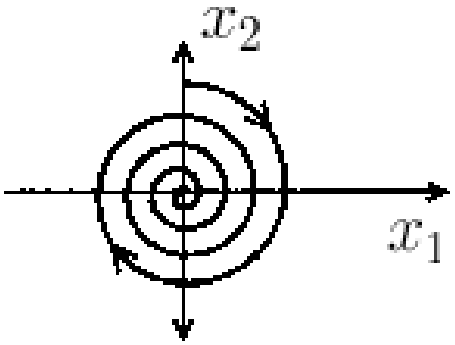

Figure 7.3: Phase portrait for the single pendulum near stable equilibrium point in the presence of dissipative forces - taken from [7]

7.1.3 Hybrid Automaton

The single inverted pendulum is a versatile model in the sense that it can, as already observed, be used to study standing still or walking, but it can also represent the trunk motion or as an abstraction of the relationship of COG (ZMP) and the base of support.

For most of those situations, it can be established an automaton based in the system energy with three modes:

1. "Pump energy" ;
2. "Remove energy"; and
3. "Wait"

In some situations, a "stabilize" mode must be added.

The transition condition and reset value will depend on the situation considered.

Consider the situation where the trunk is bending forward (as if the person is trying to touch their toes) and it is desired to return to the normal standing position. Here there is no reset map and the transition between modes translate how far from the upright position the trunk is. Specifying two boundary layers ε and δ in the neighborhood of $\theta = 0$ with $\varepsilon > \delta$, we can define the hybrid automaton as in figure 7.4. We assume $u_0 > 1$.

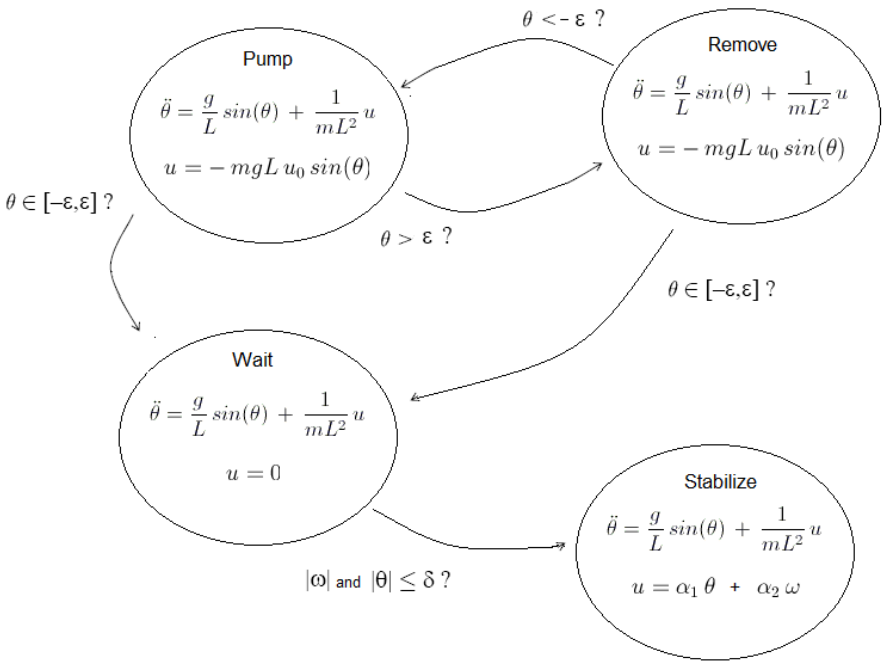

Figure 7.4: Hybrid Automaton for the single inverted pendulum

As it can be seen, the discrete is Q = {pump, remove, wait, stabilize } and the transition map is

$$\Phi(q,x) = \begin{cases} (pump,x) & q = pump\,, \theta < -\varepsilon \\ (remove,x) & q = pump\,, \theta > \varepsilon \\ (wait,x) & q = pump\,, |\,\theta\,| \leq \varepsilon \\ \\ (remove,x) & q = remove\,, \theta > \varepsilon \\ (pump,x) & q = remove\,, \theta < -\varepsilon \\ (wait,x) & q = remove\,, |\,\theta\,| \leq \varepsilon \\ \\ (wait,x) & q = wait\,, |\omega|\ and\ |\,\theta\,| > \delta \\ (stabilize,x) & q = wait\,, |\omega|\ and\ |\,\theta\,| \leq \delta \\ \\ (stabilize,x) & q = stabilize \end{cases} \tag{7.12}$$

7.2 Multi-link Model

Constructing a more complex model enables the study of other features.

Observing human locomotion, it is possible to conclude that the same joint motion does not always have the same effect on body behavior. For example, bending the knee will move the waist closer to the ground if that leg is the stance leg, but will make the foot higher if that leg is the swinging one.

In the author's perspective, it is important that the model captures these details. A way to do it is carefully assign the order of the body frames that will be used to perform the DH method in order to obtain the kinematic equations.

So, although theoretically the base frame can be placed anywhere, its location was chosen to be the toe joint of the stance foot. Another reasonable possibility would be the heel, but, despite representing the larger impact present in the system, the body weight transfer is still not completed and it would not so easily allow the simulation of the heel-lift motion.

The initial idea was to include a roll joint at the hip and ankle but that would force the study of a high dimension system so we will start by having legs with 3 links with one DOF (pitch) and one link trunk also with a pitch DOF were considered.

A global frame (also called inertial) (x_0, y_0, z_0) is placed on the ground and stationary (aligned in y with the support leg and overlapping the heel in x for time = 0) was used to facilitate the visualization of simulation results. For the same reason, a frame was also assigned to each heel, although it has no joint.

As it can be seen, it is possible to identify three subsystems: stance leg, swing leg and trunk. This three subsystems will interact and cause the appearance of an additional and virtual subsystem (in the sense that it has no physical existence), which is the position of the COG in relation with the base of support.

In the next section, DH method will be introduced and equations for each subsystem are going to be written.

7.2.1 Kinematics Equations

The DH method is a systematic path to define the motion of a system composed by rigid bodies connected by single or multiple degrees of freedom joints each. It associats a local frame to each single degree of freedom joint, having specific rules to determine every axis direction. Following these rules, the relationship between adjacent local reference frames is described by only four parameters (a,α, d and θ), which enable the construction of the homogeneous matrix H, which is

the product of four basic transformations (rotations and translations)

$$^{i-1}H_i = Rot_{z,q_i}\, Trans_{z,di}\, Trans_{x,a_i}\, Rot_{x,a_i}$$

$$^{i-1}H_i = \begin{bmatrix} cos(\theta_i) & -cos(\alpha_i)sin(\theta_i) & sin(\alpha_i) & a_i cos(\theta_i) \\ sin(\theta_i) & cos(\alpha_i)cos(\theta_i) & -sin(\alpha_i)cos(\theta_i) & a_i sin(\theta_i) \\ 0 & sin(\alpha_i) & cos(\alpha_i) & d_i \\ 0 & 0 & 0 & 1 \end{bmatrix} \tag{7.13}$$

Thus, any point can be expressed in another frame by multiplying all the $^{i-1}H_i$ matrices separating their local frames,

$$^0R_i = {}^0H_1\, {}^1H_2 ... {}^{i-2}H_{i-1}\, {}^{i-1}H_i = {}^0R_{i-1}\ {}^{i-1}H_i \tag{7.14}$$

The meaning of each column of T (or H) is known from theory: the first three rows of the first three columns give the rotation suffered by the axis when moving from frame i-1 to frame i, while the first three rows of the last column are the position vector of the origin i in frame i-1, $pos = [p_x\ p_y\ p_z]^T$.

To obtain the position of a point w, rather then the frame origin, in frame b, we just do

$$pos_b^w = {}^bR_{local}\ pos_{local}^w \tag{7.15}$$

The axis placement used to derive the equations for the human model and the signal convention for the angles are showed in the figure below. Table 7.1 contains the resulting DH parameters for the support leg.

Table 7.1: DH parameters for the support leg

DH parameters	**Frame**				
	1	2	3	4	5
a_i	$x_0 + L_{foot}$	$-L_{foot}$	$-L_{heel}$	$-L_{shin}$	$-L_{thigh}$
α_i	- 90	0	0	0	0
d_i	0	0	0	0	0
θ_i	0	θ_{toe-st}	90	$\theta_{ankle-st}$	$\theta_{knee-st}$

The variable x_0 stands for the distance in x from the global frame to the heel of the support leg, which is initially zero and increases at each step given. The letters "st" in the angles represent "stance" (synonymous for support) and helps to distinguish from the angles of the other leg.

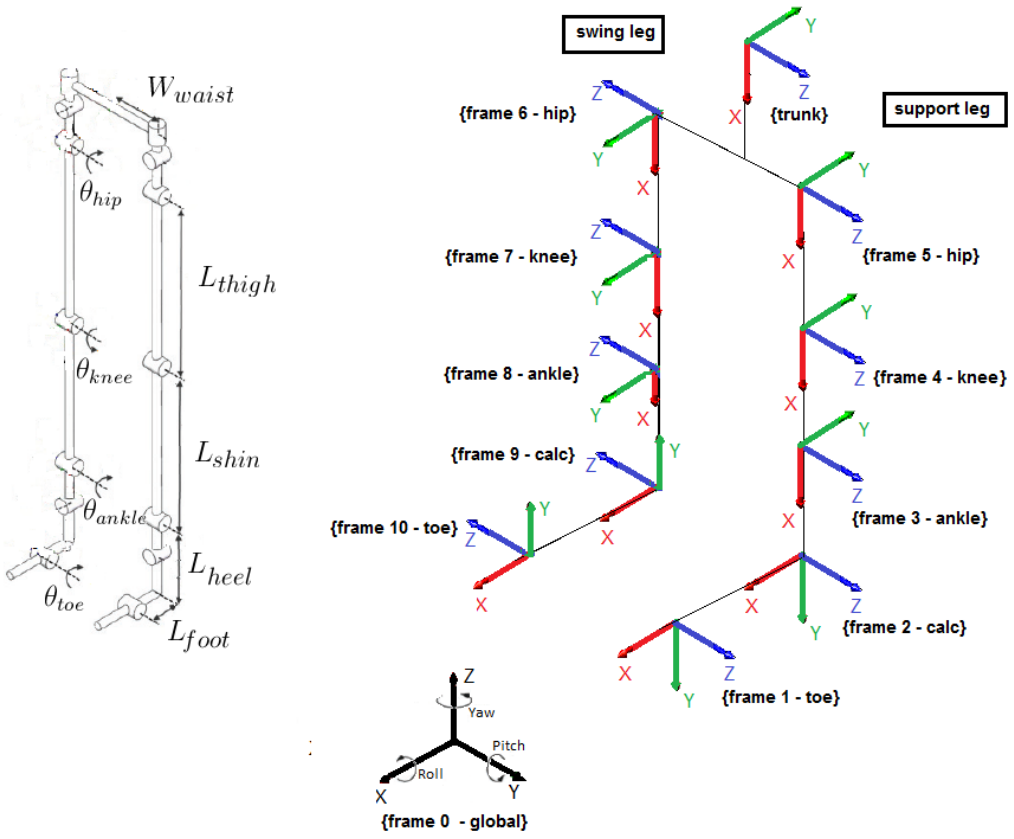

Figure 7.5: Multi-links Human model with axis placement for DH method

- **Forward Kinematics**

Changing from the joint space to the cartesian space is called Forward kinematics.

By using equations (7.13) to (7.15) and table 7.1, it is possible to express, for example, the knee position (local frame 4) in the global frame

$$\begin{aligned} x_{knee} &= x_0 + L_{foot} - L_{foot}\, cos(\theta_{toe}) + L_{shin}\, sin(\theta_{toe} + \theta_{ankle}) + L_{heel}\, sin(\theta_{toe}) \\ y_{knee} &= 0 \\ z_{knee} &= L_{shin}\, cos(\theta_{toe} + \theta_{ankle}) + L_{heel}\, cos(\theta_{toe}) + L_{foot}\, sin(\theta_{toe}) \end{aligned} \tag{7.16}$$

The notation "st" was removed from the equations above to simplify the reading.

- **Inverse Kinematics**

The opposite change is called inverse kinematics. In finding the inverse kinematics equations we get the angles necessary to give a step. One way to do it is by using a geometric approach.

Once more the expressions presented are valid to the support leg and a similar process can was done to the swing leg.

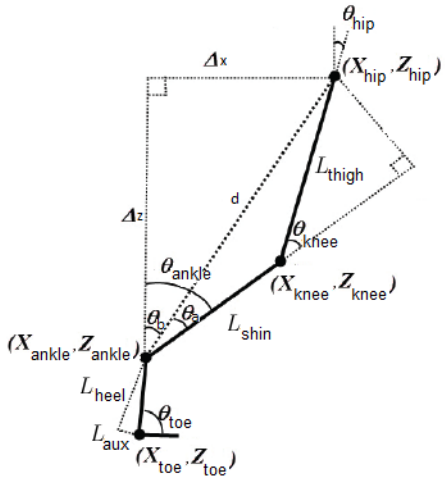

Figure 7.6: Lateral view of the robot

By examining at the figure above, we can get

$$d^2 = \Delta x^2 + \Delta z^2 \Leftrightarrow d^2 = (X_{hip} - X_{ankle})^2 + (Z_{hip} - Z_{ankle})^2 \tag{7.17}$$

So, we obtain the knee angle

$$\theta_{knee} = cos^{-1}\left(\frac{d^2 - (L_{knee}^2 + L_{ankle}^2)}{2\,L_{knee}\,L_{ankle}}\right) \tag{7.18}$$

Focusing now on the ankle area in the figure, it is possible to write

$$\begin{aligned} \theta_a &= tan^{-1}\left(\frac{L_{knee}\,sin(\theta_{knee})}{L_{ankle} + L_{knee}\,sin(\theta_{knee})}\right) \\ \theta_b &= tan^{-1}\left(\frac{X_{hip} - X_{ankle}}{Z_{hip} - Z_{ankle}}\right) \end{aligned} \tag{7.19}$$

Then, the ankle angle is

$$\theta_{ankle} = \theta_a + \theta_b \tag{7.20}$$

For the hip

$$\theta_{hip} = tan^{-1}\left(\frac{X_{hip} - X_{knee}}{Z_{hip} - Z_{knee}}\right) \tag{7.21}$$

Concerning the toe, its angle is given by

$$\theta_{toe} = tan^{-1}\left(\frac{X_{hip} - X_{toe} - (L_{knee}\,sin(\theta_{knee}) + L_{ankle}\,sin(\theta_{ankle}))}{Z_{hip} - Z_{toe} - (L_{knee}\,sin(\theta_{knee}) + L_{ankle}\,sin(\theta_{ankle}))}\right) \tag{7.22}$$

Thus, equations (7.18), (7.20), (7.21), (7.22) resume the inverse kinematics for the sagittal plane of motion.

- **Other Relevant Equations and Considerations**

The ZMP location is found computing expression (7.23)

$$\begin{aligned} x_{zmp} &= \frac{\sum_i I_i\,\dot{\omega}_i + m_i\,x_i\,(\ddot{z}_i - g) - m_i\,\ddot{x}_i\,z_i}{\sum_i m_i\,(\ddot{z}_i - g)} \\ y_{zmp} &= \frac{\sum_i I_i\,\dot{\omega}_i + m_i\,y_i\,(\ddot{z}_i - g) - m_i\,\ddot{y}_i\,z_i}{\sum_i m_i\,(\ddot{z}_i - g)} \end{aligned} \tag{7.23}$$

where $\ddot{x}$ and $\ddot{z}$ are the acceleration in the respective directions.

In a descending stairs or a slope situation the term $(\ddot{z}_i - g)$ becomes $(\ddot{z}_i + g)$, since both accelerations point in the same way.

The ZMP is related with the COG by the expression below

$$\begin{aligned} x_{zmp} &= x_{COG} - \frac{z}{\ddot{z} - g}\,\ddot{x}_{COG} \\ y_{zmp} &= y_{COG} - \frac{z}{\ddot{z} - g}\,\ddot{y}_{COG} \end{aligned} \tag{7.24}$$

Related with the ZMP is the dynamic balance margin. It is crucial to understand how far from unbalance is the body and has the following expression

$$DBM = \left(\frac{L_7}{2}\,cos(\Phi) - dist_{ZMP}\right) \tag{7.25}$$

where $dist_{ZMP}$ is the distance between the ZMP location and the ankle joint and Φ is the ground slope, which for even ground is zero.

In order to achieve the coordination between both legs some conditions should verify. This conditions came directly from human locomotion observation. They can be summarized in the following three conditions:

- the joints' configuration of both legs has to be similar, with the convenient time-shift,
- the distance between feet in the direction of motion has an upper bound,

- the lateral distance between feet has a lower bound ($\geq$ 3cm) and an upper bound,

Now that forward and inverse kinematics analysis are concluded, the analysis of the dynamics of the system is going to be done.

7.2.2 Dynamics Equations

The kinematics analysis previously made relates the robot angles with the position in space. The dynamics equations associate the movement with the forces or torques needed to originate it. with the configurations in space over time.

Like kinematics, there is the direct (also called forward) relation and the inverse relation. In direct dynamics, the forces/torques are the input and the joint variables are the output. In inverse dynamics, it is the other way around.

Instead of Newton′s Laws, which were used for the single inverted pendulum, the Euler- Lagrange equation is going to be used now, because the Lagrangian approach is beneficial in more complex systems and has "several very important properties that can be exploited to design and analyze feedback control algorithms", [12]. Other often used possibility was the Newton-Euler formulation. It has not chosen because, despite being good for implementation, does not allow a so good perception of the body behavior as a whole.

- **Euler-Lagrange Formulation**

The Euler-Lagrange equation is a set of differential equations that describe the evolution of mechanical systems submitted to holonomic constraints.

To write the equation it is necessary to form the Lagrangian of the system, $\mathcal{L}$.

The formal method chosen for the derivation of the robot dynamic model is the principle of virtual displacement. Under the assumption that each link behaves as a rigid body, we determine the Lagrangian (expression (7.26)) and the Euler-Lagrange equation (expression (7.27)).

$$\mathcal{L} = \mathcal{K} - \mathcal{P} \tag{7.26}$$

$$u_i = \frac{\mathrm{d}}{\mathrm{d}t}\left(\frac{\partial \mathcal{L}}{\partial \dot{q}_i}\right) - \frac{\partial \mathcal{L}}{\partial q_i} \tag{7.27}$$

$\mathcal{K}$ and $\mathcal{P}$ are the kinetic and potential energy, in this order. $q_i \in R^n$ represents the generalized coordinates and u_i is the generalized torque/force performing work on q_i, $(i = 1,...,N)$. Beware that u_i are non-conservative and N is the number of links of the robot.

The N joint variables used in the DH method can be a set of generalized coordinates for a rigid robot, [12].

Each link being a rigid body brings the following constraint in expression (7.28). This brings no trouble since it is an holonomic constraint.

$$\|r_i - r_{i-1}\| = L_i \tag{7.28}$$

The fundamental kinematic relationship of a rigid body states that

$$v = v_c + \omega\, r \Leftrightarrow v = v_c + S(\omega)\, r \tag{7.29}$$

$S(\omega)$ is the skew-symmetric matrix and can be computed form the transformation matrix ${}^0R_i$ already presented in the kinematics section. It allow us to find ω.

$$S(\omega) = \dot{R}\, R^T \tag{7.30}$$

The kinetic energy of a N links rigid body is the sum of the of the kinetic energy of each link, which in its turn is, according to the König theorem, the sum of the energy generated by the motion of the center of mass and the energy generated by the rotation (expression (7.31)).

$$\mathcal{K}_i = \frac{1}{2} m_i\, v_{ci}^T\, v_{ci} + \frac{1}{2} \omega_{ci}^T I_i \omega_{ci} \tag{7.31}$$

In the equation above, I is the inertia tensor, which is given by the integration over volume for the position vectors of each body particle. The elements in the diagonal are called the principal moments of inertia about the x,y,z axes,respectively, while remaining terms are called the cross products of inertia. Assuming a uniform distribution of mass, all the cross products of inertia will be zero. For a parallelepiped body with length a (in the x-axis) , height b (in the y-axis) and width c, the principal moments of inertia are

$$\begin{aligned} I_{xx} &= \frac{1}{12} m(b^2 + c^2) \\ I_{yy} &= \tfrac{1}{12} m(a^2 + c^2) \\ I_{zz} &= \tfrac{1}{12} m(a^2 + b^2) \end{aligned} \tag{7.32}$$

If we consider each link to be just a line along the x-axis, it results

$$\begin{aligned} I_{xx} &= 0 \\ I_{yy} &= \tfrac{1}{12} m a^2 \\ I_{zz} &= \tfrac{1}{12} m a^2 \end{aligned} \tag{7.33}$$

It could also be expressed in the global frame, using the transformation

$$\mathcal{I} = {}^0R_i \, I \, {}^0R_i^T \tag{7.34}$$

Through the Jacobian and the variation of the joint variables is possible to write the linear velocity v and the angular velocity ω

$$\begin{aligned} v_{ci} &= J_{v_i} \dot{q} \\ \omega_{ci} &= J_{\omega_i} \dot{q} \end{aligned} \tag{7.35}$$

The Jacobians are calculated according to

$$\begin{aligned} J_{v_i} &= \begin{bmatrix} \frac{\partial p_i}{\partial q_1} & \frac{\partial p_i}{\partial q_2} & \dots & \frac{\partial p_i}{\partial q_i} & 0 & 0 & \dots \end{bmatrix} \\ J_{\omega_i} &= \begin{bmatrix} \varepsilon_1 z_1 & \varepsilon_2 z_2 & \dots & \varepsilon_i z_i & 0 & 0 & \dots \end{bmatrix} \end{aligned} \tag{7.36}$$

$\varepsilon = 1$ for a revolute joint. The position vector of the center of mass of each link p_i and z_i can be found in the first three element of the fourth and third column of the ${}^0R_i$ matrix, respectively.

Replacing the previous equations in (7.31), we obtain

$$\mathcal{K} = \frac{1}{2} \, \dot{q}^T \sum_{i=0}^{N} \left(m_i \, J_{vi}^T \, J_{vi} + J_{\omega i}^T \, \mathcal{I} \, J_{\omega i} \right) \dot{q} \tag{7.37}$$

In a more compact form,

$$\mathcal{K} = \frac{1}{2} \, \dot{q}^T \, B(q) \, \dot{q} \tag{7.38}$$

B(q) is the generalized inertia matrix of the system. It is symmetric and positive definite, which makes it always invertible, $\forall \, q$

There are two different ways of applying the Euler-Lagrange equations: the scalar derivation or the vector format derivation. The scalar derivation is going to be presented converging in the final into the vector format.

Thus, the scalar format of equation (7.38) is

$$\mathcal{K} = \frac{1}{2} \sum_{i \, j} b_{ij}(q) \, \dot{q}_i \, \dot{q}_i \tag{7.39}$$

Notice that in the above equation, $\mathcal{K}$ is always positive ($unless \dot{q} = 0 \Leftrightarrow K = 0$), is a quadratic function of $\dot{q}$.

The Potential energy of the system is also the sum of the potential energy of each link, which

is given by

$$\mathcal{P}_i = -m_i g^T p_{0,ci} \tag{7.40}$$

where g is the gravity acceleration vector, m_i and $p_{0,ci}$ are the mass and the position of the center of mass of the i-th link, respectively.

With this knowledge and since $\mathcal{P}$ is independent from $\dot{q}$ we can rewrite the Lagrangian and the terms of expression (7.27) for the k-th equation

$$\mathcal{L}(q,\dot{q}) = \frac{1}{2}\sum_{ij} b_{ij}(q)\,\dot{q}_i\,\dot{q}_i - \mathcal{P}(q) \tag{7.41}$$

$$\begin{gathered}\left(\frac{\partial \mathcal{L}}{\partial \dot{q}_k}\right) = \sum_j b_{kj}\,\dot{q}_j \Rightarrow \frac{\mathrm{d}}{\mathrm{d}t}\left(\frac{\partial \mathcal{L}}{\partial \dot{q}_k}\right) = \sum_j b_{kj}\,\ddot{q}_j + \sum_{i,j}\frac{\partial\, b_{kj}}{\partial q_i}\,\dot{q}_i\dot{q}_j \\ \frac{\partial \mathcal{L}}{\partial q_k} = \frac{1}{2}\sum_{i,j}\frac{\partial\, b_{ij}}{\partial q_k}\,\dot{q}_i\dot{q}_j - \frac{\partial \mathcal{P}}{\partial q_k}\end{gathered} \tag{7.42}$$

As it can be seen, there are linear terms in acceleration $\ddot{q}$, quadratic terms in velocity $\dot{q}$ and nonlinear terms in configuration q.

Putting the expression together

$$u_k = \sum_j b_{kj}\,\ddot{q}_j + \sum_{i,j}\left(\frac{\partial\, b_{kj}}{\partial q_i} - \frac{1}{2}\frac{\partial\, b_{ij}}{\partial q_k}\right)\dot{q}_i\dot{q}_j + \frac{\partial \mathcal{P}}{\partial q_k} \tag{7.43}$$

Focusing in the first term inside the summatory, if we change the order of addition and take advantage of symmetry, we get

$$\sum_{i,j}\frac{\partial\, b_{kj}}{\partial q_i} = \sum_{i,j}\frac{1}{2}\left(\frac{\partial\, b_{kj}}{\partial q_i} - \frac{\partial\, b_{ki}}{\partial q_j}\right) \tag{7.44}$$

Replacing in expression (7.43)

$$u_k = \sum_j b_{kj}\,\ddot{q}_j + \sum_{i,j}\frac{1}{2}\left(\frac{\partial\, b_{ij}}{\partial q_k} + \frac{\partial\, b_{ik}}{\partial q_j} - \frac{\partial\, b_{jk}}{\partial q_i}\right)\dot{q}_i\dot{q}_j + \frac{\partial \mathcal{P}}{\partial q_k} \tag{7.45}$$

The terms inside the sum are called Christoffel symbols of the first kind, c_{ijk}.

Rewriting,

$$u_k = \sum_j b_{kj}\,\ddot{q}_j + \sum_{i,j} c_{ijk}\,\dot{q}_i\dot{q}_j + \frac{\partial \mathcal{P}}{\partial q_k} \tag{7.46}$$

The first term of the equation are the inertial terms, the ones in the middle are the centrifugal (if $i = j$) and coriolis (if $i \neq j$) terms and the last ones are the gravity terms.

Is crucial to understand the physical meaning of each set of terms (see table 7.1)

Table 7.2: Physical meaning of each set of terms in the dymanics equation

Term	Physical Meaning
b_{kk}	inertia at joint k when joint k accelerates
b_{kj}	inertia "seen" at joint k when joint j accelerates
c_{kii}	coefficient of the centrifugal force at joint k when joint i is moving ($c_{iii} = 0$)
c_{kij}	coefficient of the Coriolis force at joint k when both joint i and joint j are moving

Notice that, since b_{kk} is a function of the following links, the last coefficient is always constant.

We can also write (7.46) in vector format, which can be useful when computing the equations. To that end,

$$C(q,\dot{q}) = \begin{bmatrix} c_{111} & c_{122} & \dots & c_{1NN} \\ c_{211} & c_{222} & \dots & c_{2NN} \\ \dots & \dots & \dots & \dots \\ c_{N11} & c_{N22} & \dots & c_{NNN} \end{bmatrix} \begin{bmatrix} \dot{q}_1^2 \\ \dot{q}_2^2 \\ \dots \\ \dot{q}_N^2 \end{bmatrix} + 2 \begin{bmatrix} c_{112} & c_{113} & \dots & c_{1(N-1)N} \\ c_{212} & c_{213} & \dots & c_{2(N-1)N} \\ \dots & \dots & \dots & \dots \\ c_{N12} & c_{N13} & \dots & c_{N(N-1)N} \end{bmatrix} \begin{bmatrix} \dot{q}_1\,\dot{q}_2 \\ \dot{q}_1\,\dot{q}_3 \\ \dots \\ \dot{q}_{N-1}\,\dot{q}_N \end{bmatrix} \tag{7.47}$$

It is possible to put $\dot{q} = [\dot{q}_1\ \dot{q}_2 \dots \dot{q}_N]'$ in evidence and get $C(q,\dot{q})\,\dot{q}$. By separating the centrifugal and the coriolis matrix, the above equation helps to understand the dimensions of each one of them - $(N,N)x(N,1) + (N,(\frac{N(N-1)}{2}))x((\frac{N(N-1)}{2}),1)$. So, $C(q,\dot{q})$ results in an Nx1 vector.

The partial derivative of the potential energy in equation (7.40) can be called G(q) and it can be expressed using J_v, as

$$G(q) = \frac{\partial \mathcal{P}}{\partial q_k} = \begin{bmatrix} J_{v_1} & J_{v_2} & \dots & J_{v_N} \end{bmatrix} \begin{bmatrix} m_1 \\ m_2 \\ \dots \\ m_N \end{bmatrix} g \tag{7.48}$$

Reaching the generic vector format for the dynamic model of the system

$$u = B(q)\,\ddot{q} + C(q,\dot{q}) + G(q) \tag{7.49}$$

Having the symbolic expression of position for center of mass of each link (from kinematics) makes it possible to compute (7.49) for each leg. In appendix A, the resulting matrices for the swing leg are presented. One way to inspect the resulting expression is though the matrices

properties referred above: as expected, the inertia matrix is symmetric, its last coefficient ($B_{3,3}$) is constant and the elements on the centrifugal matrix diagonal are null.

An identical process was followed for the other subsystems.

To obtain the one-dimensional representation introduced in section 6.3 first we have to solve (7.49) in order to $\ddot{q}$

$$\ddot{q} = B(q)^{-1}\left[U - C(q,\dot{q}) - G(q)\right] \tag{7.50}$$

Notice that the inversion of B is only possible if its determinant is not null, which in this case is not a problem because the mass matrix is, by definition, positive definite.

Then, doing the change of variable

$$x = \begin{bmatrix} q \\ \dot{q} \end{bmatrix} \tag{7.51}$$

We reach

$$\begin{gathered} \dot{x} = f(x,u,t) \\ \Leftrightarrow \\ \dot{x} = \begin{bmatrix} \dot{q} \\ B(q)^{-1}\left[U - C(q,\dot{q}) - G(q)\right] \end{bmatrix} \end{gathered} \tag{7.52}$$

It can be written as in (6.33) by separating what depends on U

$$\dot{x} = \begin{bmatrix} \dot{q} \\ B(q)^{-1}\left[-C(q,\dot{q}) - G(q)\right] \end{bmatrix} + \begin{bmatrix} 0 \\ B(q)^{-1} \end{bmatrix} U \tag{7.53}$$

- **Ground Impact Forces**

In the heel-strike stage, a significant impact between the swing leg and the ground occurs.

This contact forces bring a new term into expression (7.49), which is now written as

$$u + J^T F_c = B(q)\,\ddot{q} + C(q,\dot{q}) + G(q) \tag{7.54}$$

In a real situation, the impact is instantaneous (when compared with the gait cycle duration) and the foot does not rebound. This constraints impose that the new term is a set of impulses and the velocity profile has a discontinuity (but no discontinuity in configuration). Mathematically,

$$\begin{gathered} B(\dot{q}^+ - \dot{q}^-) = J^T \lim_{\Delta t \to 0} \int_{\Delta t} F_c \\ \Leftrightarrow B(\dot{q}^+ - \dot{q}^-) = J^T \lambda \end{gathered} \tag{7.55}$$

λ and J denote the external impulses at collision points and the Jacobian. We assume the collision occurs only in one point, resulting λ in a 2x1 vector.

Notice that joint torque, coriolis, centrifugal and gravitational forces disappear because they are constant in the integration period. Furthermore, the impulse must have a positive value, since the ground will always react by imposing a force in the opposite direction. The velocity of the foot along the y axis will also be always positive, once we consider that macroscopically the ground has no elasticity.

Thus,

$$J\dot{q}^{+} = 0 \tag{7.56}$$

Combining it with (7.55)

$$\begin{array}{rl} B\dot{q}^{+} - J^{T}\lambda & = B\dot{q}^{-} \\ J^{T}\dot{q}^{+} & = 0 \end{array} \tag{7.57}$$

It can also be written in matrix form

$$\begin{bmatrix} B & -J^{T} \\ J & 0 \end{bmatrix} \begin{bmatrix} \dot{q}^{+} \\ \lambda \end{bmatrix} = \begin{bmatrix} B\dot{q}^{-} \\ 0 \end{bmatrix} \tag{7.58}$$

To solve the upper equation in equation system (7.57) two different situations have to be considered:

1. J is full-ranked
2. J is rank-deficient

In the first situation, we can multiply both sides of the equation by JB^{-1} we obtain

$$JB^{-1}J^{T}\lambda = -J\dot{q}^{-} \tag{7.59}$$

Since J and B are full-ranked, $JB^{-1}J^{T}$ is invertible. Not yet that the rate of displacement previous to impact is related with the joint velocity by the Jacobian, this is, $\Delta\dot{pos}^{-} = (J\dot{q}^{-})$, resulting

$$\begin{array}{rl} \lambda & = (JB^{-1}J^{T})^{-1}(-J\dot{q}^{-}) \\ \dot{q}^{+} & = \dot{q}^{-} + B^{-1}J^{T}(JB^{-1}J^{T})^{-1}(-J\dot{q}^{-}) \end{array} \tag{7.60}$$

When J is rank-deficient a little more wok is needed. The rank-deficit can have two distinguish origins: the number of contact constraints (2k , k being the number of collision points) is higher than the DOF prior to impact(n) or the constraint equations are not independent. Both lead to a

non-unique of $\dot{q}^+$ and λ. To overpass it, we create a new row equivalent matrix $\tilde{J}$, which contains the full-rank sub-matrix of J $\tilde{J}_1$ and 2k-r zero vectors, this is

$$\tilde{J} = TJ = \begin{bmatrix} \tilde{J}_{1\,(r,n)} \\ 0_{(2k-r,n)} \end{bmatrix} \tag{7.61}$$

T is an invertible transformation matrix, that enables the partition done.
The same condition in (7.56)

$$\tilde{J}\dot{q}^+ = 0 \tag{7.62}$$

The term $-J^T\lambda$ in equation (7.57) should be replaced by $-\tilde{J}^T T^T \lambda$
Note that

$$T^T\lambda = F(\lambda) = \begin{bmatrix} F_{1\,(r,1)} \\ F_{2\,(2k-r,1)} \end{bmatrix} \tag{7.63}$$

with F_1 and F_2 being the vectors of linear combinations of the external impulses λ
Thus, equation (7.58) becomes

$$\begin{bmatrix} B & -\tilde{J}_1^T \\ \tilde{J}_1 & 0 \end{bmatrix} \begin{bmatrix} \dot{q}^+ \\ F_1 \end{bmatrix} = \begin{bmatrix} B\dot{q}^- \\ 0 \end{bmatrix} \tag{7.64}$$

And results in a equations system very similar to (7.60)

$$\begin{aligned} F_1 &= (\tilde{J}_1 B^{-1} \tilde{J}_1^T)^{-1} (-\tilde{J}_1 \dot{q}^-) \\ \dot{q}^+ &= \dot{q}^- + B^{-1}\tilde{J}_1^T (\tilde{J}_1 B^{-1} \tilde{J}_1^T)^{-1} (-\tilde{J}_1 \dot{q}^-) \end{aligned} \tag{7.65}$$

As you could see expressions (7.60) and (7.65) allow us to know the magnitude of the impact force and the velocity afterwards.

7.2.3 Hybrid Automaton

The hybrid automaton presented in this section takes into consideration the walking style where the heel-strike happens before the toe-lift of the opposite leg and the foot lands on the ground using the heel and, only after that, the toe reaches the ground. The toe lift is preceded by the heel-lift and the swing knee must reach a considerably good extension before foot landing.

Thus, the existence of feet with these motion particulars provokes periods of full-actuation and under-actuation during a step.

The system is underactuated whenever the system is in single support exclusively in heel contact or in single support exclusively in toe contact. Although these periods of time are small

when compared with step duration they are significant enough to endanger the biped stability if not controlled.

The resulting automaton is presented in figure 7.7

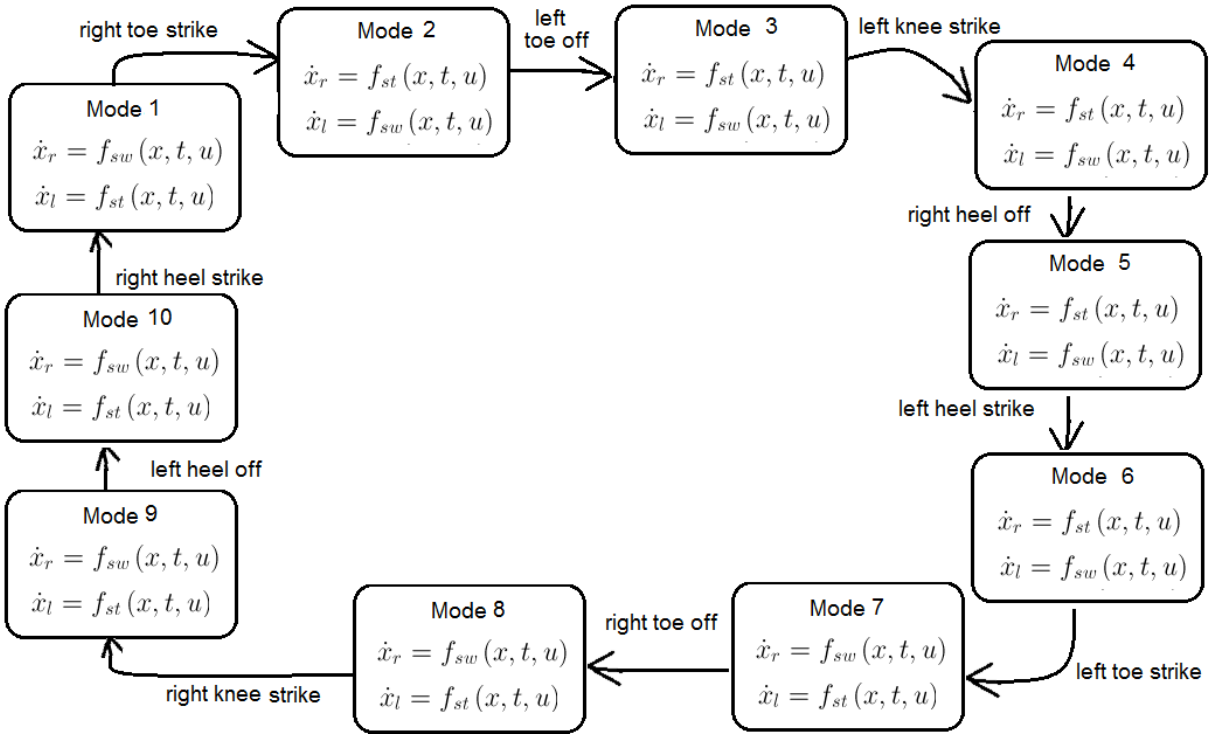

Figure 7.7: Hybrid automaton for the multi-link model

The subscripts "l" and "r" identify the left or the right leg while "st" and "sw" stand for stance and swing, respectively.

Observe that there are only two different continuous dynamics involved but a new state has to be considered because the transition condition and control action will be different in every state. This automaton also reflects the symmetry that exist in a step, since guard conditions to exist modes 1 to 5 only differ from the ones in 6 to 10 on the foot they refer to. The double-support occorus in modes {1,2} and {6,7}. The guard that leads to mode 4 (or 9) does not have the same nature then the others once it does not represent a interaction with the environment - the impact is internal to the system.

Now that modeling is concluded, the implementation results will be presented.

Chapter 8

Implementation Results

Based on the architecture discussed in chapter 5, multiple tests were conducted to simulate the different blocks. Next the results are presented together with a brief descrition comment about what was obtained in comparation which the pre-defined goal and eventual problems found during the development.

Once the simulations illustrate continuous motion they are presented below in sample-frames, that should be visualized by lines and from left to right.

block "Planning"

Recall that the goal for this block is to perform locomotion based on the input parameters chosen to describe it.

Two parameters from the possible input parameters list were chosen (average motion speed and step length) and they were varied to perform the simulation.

The figure is a top-view of the feet during the execution of a step. Each rectangles represents a foot touching the ground and therefore the frames where two rectangles are visible represent the double support phase and the other represent the single support phase.

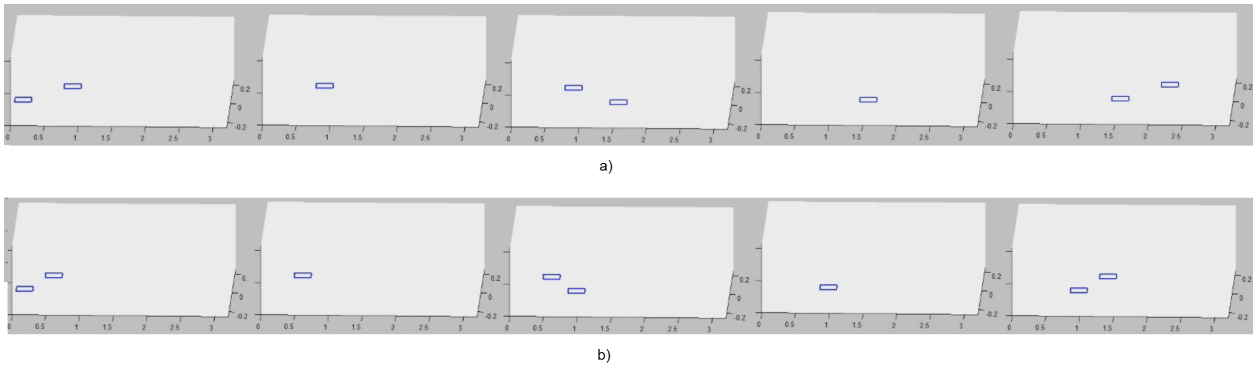

Figure 8.1: Simulation results for the "Planning" block

In a) the step length is 0.7m and the average walking speed is 1.3 m/s. In b) the step length is 0.4m and the average walking speed is 0.8 m/s.

Although the change in the motion speed is not understandable though the frames below, is can be observed that the position reached in the curse of a step is clearly different.

block "Feasibility Verification"

The general goal is to guarantee the respect for the constraints, specially the strongest ones.

The set of results presented exemplify the feasibility verification for the stance leg and were obtained using Excel.

Figure 8.2 is the user-interface were the height of the person/robot is introduced. Then the length of each segment is automatically obtained, assuming that the human proportions collected from the literature (presented in chapter 4) are valid.

The table starting in line 13, has the constraints concerning the joint limitations and in the table starting in line 20 were introduced the behavior pretended for the hip, which is the extremity, indicating the allowable amplitude of oscillation and when on the gait cycle should it occur.

	A	B	C	D	E	F
2						
3	**lengths of interest (m)**		**calculated for verification**			
4	total height	1,65	altura total da perna ao chao	0,875		
5	dist_hip_knee	0,437	altura joelho ao chao	0,437		
6	dist_knee_ankle	0,373				
7	dist_ankle_chao	0,064				
8	tamanho_pe	0,150				
9	largura_anca	0,322				
10	largura_umbigo_anca	0,161				
11						
12						
13			**Constraints**			
14		**Human limits (generic situation)**		**usual human limits when walking in flat surface**		
15	joint	minimum angle (degrees)	maximum angle (degrees)	minimum angle (degrees)	maximum angle (degrees)	
16	hip	-40	40	-20	30	
17	knee	1	270	2	65	
18	ankle	10	-30	7	-25	
19						
20			**Expected behavior**			
21	**Support leg**					
22		maximum (m)	instant of the gait cycle (%)	minimum (m)	instant of the gait cycle (%)	
23	hip height	0,875	30,0	0,825	0	50
24	ankle height			0,0	0 to 40	100
25						
26	**sheet 3 -> admissable combinations that ensure the hip's height constraint**					
27	**in red is the minimum height and in blue the maximum height**					

Figure 8.2: Simulation results for the "Feasibility Verification" block - configurable values and constraints

The introduction of different parameters result in different region of admissibility. The region of admissibility is colored in green with the lower extremity colored in red and the upper extremity colored in blue.

For the period of the gait cycle where the foot is flat on the ground, there are still three modalities, which need to cooperate to ensure the desired waist height (be aware that a waist height different from the expected will force the modification of the values assigned for the entire swing leg). Hence, its consistency has to be ratified. The option was to verify two of the modalities in a double entry table and use an additional set of tables to find the suitable value for the remaining modality.

So, figures 8.3 and 8.4 show the region of admissibility for two individuals with different body height: individual 1 is 1,65m height and individual 2 is 1,80m height. The knee and hip angles become defined from this table.

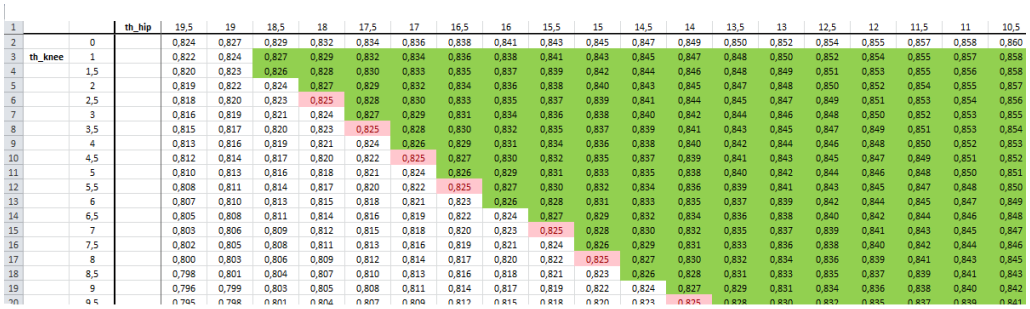

		th_hip	19,5	19	18,5	18	17,5	17	16,5	16	15,5	15	14,5	14	13,5	13	12,5	12	11,5	11	10,5
	0		0,824	0,827	0,829	0,832	0,834	0,836	0,838	0,841	0,843	0,845	0,847	0,849	0,850	0,852	0,854	0,855	0,857	0,858	0,860
th_knee	1		0,822	0,824	0,827	0,829	0,832	0,834	0,836	0,838	0,841	0,843	0,845	0,847	0,848	0,850	0,852	0,854	0,855	0,857	0,858
	1,5		0,820	0,823	0,826	0,828	0,830	0,833	0,835	0,837	0,839	0,842	0,844	0,846	0,848	0,849	0,851	0,853	0,855	0,856	0,858
	2		0,819	0,822	0,824	0,827	0,829	0,832	0,834	0,836	0,838	0,840	0,843	0,845	0,847	0,848	0,850	0,852	0,854	0,855	0,857
	2,5		0,818	0,820	0,823	0,825	0,828	0,830	0,833	0,835	0,837	0,839	0,841	0,844	0,845	0,847	0,849	0,851	0,853	0,854	0,856
	3		0,816	0,819	0,821	0,824	0,827	0,829	0,831	0,834	0,836	0,838	0,840	0,842	0,844	0,846	0,848	0,850	0,852	0,853	0,855
	3,5		0,815	0,817	0,820	0,823	0,825	0,828	0,830	0,832	0,835	0,837	0,839	0,841	0,843	0,845	0,847	0,849	0,851	0,853	0,854
	4		0,813	0,816	0,819	0,821	0,824	0,826	0,829	0,831	0,834	0,836	0,838	0,840	0,842	0,844	0,846	0,848	0,850	0,852	0,853
	4,5		0,812	0,814	0,817	0,820	0,822	0,825	0,827	0,830	0,832	0,835	0,837	0,839	0,841	0,843	0,845	0,847	0,849	0,851	0,852
	5		0,810	0,813	0,816	0,818	0,821	0,824	0,826	0,829	0,831	0,833	0,835	0,838	0,840	0,842	0,844	0,846	0,848	0,850	0,851
	5,5		0,808	0,811	0,814	0,817	0,820	0,822	0,825	0,827	0,830	0,832	0,834	0,836	0,839	0,841	0,843	0,845	0,847	0,848	0,850
	6		0,807	0,810	0,813	0,815	0,818	0,821	0,823	0,826	0,828	0,831	0,833	0,835	0,837	0,839	0,842	0,844	0,845	0,847	0,849
	6,5		0,805	0,808	0,811	0,814	0,816	0,819	0,822	0,824	0,827	0,829	0,832	0,834	0,836	0,838	0,840	0,842	0,844	0,846	0,848
	7		0,803	0,806	0,809	0,812	0,815	0,818	0,820	0,823	0,825	0,828	0,830	0,832	0,835	0,837	0,839	0,841	0,843	0,845	0,847
	7,5		0,802	0,805	0,808	0,811	0,813	0,816	0,819	0,821	0,824	0,826	0,829	0,831	0,833	0,836	0,838	0,840	0,842	0,844	0,846
	8		0,800	0,803	0,806	0,809	0,812	0,814	0,817	0,820	0,822	0,825	0,827	0,830	0,832	0,834	0,836	0,839	0,841	0,843	0,845
	8,5		0,798	0,801	0,804	0,807	0,810	0,813	0,816	0,818	0,821	0,823	0,826	0,828	0,831	0,833	0,835	0,837	0,839	0,841	0,843
	9		0,796	0,799	0,803	0,805	0,808	0,811	0,814	0,817	0,819	0,822	0,824	0,827	0,829	0,831	0,834	0,836	0,838	0,840	0,842
	9,5		0,795	0,798	0,801	0,804	0,807	0,809	0,812	0,815	0,818	0,820	0,823	0,825	0,828	0,830	0,832	0,835	0,837	0,839	0,841

1)

		th_hip	19,5	19	18,5	18	17,5	17	16,5	16	15,5	15	14,5	14	13,5	13	12,5	12	11,5	11	10,5
	0		0,899	0,902	0,905	0,907	0,910	0,912	0,915	0,917	0,919	0,921	0,924	0,926	0,928	0,930	0,931	0,933	0,935	0,936	0,938
th_knee	1		0,896	0,899	0,902	0,905	0,907	0,910	0,912	0,915	0,917	0,919	0,921	0,924	0,926	0,928	0,930	0,931	0,933	0,935	0,936
	1,5		0,895	0,898	0,901	0,903	0,906	0,909	0,911	0,913	0,916	0,918	0,920	0,922	0,925	0,927	0,929	0,930	0,932	0,934	0,936
	2		0,893	0,896	0,899	0,902	0,905	0,907	0,910	0,912	0,915	0,917	0,919	0,921	0,923	0,926	0,927	0,929	0,931	0,933	0,935
	2,5		0,892	0,895	0,898	0,900	0,903	0,906	0,908	0,911	0,913	0,916	0,918	0,920	0,922	0,924	0,926	0,928	0,930	0,932	0,934
	3		0,890	0,893	0,896	0,899	0,902	0,904	0,907	0,910	0,912	0,914	0,917	0,919	0,921	0,923	0,925	0,927	0,929	0,931	0,933
	3,5		0,889	0,892	0,895	0,897	0,900	0,903	0,906	0,908	0,911	0,913	0,915	0,918	0,920	0,922	0,924	0,926	0,928	0,930	0,932
	4		0,887	0,890	0,893	0,896	0,899	0,901	0,904	0,907	0,909	0,912	0,914	0,916	0,919	0,921	0,923	0,925	0,927	0,929	0,931
	4,5		0,885	0,888	0,891	0,894	0,897	0,900	0,903	0,905	0,908	0,910	0,913	0,915	0,917	0,920	0,922	0,924	0,926	0,928	0,930
	5		0,884	0,887	0,890	0,893	0,896	0,898	0,901	0,904	0,906	0,909	0,911	0,914	0,916	0,918	0,921	0,923	0,925	0,927	0,929
	5,5		0,882	0,885	0,888	0,891	0,894	0,897	0,900	0,902	0,905	0,908	0,910	0,912	0,915	0,917	0,919	0,921	0,924	0,926	0,928
	6		0,880	0,883	0,886	0,889	0,892	0,895	0,898	0,901	0,903	0,906	0,909	0,911	0,913	0,916	0,918	0,920	0,922	0,924	0,926
	6,5		0,878	0,882	0,885	0,888	0,891	0,894	0,896	0,899	0,902	0,905	0,907	0,910	0,912	0,914	0,917	0,919	0,921	0,923	0,925
	7		0,877	0,880	0,883	0,886	0,889	0,892	0,895	0,898	0,900	0,903	0,906	0,908	0,911	0,913	0,915	0,918	0,920	0,922	0,924
	7,5		0,875	0,878	0,881	0,884	0,887	0,890	0,893	0,896	0,899	0,901	0,904	0,907	0,909	0,912	0,914	0,916	0,918	0,921	0,923
	8		0,873	0,876	0,879	0,882	0,885	0,888	0,891	0,894	0,897	0,900	0,902	0,905	0,908	0,910	0,912	0,915	0,917	0,919	0,921
	8,5		0,871	0,874	0,877	0,881	0,884	0,887	0,890	0,893	0,895	0,898	0,901	0,904	0,906	0,909	0,911	0,913	0,916	0,918	0,920
	9		0,869	0,872	0,875	0,879	0,882	0,885	0,888	0,891	0,894	0,897	0,899	0,902	0,905	0,907	0,910	0,912	0,914	0,916	0,919
	9,5																				

2)

Figure 8.3: Simulation results for the "Feasibility Verification" block - region of admissibility (lower extremity for individuals with different body height)

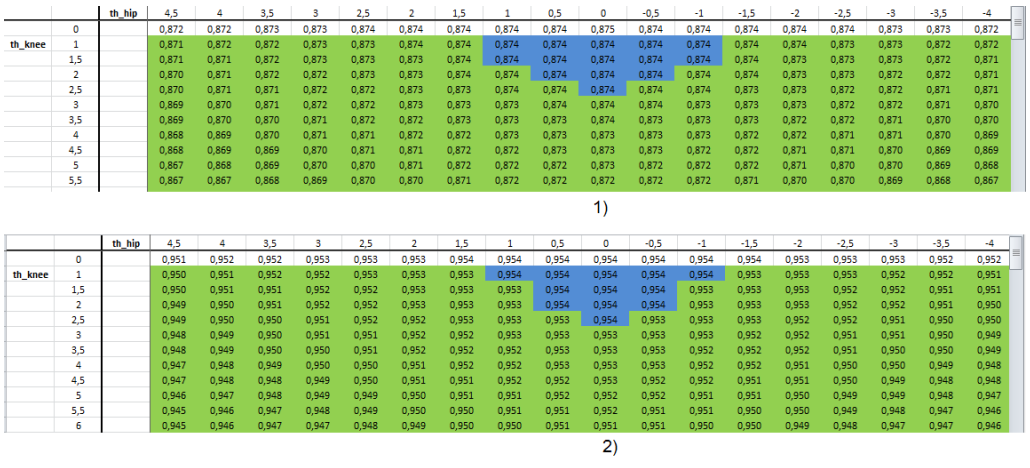

		th_hip	4,5	4	3,5	3	2,5	2	1,5	1	0,5	0	-0,5	-1	-1,5	-2	-2,5	-3	-3,5	-4
	0		0,872	0,872	0,873	0,873	0,874	0,874	0,874	0,874	0,874	0,875	0,874	0,874	0,874	0,874	0,874	0,873	0,873	0,872
th_knee	1		0,871	0,872	0,872	0,873	0,873	0,874	0,874	0,874	0,874	0,874	0,874	0,874	0,874	0,874	0,874	0,873	0,873	0,872	0,872
	1,5		0,871	0,871	0,872	0,873	0,873	0,873	0,874	0,874	0,874	0,874	0,874	0,874	0,874	0,873	0,873	0,873	0,872	0,872	0,871
	2		0,870	0,871	0,872	0,872	0,873	0,873	0,874	0,874	0,874	0,874	0,874	0,874	0,874	0,873	0,873	0,873	0,872	0,872	0,871
	2,5		0,870	0,871	0,871	0,872	0,872	0,873	0,873	0,874	0,874	0,874	0,874	0,874	0,873	0,873	0,872	0,872	0,871	0,871
	3		0,869	0,870	0,871	0,872	0,872	0,873	0,873	0,874	0,874	0,874	0,874	0,873	0,873	0,873	0,872	0,872	0,871	0,870
	3,5		0,869	0,870	0,870	0,871	0,872	0,872	0,873	0,873	0,873	0,874	0,873	0,873	0,873	0,872	0,872	0,871	0,870	0,870
	4		0,868	0,869	0,870	0,871	0,871	0,872	0,872	0,873	0,873	0,873	0,873	0,873	0,872	0,872	0,871	0,871	0,870	0,869
	4,5		0,868	0,869	0,869	0,870	0,871	0,871	0,872	0,872	0,873	0,873	0,873	0,872	0,872	0,871	0,871	0,870	0,869	0,869
	5		0,867	0,868	0,869	0,870	0,870	0,871	0,872	0,872	0,872	0,873	0,872	0,872	0,872	0,871	0,870	0,870	0,869	0,868
	5,5		0,867	0,867	0,868	0,869	0,870	0,870	0,871	0,872	0,872	0,872	0,872	0,872	0,871	0,870	0,870	0,869	0,868	0,867

1)

		th_hip	4,5	4	3,5	3	2,5	2	1,5	1	0,5	0	-0,5	-1	-1,5	-2	-2,5	-3	-3,5	-4
	0		0,951	0,952	0,952	0,953	0,953	0,953	0,954	0,954	0,954	0,954	0,954	0,954	0,954	0,953	0,953	0,953	0,952	0,952
th_knee	1		0,950	0,951	0,952	0,952	0,953	0,953	0,954	0,954	0,954	0,954	0,954	0,954	0,953	0,953	0,953	0,952	0,952	0,951
	1,5		0,950	0,951	0,951	0,952	0,952	0,953	0,953	0,953	0,954	0,954	0,954	0,953	0,953	0,953	0,952	0,952	0,951	0,951
	2		0,949	0,950	0,951	0,952	0,952	0,953	0,953	0,953	0,954	0,954	0,954	0,953	0,953	0,953	0,952	0,952	0,951	0,950
	2,5		0,949	0,950	0,950	0,951	0,952	0,952	0,953	0,953	0,953	0,954	0,953	0,953	0,953	0,952	0,952	0,951	0,950	0,950
	3		0,948	0,949	0,950	0,951	0,951	0,952	0,952	0,953	0,953	0,953	0,953	0,953	0,952	0,952	0,951	0,951	0,950	0,949
	3,5		0,948	0,949	0,950	0,950	0,951	0,952	0,952	0,952	0,953	0,953	0,953	0,952	0,952	0,952	0,951	0,950	0,950	0,949
	4		0,947	0,948	0,949	0,950	0,950	0,951	0,952	0,952	0,953	0,953	0,953	0,952	0,952	0,951	0,950	0,950	0,949	0,948
	4,5		0,947	0,948	0,948	0,949	0,950	0,951	0,951	0,952	0,952	0,953	0,952	0,952	0,951	0,951	0,950	0,949	0,948	0,948
	5		0,946	0,947	0,948	0,949	0,949	0,950	0,951	0,951	0,952	0,952	0,952	0,951	0,951	0,950	0,949	0,949	0,948	0,947
	5,5		0,945	0,946	0,947	0,948	0,949	0,950	0,950	0,951	0,951	0,952	0,951	0,951	0,950	0,950	0,949	0,948	0,947	0,946
	6		0,945	0,946	0,947	0,947	0,948	0,949	0,950	0,950	0,951	0,951	0,951	0,950	0,950	0,949	0,948	0,947	0,947	0,946

2)

Figure 8.4: Simulation results for the "Feasibility Verification" block - region of admissibility (upper extremity for individuals with different body height)

In figure 8.5 is presented one table from the second set of tables.

Here, the knee angle is fixed and a search is maid in the hip angle's column to see if there is an ankle angle value not too distant from the one previously assigned to it, that falls inside the region of interest. If not, the first alternative would be change the hip angle. In the situation that a valid solution is not find in the neighborhood of the combination (hip, ankle) a new search is done in the (knee,hip) table. A plausible way to do this second search would be doing it backwards.

h_knee	2	th_hip	24	23,5	23	22,5	22	21,5	21	20,5	20	19,5	19	18,5	18	17
th_ank	4,5		0,067	0,066	0,064	0,063	0,062	0,061	0,060	0,059	0,057	0,056	0,055	0,054	0,052	0
	4		0,066	0,064	0,063	0,062	0,061	0,060	0,059	0,057	0,056	0,055	0,054	0,052	0,051	0,
	3,5		0,064	0,063	0,062	0,061	0,060	0,059	0,057	0,056	0,055	0,054	0,052	0,051	0,050	0,
	3		0,063	0,062	0,061	0,060	0,059	0,057	0,056	0,055	0,054	0,052	0,051	0,050	0,049	0,
	2,5		0,062	0,061	0,060	0,059	0,057	0,056	0,055	0,054	0,052	0,051	0,050	0,049	0,048	0,
	2		0,061	0,060	0,059	0,057	0,056	0,055	0,054	0,052	0,051	0,050	0,049	0,048	0,046	0,
	1,5		0,060	0,059	0,057	0,056	0,055	0,054	0,052	0,051	0,050	0,049	0,048	0,046	0,045	0,
	1		0,059	0,057	0,056	0,055	0,054	0,052	0,051	0,050	0,049	0,048	0,046	0,045	0,044	0,
	0,5		0,057	0,056	0,055	0,054	0,052	0,051	0,050	0,049	0,048	0,046	0,045	0,044	0,043	0
	0		0,056	0,055	0,054	0,052	0,051	0,050	0,049	0,048	0,046	0,045	0,044	0,043	0,041	0,
	-0,5		0,055	0,054	0,052	0,051	0,050	0,049	0,048	0,046	0,045	0,044	0,043	0,041	0,040	0,
	-1		0,054	0,052	0,051	0,050	0,049	0,048	0,046	0,045	0,044	0,043	0,041	0,040	0,039	0,
	-1,5		0,052	0,051	0,050	0,049	0,048	0,046	0,045	0,044	0,043	0,041	0,040	0,039	0,038	0,
	-2		0,051	0,050	0,049	0,048	0,046	0,045	0,044	0,043	0,041	0,040	0,039	0,038	0,036	0,
	-2,5		0,050	0,049	0,048	0,046	0,045	0,044	0,043	0,041	0,040	0,039	0,038	0,036	0,035	0,
	-3		0,049	0,048	0,046	0,045	0,044	0,043	0,041	0,040	0,039	0,038	0,036	0,035	0,034	0,
	-3,5		0,048	0,046	0,045	0,044	0,043	0,041	0,040	0,039	0,038	0,036	0,035	0,034	0,032	0
	-4		0,046	0,045	0,044	0,043	0,041	0,040	0,039	0,038	0,036	0,035	0,034	0,032	0,031	0,
	-4,5		0,045	0,044	0,043	0,041	0,040	0,039	0,038	0,036	0,035	0,034	0,032	0,031	0,030	0,
	-5		0,044	0,043	0,041	0,040	0,039	0,038	0,036	0,035	0,034	0,032	0,031	0,030	0,029	0,
	-5,5		0,043	0,041	0,040	0,039	0,038	0,036	0,035	0,034	0,032	0,031	0,030	0,029	0,027	0,
	-6		0,041	0,040	0,039	0,038	0,036	0,035	0,034	0,032	0,031	0,030	0,029	0,027	0,026	0,
	-6,5		0,040	0,039	0,038	0,036	0,035	0,034	0,032	0,031	0,030	0,029	0,027	0,026	0,025	0,
	-7		0,039	0,038	0,036	0,035	0,034	0,032	0,031	0,030	0,029	0,027	0,026	0,025	0,023	0,
	-7,5		0,038	0,036	0,035	0,034	0,032	0,031	0,030	0,029	0,027	0,026	0,025	0,023	0,022	0
	-8		0,036	0,035	0,034	0,032	0,031	0,030	0,029	0,027	0,026	0,025	0,023	0,022	0,021	0,
	-8,5		0,035	0,034	0,032	0,031	0,030	0,029	0,027	0,026	0,025	0,023	0,022	0,021	0,020	0
	-9		0,034	0,032	0,031	0,030	0,029	0,027	0,026	0,025	0,023	0,022	0,021	0,020	0,018	0
	-9,5		0,032	0,031	0,030	0,029	0,027	0,026	0,025	0,023	0,022	0,021	0,020	0,018	0,017	0
	-10		0,031	0,030	0,029	0,027	0,026	0,025	0,023	0,022	0,021	0,020	0,018	0,017	0,016	0
	-10,5		0,030	0,029	0,027	0,026	0,025	0,023	0,022	0,021	0,020	0,018	0,017	0,016	0,014	0
	-11		0,029	0,027	0,026	0,025	0,023	0,022	0,021	0,020	0,018	0,017	0,016	0,014	0,013	0
	-11,5		0,027	0,026	0,025	0,023	0,022	0,021	0,020	0,018	0,017	0,016	0,014	0,013	0,012	0
	-12		0,026	0,025	0,023	0,022	0,021	0,020	0,018	0,017	0,016	0,014	0,013	0,012	0,010	0,
	-12,5		0,025	0,023	0,022	0,021	0,020	0,018	0,017	0,016	0,014	0,013	0,012	0,010	0,009	0,
	-13		0,023	0,022	0,021	0,020	0,018	0,017	0,016	0,014	0,013	0,012	0,010	0,009	0,008	0,
	-13,5		0,022	0,021	0,020	0,018	0,017	0,016	0,014	0,013	0,012	0,010	0,009	0,008	0,007	0,
	-14		0,021	0,020	0,018	0,017	0,016	0,014	0,013	0,012	0,010	0,009	0,008	0,007	0,005	0,
	-14,5		0,020	0,018	0,017	0,016	0,014	0,013	0,012	0,010	0,009	0,008	0,007	0,005	0,004	0,
	-15		0,018	0,017	0,016	0,014	0,013	0,012	0,010	0,009	0,008	0,007	0,005	0,004	0,003	0
	-15,5		0,017	0,016	0,014	0,013	0,012	0,010	0,009	0,008	0,007	0,005	0,004	0,003	0,001	0,
	-16		0,016	0,014	0,013	0,012	0,010	0,009	0,008	0,007	0,005	0,004	0,003	0,001	0,000	-0
	-16,5		0,014	0,013	0,012	0,010	0,009	0,008	0,007	0,005	0,004	0,003	0,001	0,000	-0,001	-0,
	-17		0,013	0,012	0,010	0,009	0,008	0,007	0,005	0,004	0,003	0,001	0,000	-0,001	-0,003	-0,
	-17,5		0,012	0,010	0,009	0,008	0,007	0,005	0,004	0,003	0,001	0,000	-0,001	-0,003	-0,004	-0,
	-18		0,010	0,009	0,008	0,007	0,005	0,004	0,003	0,001	0,000	-0,001	-0,003	-0,004	-0,005	-0,
	-18,5		0,009	0,008	0,007	0,005	0,004	0,003	0,001	0,000	-0,001	-0,003	-0,004	-0,005	-0,007	-0,

Folha1

Figure 8.5: Simulation results for the "Feasibility Verification" block - region of admissibility (part 2)

Intra Walking Cycle

The intra walking cycle is composed by the low level controllers and the walking machine.

As stated before, controlling the legs and trunk is a mean to guarantee that the COG (ZMP) is inside the base of support, having therefor a virtual inverted pendulum to control (indirectly). The hybrid nature of the walking machine makes it more interesting because the pivot point of

this pendulum (the point where it connects to the ground) will change every time a foot strikes or leaves the ground.

The figure below shows an ideal reference trajectory. The base of support is always formed by the stance foot's area when in single support or the area of both feet plus the area that connects them, which is delimited by the green lines, when in double support. The red dot indicates the projection of the pendulum's mass on the ground while the black dot denotes the base of support's center.

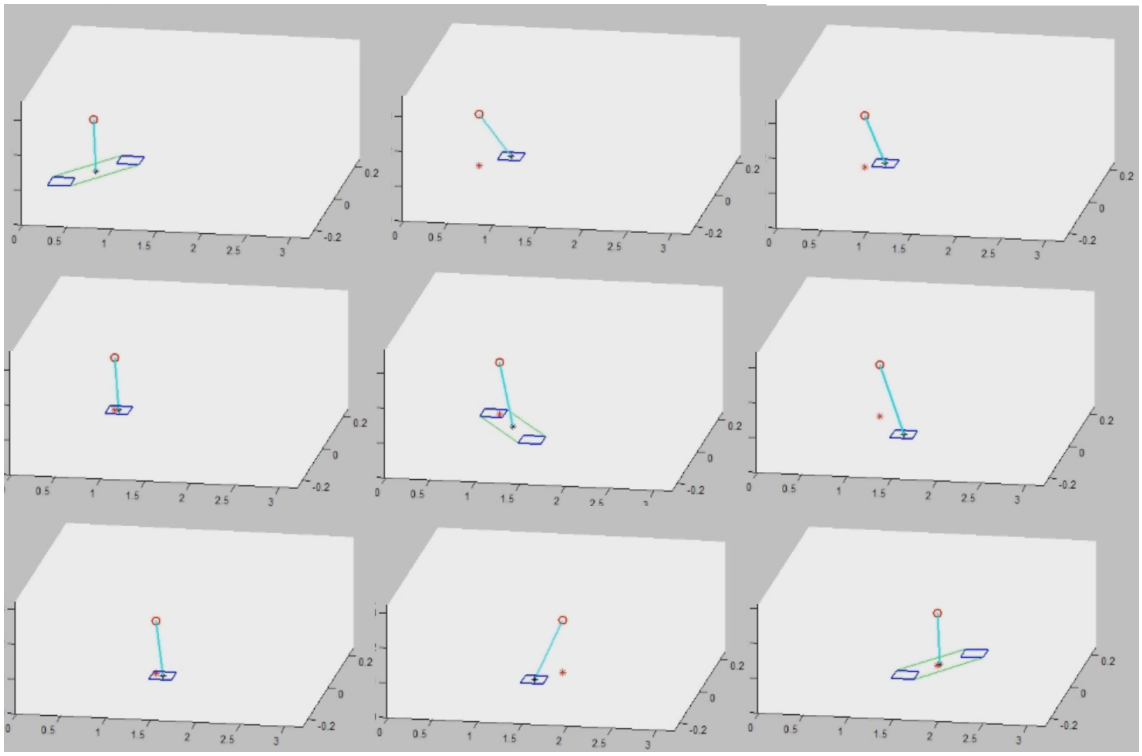

Figure 8.6: Simulation results for the "Walking Machine" block - virtual inverted pendulum and base of suppoort

Figure 8.7 illustrates an open-loop simulation of the walking machine.

It is able to walk at different speeds and for a configurable distance.

All the fundamental stages are present and its sequence in time respects what has been defined previously as "style of locomotion 2": toe-strike (frame 1) followed by toe-lift of the opposite leg. Then, it occurs the knee-strike of the swing leg and before the heel of this leg strikes the ground (frame 4) still happens the stance leg's heel-off. The process repeats itself only inverting the roles of each leg.

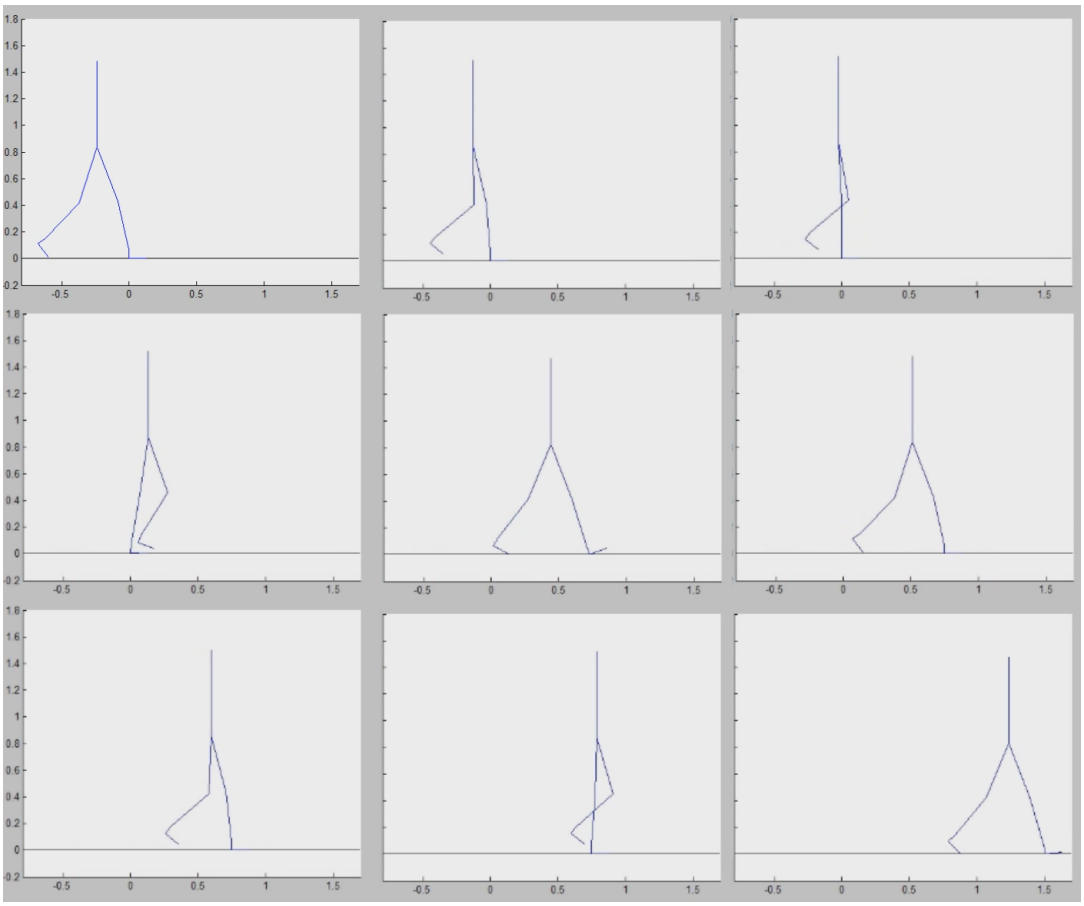

Figure 8.7: Simulation results for the "Walking Machine" block - entire body in 2D

Later, it was extended from 2D to 3D. It can be seen below.

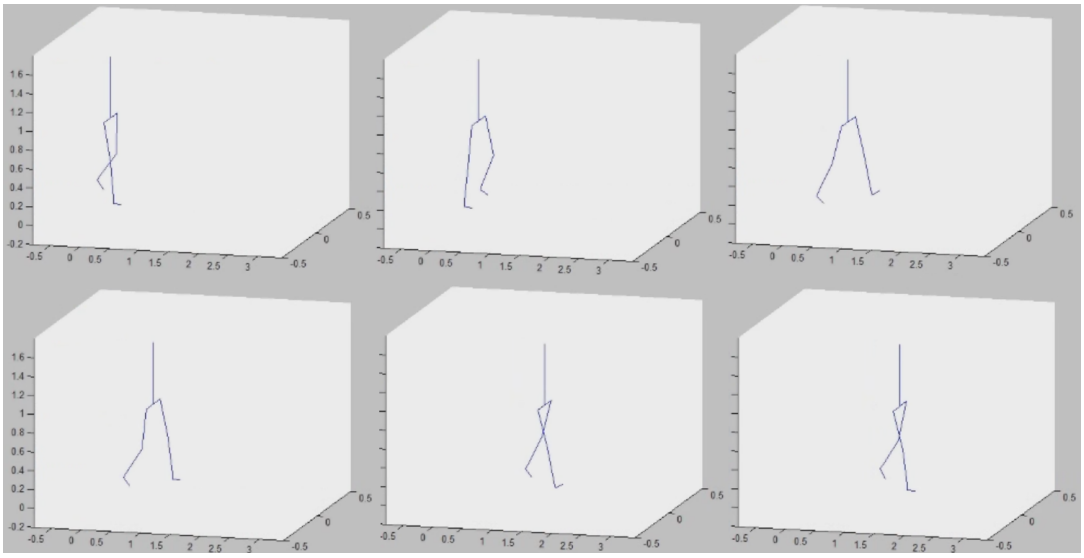

Figure 8.8: Simulation results for the "Walking Machine" block - entire body in 3D

The close-loop simulation was maid implementing a sliding mode control technique. The Simulink diagram in figure 8.9 presents part of the total system.

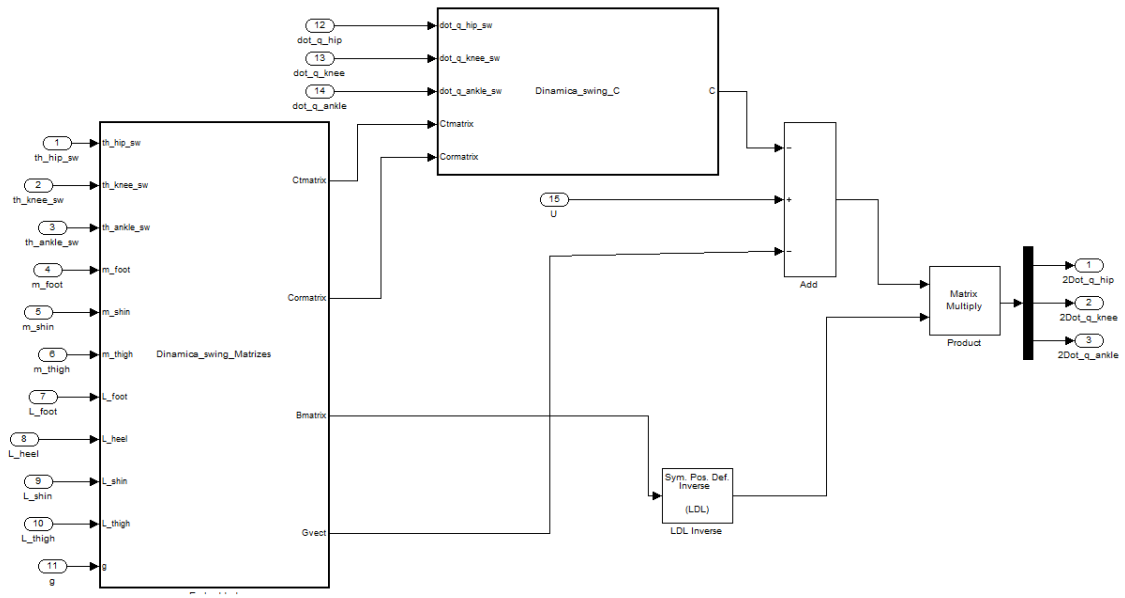

Figure 8.9: Close-loop simulation results for the "Walking Machine" block - Simulink block diagram

Aside from these, some tests were maid for the simple inverted pendulum. Below you can find the result of the simulations conducted to obtain the phase portrait.

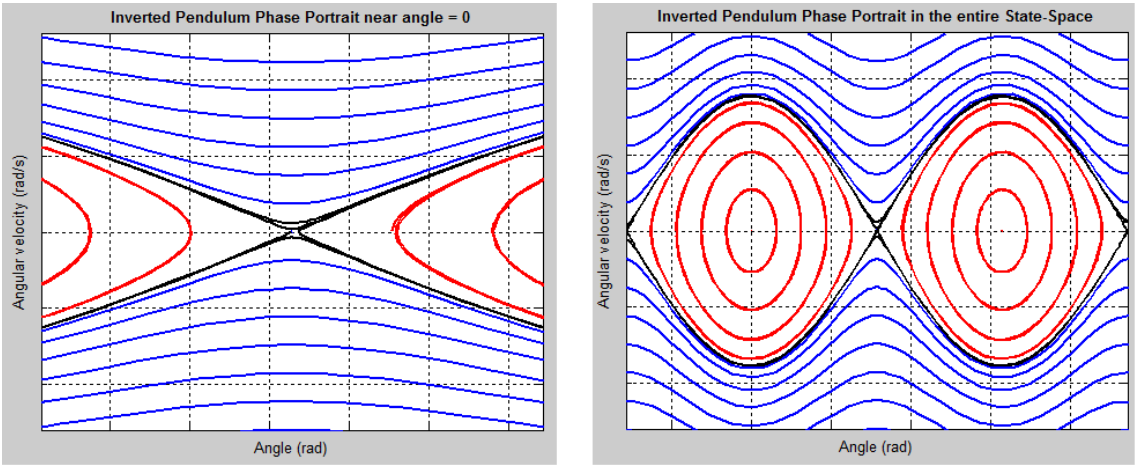

Figure 8.10: Simulation of the Phase Portrait of the single inverted pendulum: a) near $\theta = 0$; b) in the entire state space

Chapter 9

Conclusion

This dissertation work presented a great and transversal challenge.

It started with the need of doing a very good market research to find the gaps of the existing products and thus justify the purpose and scope of the selected topic.

A literature review on human locomotion, its modeling techniques and control methods used in humanoid robots was also included. It allowed the collection of relevant data about human motion (so later it could be used to test the model) and get to know the capabilities of the state-of-the art on humanoids and the available modeling and control techniques.

Then came the challenge of defining the goals and follow all the steps of a Systems Engineering Process' methodology, with culminated in the preliminary control architecture.

The locomotion modeling bought some unpredicted situations to be solved: the initial idea of using the human data collected to generate the joints' references had to be set aside because the wave forms were not periodic. This has great relevance whereas it contradicts the basic physical knowledge that the joint angle is a smooth function over time and induced a non human-like walk. The first alternative has to modify the last segment of the wave forms to make them periodic but it proved to be inefficient because the resulting amplitude of the intermediate points for each joint produced a skitter-looking walk since the combination of leg angles did not produce a constant position has it should. The second alternative was finding new and periodic wave forms in different literature. The new wave forms found were all quite different in amplitude, and some even in shape, from the previous ones, but it also did not work out since they did not originate a human-like walk.

In the author's opinion this problem has three main sources: errors in data acquisition, which led to the non-periodic wave forms; the age or height (among others) of the individuals used to collect the data was unspecified in the works used as reference and such parameters can cause the large variation of amplitude of the human joint angles that has been observed; finally, the fact that the wave form for a human joint reaches a given amplitude because it relays on the influence that the motion of other joints will have in the final position of that body segment, that is, once our model has much less degrees of freedom that a human, a "human-based" behavior of a joint will not grant an equal final position in the model.

The solution found was the artificial generation of the wave forms based on the qualitative characterization of human motion and constraints.

Still in relation to modeling, it has been concluded that, contrary to what is advocated by some other authors (as [32]), the model cannot be done for a single leg and after applied to the other. The reason for that is, as detailed earlier, that the effect a leg has in the system as a whole depends on the role it is playing (stance leg or swing leg).

This two conclusions had direct weight in the system architecture, with the introduction of the "Feasibility Verification" and "Decomposition in Motion Coordinated Modalities" blocks.

The design of a distributed architecture and organized by layers was considered essential. The ability to guarantee adaptivity, robustness and (sub-)optimality is a crucial feature.

The low level layer can be reduced to a problem of tracking for each degree of freedom that can be implemented by a nonlinear control technique such as sliding mode control or backstepping. It must have the ability to handle perturbations.

A model predictive controller was chosen to be in charge of the upper layers, verifying the feasibility of the established plan according to the system state, group constraints and all the remaining constraints. It has the capability of changing motion parameters or plans and is will optimize the low level controllers' references.

The presence of three distinct dynamics belonging to three different sub-system that need to cooperate to archive a fourth dynamic behavior, led to the reduction of degrees of freedom to make the study of each sub-system properties possible. Thus, the strategy used was to conduct individual simulations before testing the system as a whole.

Due to the nature of the system, a significant effort had to be put into the theoretical study of different fields: mechanics of rigid bodies along with Lagrangian mechanics to obtain the kinematics and dynamics' equations; hybrid systems that emerge thanks to the existence of impacts; nonlinear control including Limit cycle stability and Lyapunov stability analysis; optimal control.

Given the large complexity of the system there is still plenty of room for improvement, but a solid foundation for future developments has been accomplished.

Appendix A

Computation of the Dinamics Equation

Equation (7.49) can be materialized into the dynamical system of the swing leg. Expanding it we get

$$\begin{bmatrix} u_{hip}(t) \\ u_{knee}(t) \\ u_{ankle}(t) \end{bmatrix} = \begin{bmatrix} B_{1,1} & B_{1,2} & B_{1,3} \\ B_{2,1} & B_{2,2} & B_{2,3} \\ B_{3,1} & B_{3,2} & B_{3,3} \end{bmatrix} \begin{bmatrix} \ddot{\theta}_{hip}(t) \\ \ddot{\theta}_{knee}(t) \\ \ddot{\theta}_{ankle}(t) \end{bmatrix} + \begin{bmatrix} Ct_{1,1} & Ct_{1,2} & Ct_{1,3} \\ Ct_{2,1} & Ct_{2,2} & Ct_{2,3} \\ Ct_{3,1} & Ct_{3,2} & Ct_{3,3} \end{bmatrix} \begin{bmatrix} \dot{\theta}_{hip}(t)^2 \\ \dot{\theta}_{knee}(t)^2 \\ \dot{\theta}_{ankle}(t)^2 \end{bmatrix} \tag{A.1}$$

$$+ \begin{bmatrix} Cor_{1,1} & Cor_{1,2} & Cor_{1,3} \\ Cor_{2,1} & Cor_{2,2} & Cor_{2,3} \\ Cor_{3,1} & Cor_{3,2} & Cor_{3,3} \end{bmatrix} \begin{bmatrix} \dot{\theta}_{hip}(t)\,\dot{\theta}_{knee}(t) \\ \dot{\theta}_{hip}(t)\,\dot{\theta}_{ankle}(t) \\ \dot{\theta}_{knee}(t)\,\dot{\theta}_{ankle}(t) \end{bmatrix} + \begin{bmatrix} G_{1,1} \\ G_{2,1} \\ G_{3,1} \end{bmatrix}$$

with the coefficients

$$\begin{aligned} B_{1,1} = & -2\,m_{foot} L_{foot}\, L_{shin} \sin(\theta_{ankle}(t)) \\ & + m_{foot} {L_{thigh}}^2 + 2\,m_{foot} L_{thigh} L_{shin} \cos(\theta_{knee}(t)) \\ & - 2\,m_{foot} L_{foot}\, L_{thigh} \sin(\theta_{ankle}(t) - \theta_{knee}(t)) \\ & + m_{foot} {L_{heel}}^2 + 2\,m_{foot} L_{heel}\, L_{shin} \cos(\theta_{ankle}(t)) \\ & + 2\,m_{foot} L_{heel}\, L_{thigh} \cos(\theta_{ankle}(t) - \theta_{knee}(t)) \\ & + 0.25\,m_{thigh} L_{thigh}^2 + m_{shin} L_{thigh}\, L_{shin} \cos(\theta_{knee}(t)) \\ & + m_{foot} {L_{foot}}^2 + m_{shin} {L_{thigh}}^2 + 0.25\,m_{shin} L_{shin}^2 + m_{foot} {L_{shin}}^2 \end{aligned} \tag{A.2}$$

$$
\begin{aligned}
B_{1,2} = & -0.5\,m_{shin}L_{thigh}L_{shin}\cos(\theta_{knee}(t)) - m_{foot}{L_{shin}}^2 \\
& - m_{foot}{L_{foot}}^2 - m_{foot}{L_{heel}}^2 + m_{foot}L_{foot}L_{thigh}\sin(\theta_{ankle}(t) - \theta_{knee}(t)) \\
& - m_{foot}L_{thigh}L_{shin}\cos(\theta_{knee}(t)) \\
& - m_{foot}L_{heel}L_{thigh}\cos(\theta_{ankle}(t) - \theta_{knee}(t)) \\
& + 2\,m_{foot}L_{foot}L_{shin}\sin(\theta_{ankle}(t)) \\
& - 2\,m_{foot}L_{heel}L_{shin}\cos(\theta_{ankle}(t)) - 0.25\,m_{shin}L_{shin}^2
\end{aligned}
$$

$$
\begin{aligned}
B_{1,3} = & -m_{foot}[-{L_{foot}}^2 + L_{foot}L_{shin}\sin(\theta_{ankle}(t)) \\
& - {L_{heel}}^2 - L_{heel}L_{thigh}\cos(\theta_{ankle}(t) - \theta_{knee}(t)) \\
& + L_{foot}L_{thigh}\sin(\theta_{ankle}(t) - \theta_{knee}(t)) \\
& - L_{heel}L_{shin}\cos(\theta_{ankle}(t))]
\end{aligned}
$$

$$
\begin{aligned}
B_{2,1} = & -0.5\,m_{shin}L_{thigh}L_{shin}\cos(\theta_{knee}(t)) \\
& - m_{foot}{L_{shin}}^2 - m_{foot}{L_{foot}}^2 - m_{foot}{L_{heel}}^2 \\
& + m_{foot}L_{foot}L_{thigh}\sin(\theta_{ankle}(t) - \theta_{knee}(t)) \\
& - m_{foot}L_{thigh}L_{shin}\cos(\theta_{knee}(t)) \\
& - m_{foot}L_{heel}L_{thigh}\cos(\theta_{ankle}(t) - \theta_{knee}(t)) \\
& + 2\,m_{foot}L_{foot}L_{shin}\sin(\theta_{ankle}(t)) - 2\,m_{foot}L_{heel}L_{shin}\cos(\theta_{ankle}(t)) \\
& - 0.25\,m_{shin}L_{shin}^2
\end{aligned}
$$

$$
\begin{aligned}
B_{2,2} = & \, m_{foot}{L_{foot}}^2 + 0.25\,m_{shin}L_{shin}^2 + m_{foot}{L_{heel}}^2 + m_{foot}{L_{shin}}^2 \\
& - 2\,m_{foot}L_{foot}L_{shin}\sin(\theta_{ankle}(t)) \\
& + 2\,m_{foot}L_{heel}L_{shin}\cos(\theta_{ankle}(t))
\end{aligned}
$$

$$
\begin{aligned}
B_{2,3} = & -m_{foot}{L_{foot}}^2 - m_{foot}{L_{heel}}^2 \\
& + m_{foot}L_{foot}L_{shin}\sin(\theta_{ankle}(t)) - m_{foot}L_{heel}L_{shin}\cos(\theta_{ankle}(t))
\end{aligned}
$$

$$
\begin{aligned}
B_{3,1} = & \, m_{foot}{L_{foot}}^2 - m_{foot}L_{foot}L_{shin}\sin(\theta_{ankle}(t)) \\
& + m_{foot}{L_{heel}}^2 + m_{foot}L_{heel}L_{thigh}\cos(\theta_{ankle}(t) - \theta_{knee}(t)) \\
& - m_{foot}L_{foot}L_{thigh}\sin(\theta_{ankle}(t) - \theta_{knee}(t)) + m_{foot}L_{heel}L_{shin}\cos(\theta_{ankle}(t))
\end{aligned}
$$

$$B_{3,2} = - m_{foot} {L_{foot}}^2 - m_{foot} {L_{heel}}^2 + m_{foot} L_{foot} L_{shin} \sin(\theta_{ankle}(t)) - m_{foot} L_{heel} L_{shin} \cos(\theta_{ankle}(t))$$

$$B_{3,3} = m_{foot} {L_{foot}}^2 + m_{foot} {L_{heel}}^2$$

- - - - - - - - - - - - - - - - (centrifugal matrix coefficients) - - - - - - - - - - - - - - - - - -

$$Ct_{1,1} = 0$$

$$\begin{aligned} Ct_{1,2} = & L_{thigh} [0.5 m_{shin} L_{shin} \sin(\theta_{knee}(t)) \\ & + m_{foot} L_{shin} \sin(\theta_{knee}(t)) - m_{foot} L_{foot} \cos(\theta_{ankle}(t) - \theta_{knee}(t)) \\ & - m_{foot} L_{heel} \sin(\theta_{ankle}(t) - \theta_{knee}(t))] \end{aligned} \tag{A.3}$$

$$\begin{aligned} Ct_{1,3} = & - m_{foot} [L_{foot} L_{thigh} \cos(\theta_{ankle}(t) - \theta_{knee}(t)) \\ & + L_{heel} L_{thigh} \sin(\theta_{ankle}(t) - \theta_{knee}(t)) \\ & + L_{foot} L_{shin} \cos(\theta_{ankle}(t)) + L_{heel} L_{shin} \sin(\theta_{ankle}(t))] \end{aligned}$$

$$\begin{aligned} Ct_{2,1} = & L_{thigh} [0.5 m_{shin} L_{shin} \sin(\theta_{knee}(t)) \\ & + m_{foot} L_{shin} \sin(\theta_{knee}(t)) - m_{foot} L_{foot} \cos(\theta_{ankle}(t) - \theta_{knee}(t)) \\ & - m_{foot} L_{heel} \sin(\theta_{ankle}(t) - \theta_{knee}(t))] \end{aligned}$$

$$Ct_{2,2} = 0$$

$$Ct_{2,3} = m_{foot} L_{foot} L_{shin} \cos(\theta_{ankle}(t)) + m_{foot} L_{heel} L_{shin} \sin(\theta_{ankle}(t))$$

$$\begin{aligned} Ct_{3,1} = & m_{foot} [L_{foot} L_{thigh} \cos(\theta_{ankle}(t) - \theta_{knee}(t)) \\ & + L_{heel} L_{thigh} \sin(\theta_{ankle}(t) - \theta_{knee}(t)) \\ & + L_{foot} L_{shin} \cos(\theta_{ankle}(t)) + L_{heel} L_{shin} \sin(\theta_{ankle}(t))] \end{aligned}$$

$$Ct_{3,2} = m_{foot} L_{foot} L_{shin} \cos(\theta_{ankle}(t)) + m_{foot} L_{heel} L_{shin} \sin(\theta_{ankle}(t))$$

$$Ct_{3,3} = 0$$

- - - - - - - - - - - - - - - - (coriolis matrix coefficients) - - - - - - - - - - - - - - - - - -

$$
\begin{aligned}
Cor_{1,1} = & -2L_{thigh}\,[m_{shin}(0.5L_{shin})\,\sin(\theta_{knee}(t)) \\
& + m_{foot}L_{shin}\,\sin(\theta_{knee}(t)) - m_{foot}L_{foot}\,\cos(\theta_{ankle}(t) - \theta_{knee}(t)) \\
& - m_{foot}L_{heel}\,\sin(\theta_{ankle}(t) - \theta_{knee}(t))\,]
\end{aligned}
$$

$$
\begin{aligned}
Cor_{1,2} = & -2m_{foot}[L_{foot}\,L_{thigh}\,\cos(\theta_{ankle}(t) - \theta_{knee}(t)) \\
& + L_{heel}\,L_{thigh}\,\sin(\theta_{ankle}(t) - \theta_{knee}(t)) \\
& + L_{foot}\,L_{shin}\,\cos(\theta_{ankle}(t)) + L_{heel}\,L_{shin}\,\sin(\theta_{ankle}(t))\,]
\end{aligned}
\tag{A.4}
$$

$$
\begin{aligned}
Cor_{1,3} = & \,2m_{foot}[L_{foot}\,L_{thigh}\,\cos(\theta_{ankle}(t) - \theta_{knee}(t)) \\
& + L_{heel}\,L_{thigh}\,\sin(\theta_{ankle}(t) - \theta_{knee}(t)) + L_{foot}\,L_{shin}\,\cos(\theta_{ankle}(t)) \\
& + L_{heel}\,L_{shin}\,\sin(\theta_{ankle}(t))\,]
\end{aligned}
$$

$$
\begin{aligned}
Cor_{2,1} = & L_{thigh}\,(m_{shin}(0.5L_{shin})\,\sin(\theta_{knee}(t)) + m_{foot}L_{shin}\,\sin(\theta_{knee}(t)) \\
& - m_{foot}L_{foot}\,\cos(\theta_{ankle}(t) - \theta_{knee}(t)) \\
& - m_{foot}L_{heel}\,\sin(\theta_{ankle}(t) - \theta_{knee}(t)))
\end{aligned}
$$

$$
Cor_{2,2} = 2m_{foot}L_{shin}\,(L_{foot}\,\cos(\theta_{ankle}(t)) + L_{heel}\,\sin(\theta_{ankle}(t)))
$$

$$
Cor_{2,3} = -2m_{foot}L_{shin}\,(L_{foot}\,\cos(\theta_{ankle}(t)) + L_{heel}\,\sin(\theta_{ankle}(t)))
$$

$$
Cor_{3,1} = -2m_{foot}L_{shin}\,(L_{foot}\,\cos(\theta_{ankle}(t)) + L_{heel}\,\sin(\theta_{ankle}(t)))
$$

$$
\begin{aligned}
Cor_{3,2} = & -m_{foot}(L_{foot}\,L_{thigh}\,\cos(\theta_{ankle}(t) - \theta_{knee}(t)) \\
& + L_{heel}\,L_{thigh}\,\sin(\theta_{ankle}(t) - \theta_{knee}(t)) \\
& + L_{foot}\,L_{shin}\,\cos(\theta_{ankle}(t)) + L_{heel}\,L_{shin}\,\sin(\theta_{ankle}(t)))
\end{aligned}
$$

$$
Cor_{3,3} = m_{foot}L_{shin}\,(L_{foot}\,\cos(\theta_{ankle}(t)) + L_{heel}\,\sin(\theta_{ankle}(t)))
$$

- - - - - - - - - - - - - - - - (gravitical vector coefficients) - - - - - - - - - - - - - - - - - -

$$
\begin{aligned}
G_{1,1} = & - g\,[0.5\,L_{thigh}\,m_{thigh}\sin(\theta_{hip}(t)) \\
& + m_{foot}L_{shin}\,\sin(\theta_{hip}(t) - \theta_{knee}(t)) + m_{shin}L_{thigh}\,\sin(\theta_{hip}(t)) \\
& + m_{shin}(0.5\,L_{shin})\,\sin(\theta_{hip}(t) - \theta_{knee}(t)) + m_{foot}L_{thigh}\,\sin(\theta_{hip}(t)) \\
& + m_{foot}L_{foot}\,\cos(\theta_{ankle}(t) + \theta_{hip}(t) - \theta_{knee}(t)) \\
& + m_{foot}L_{heel}\,\sin(\theta_{ankle}(t) + \theta_{hip}(t) - \theta_{knee}(t))\,] \\
G_{2,1} = & \, g\,[m_{foot}L_{heel}\,\sin(\theta_{ankle}(t) + \theta_{hip}(t) - \theta_{knee}(t)) \\
& + m_{foot}L_{foot}\,\cos(\theta_{ankle}(t) + \theta_{hip}(t) - \theta_{knee}(t)) \\
& + m_{foot}L_{shin}\,\sin(\theta_{hip}(t) - \theta_{knee}(t)) + m_{shin}(0.5\,L_{shin})\,\sin(\theta_{hip}(t) - \theta_{knee}(t))\,] \\
G_{3,1} = & - g\,m_{foot}\,[L_{foot}\,\cos(\theta_{ankle}(t) + \theta_{hip}(t) - \theta_{knee}(t)) \\
& + L_{heel}\,\sin(\theta_{ankle}(t) + \theta_{hip}(t) - \theta_{knee}(t))\,]
\end{aligned}
\tag{A.5}
$$

References

[1] Pandu R Vundavilli and Dilip K Pratihar. Dynamically balanced optimal gaits of a ditch-crossing biped robot. *Robotics and Autonomous Systems*, pages 349–361, 2010.

[2] Gill Pratt Jerry Pratt. Intuitive control of a planar bipedal walking robot. *1998 Internattonal Conference on Robotics and Autornat on (JCRA '98), Relgium*, 1998.

[3] Ottobock. Genium costumer catalog. http://www.ottobockknees.com/knee-family/genium-bionic-prosthetic-system/advanced-technology/, accessed in November 2012.

[4] Lutfi Mutlu et al. Modelling of an under-hip prosthesis with ankle and knee trajectory control by using human gait analysis. *18th IFAC World Congress Milano (Italy)*, pages 9672–9673, August 2011.

[5] David A Winter. Foot trajectory in human gait: A precise and multifactorial motor control task. *Journal of the American Physical Therapy Association, Vol 72*, pages 45–55, July 1991.

[6] Joao Hespanha. Hybrid systems lecture notes, 2005.

[7] Seth Hutchinson Mark W Spong and M Vidyasagar. *Robot Modeling and Control*. John Wiley and Sons, Inc, First edition, 2006.

[8] Paolo de Leva. Adjustments to zatsiorsky-seluyanov's segment inertia parameters, 1996. http://www.exrx.net/Kinesiology/Segments.html, accessed in January 2013.

[9] Pamela Levangie and Cynthia Norkin. *Joint Structure and function - A Comprehensive analysis*. MacLennan and Petty, Eastgardens, N.S.W., Fourth edition, 2005.

[10] Postural balance definition according to pollock as et al. http://www.ncbi.nlm.nih.gov/pubmed/10945424, accessed in November 2012.

[11] Hanger Inc. Kafo definition. http://www.hanger.com/orthotics/services/Pages/LowerExtremity.aspx, accessed in November 2012.

[12] Steven H. Strogatz. *Nonlinear Dynamics and Chaos: With Applications to Physics, Biology, Chemistry, and Engineering*. Perseus Books, 1994.

[13] Ill-Woo Park Jung-Yup Kim and Jun-Ho Oh. Walking control algorithm of biped humanoid robot on uneven and inclined floor.

[14] IEEE. Standard for application and management of the systems engineering process - description, 1998. IEEE Std 1220-1998.

[15] Roland Siegwart and Illah Nourbakhsh. *Introduction to Autonomous Mobile Robots*. MIT Press, First edition, 2004.

[16] Rui Monteiro. Desenvolvimento de um controlador dinâmico para rôbos humanoides nao. Technical report, Faculdade de Engenharia da Universidade do Porto, Julho 2012.

[17] Fabio Zonfrilli. Theoretical and experimental issues in biped walking control based on passive dynamics. Technical report, Universita degli Studi di Roma "La Sapienza", December 2004.

[18] Eric R. Westervelt. Toward a coherent framework for the control of planar biped locomotion. Technical report, University of Michigan, 2003.

[19] Daniele Nardi Fabio Zonfrilli, Giuseppe Oriolo. A biped locomotion strategy for the quadruped robot sony ers-210. September 2001.

[20] Yao Li. An optimal control model for human postural regulation. Technical report, University of Maryland, 2010.

[21] William S. Levine Yao Li and Gerald E. Loeb et al. A two-joint human posture control model with realistic neural delays. *IEEE Transactions on Neural Systems and Rehabilitation engineering, Vol. 20, No. 5*, pages 738–748, September 2012.

[22] R. Fluit et al. A simple controller for the prediction of three-dimensional gait. *Journal of Biomechanics 45*, page 2610–2617, September 2012.

[23] Luiz R Douat. Estabilização do caminhar de um robot bipede de 5 elos com compensação do movimento dorsal. Technical report, Universidade Federal de Santa Catarina, June 2008.

[24] André Q. Gonçalves. Locomoção bípede. Technical report, Universidade do Minho, December 2011.

[25] Joao Paulo Ferreira Manuel Crisóstomo and A. Paulo Coimbra. Controlo de um robô bípede com base em sensores de força nos pés. *9th Spanish Portuguese Congress on Electrical Engineering. Edited by Asociación Española para el Desarrollo de la Ingeniería Eléctrica. Marbella, Spain*, 30 of June to 2 of July, 2005 ISBN 84-609-5231-2.

[26] XU Tao and CHEN Qijun. A simple rebalance strategy for omnidirectional humanoids walking by learning foot positioning. *2011 8th Asian Control Conference, Taiwan*, pages 1340–1345, May 2011.

[27] Kanako Miura et al. Human-like walking with toe supporting for humanoids. *2011 IEEE/RSJ International Conference on Intelligent Robots and Systems*, pages 4428–4435, September 2011.

[28] M. Matsumoto K. Suwanratchatamanee and S. Hashimoto. Walking on the slopes with tactile sensing system for humanoid robot. *International Conference on Control, Automation and Systems 2010, Korea*, pages 350–355, October 2010.

[29] Ill-Woo Park Jung-Yup Kim and Jun-Ho Oh. Realization of dynamic stair climbing for biped humanoid robot using force/torque sensors. *J Intell Robot Syst 56*, page 389–423, 2009.

[30] Fei Wang et al. A coordinated control strategy for stable walking of biped robot with heterogeneous legs. *Industrial Robot: An International Journal, Vol. 36 Iss: 5*, pages 503–512, 2009.

[31] A. Chemori et al. A control architecture with stabilizer for 3d stable dynamic walking of sherpa biped robot on compliant ground. *2010 IEEE-RAS International Conference on Humanoid Robots*, pages 480–485, December 2010.

[32] R. Soto1 C. Hernández-Santos, E. Rodriguez-Leal and J.L. Gordillo. Kinematics and dynamics of a new 16 dof humanoid biped robot with active toe joint. *International Journal of Advanced Robotic Systems, Vol. 9*, August 2012.

[33] Christine Azevedo and the BIP team. Control architecture and algorithms of the anthropomorphic biped robot bip2000. 2000.

[34] World Health Organization. 2011 world report on disability. http://whqlibdoc.who.int/publications/2011/9789240685215_eng.pdf, accessed in October 2012.

[35] Paul Hochman. Bionic legs, i-limbs, and other super human prostheses you'll envy, February 2010. http://www.fastcompany.com/1514543/bionic-legs-i-limbs-and-other-super-human-prostheses-youll-envy, accessed in October 2012.

[36] Ottobock. Ottobock sales' report, 2011. http://www.ottobock.com/cps/rde/xchg/ob_com_en/hs.xsl/988.html, accessed in October 2012.

[37] International Organization for Standardization. Iso standards for prosthetics and orthotics. http://www.iso.org/iso/home/store/catalogue_tc/catalogue_tc_browse.htm?commid=53630, accessed in Noverber 2012.

[38] Prosthesis cost and date of criation http://en.wikipedia.org/wiki/Prosthesis, accessed in October 2012.

[39] Prosthesis release date and comparative Study http://prostheticleg.info/content/what-best-prosthetic-knee-me, accessed in October 2012.

[40] Amputee support group - differnt brand phosthesis' issues. http://www.dailystrength.org/c/Amputees/forum/7216042-freedom-innovations-plie-knee-issues, accessed in October 2012.

[41] Ottobock. Socket technology. http://www.ottobock.com/cps/rde/xchg/ob_com_en/hs.xsl/20381.html, accessed in November 2012.

[42] Bespoke Innovations. Costumized add-ons. http://www.bespokeinnovations.com/content/what-fairing, accessed in November 2012.

[43] Paul Seibert. iwalk powerfoot features. Hub Tech Insider http://hubtechinsider.wordpress.com/category/robotics/, accessed in November 2012.

[44] Hugh Herr. Hugh herr speech on "the world we dream - zeitgeist americas 2012 conference"), 2012. minute 8.15 to 9.45 http://www.youtube.com/watch?v=it1A4qT1cHs, accessed in November 2012.

[45] Mary L. Jerrell. Stance control orthoses: revolutionizing-patient-care, October 2003. http://www.healio.com/orthotics-prosthetics/orthotics/news/online/%7Bc77b0f4f-fef2-4aa0-baf5-0d1beb654bb3%7D/stance-control-orthoses-revolutionizing-patient-care, accessed in November 2012.

[46] Ottobock. Free walk operating principal. http://www.ottobockus.com/cps/rde/xchg/ob_us_en/hs.xsl/20606.html?id=19260#t19260, accessed in November 2012.

[47] Step of Mind. Re-step operating principal, 2008. http://www.stepofmind.com/Re-Step.aspx, accessed in November 2012.

[48] Frank Bell. *Principles of Mechanics and Biomechanics*. Stanley Thornes (Publishers) Ltd, Fourth edition, 1998.

[49] Kagaya et al. Ankle, knee, and hip moments during standing, 1998. US National Library of Medicine National Institutes of Health Search, http://www.ncbi.nlm.nih.gov/pubmed/9482379, abstract accessed in November 2012.

[50] Richard C. Schafer. *Clinical Biomechanics:Musculoskeletal Actions and Reactions*. Williams and Wilkins, 1987.

[51] Anthony Tongen and Roshna E. Wunderlich. Biomechanics of running and walking.

[52] Salvatore Grande Erika Ottaviano, Marco Ceccarelli. An experimental evaluation of human walking. *3rd International Congress Design and Modelling of Mechanical Systems CMSM'2009 (Turkey)*, March 2009.

[53] L. Pontryagin et al. *Mathematical Theory of Optimal Processes*. Interscience Publ., 1962.

[54] R. Vinter. *Optimal Control*. 2000.

[55] F. Clarke et al. *Nonsmooth analysis and control theory*. springer-Verlag, 1998.

[56] A. Arutyunov. *Optimality Conditions: Abnormal and Degenerate Problems*. Springer, 2000.

[57] F. Pereira A. Arutyunov, D. Karamzin. A generalization of the impulsive control concept: Controlling system jumps. *Discrete & Continuous Dynamical Systems, Vol 29(2)*, pages 403–415, 2011.

[58] A. Bemporad. Model predictive control, 2009. Controllo di Processo e de Sistemi di Produzione.

[59] D. Mayne et al. Constrained model predictive control: Stability and optimality. *Automatica, vol. 36*, 2000.

[60] F. Fontes. A general framework to design stabilizing nonlinear model predictive controllers. *Systems & Control Letters, vol. 42*, pages 127–143, 2001.

[61] E. Gyurkovics F. Fontes, L. Magni. *Sampled-data model predictive control for nonlinear time-varying systems: Stability and robustness*. Springer, 2007.

[62] F. Pereira F. Fontes. Model predictive control of impulsive dynamical systems. *NMPC2012 - 4th IFAC Nonlinear Model Predictive Control Conference*, August 2012.

[63] J. Sousa J. Silva. A dynamic programming based path-following controller for autonomous vehicles. *Control & Intel. Sys., vol. 39(4)*, pages 245–253, 2011.

[64] G. Silva F. Pereira. Necessary conditions of optimality for state constrained infinite horizon differential inclusions. *50th IEEE Conference on Decision and Control & European Control Conference*, pages 6717–6722, December 2011.

[65] M. Caputo. Necessary and sufficient conditions for infinite horizon control problems. *Foundations of Dynamic Economic Analysis Optimal Control Theory and Applications*, pages 381–411, 2005.

[66] Lygeros. Hybrid systems lecture notes, 2004.

[67] Hassan Khalil. *Nonlinear Systems*. Prentice-Hall, Second edition, 1996.

[68] Antonio Pedro Aguiar. Nonlinear control systems lecture notes, 2012. FEUP-PDEEC PhD Course.